Oscillatory Stability of Power Systems with High Shares of Renewable Generation: Investigation of the Effectiveness of Wide-Area Selective Damping Control

NextGen GridOps Knowledge Framework Supporting Future Grid Operations

Jan Vit Suntar

TUDelft

Oscillatory Stability of Power Systems with High Shares of Renewable Generation: Investigation of the Effectiveness of Wide-Area Selective Damping Control

NextGen GridOps Knowledge Framework Supporting Future Grid Operations

by

Jan Vit Suntar

to obtain the degree of Master of Science
at the Delft University of Technology,
to be defended publicly on Tuesday August 31, 2021 at 11:00 AM.

This thesis is confidential and cannot be made public until August 31, 2023.

An electronic version of this thesis is available at `http://repository.tudelft.nl/`.

Abstract

A large contribution to the total share of electricity generated in European power grid will come from renewable sources of energy in the near future due to European initiative to become carbon neutral. Renewable Energy Sources (RES) are connected to the grid with Power Electronic (PE) devices, which if not modelled correctly provide lower level of system stability and security of supply. The existing power grid with mainly synchronous generators will not be suited to operate in the future, when synchronous machines will become less important sources of energy. An increase in dynamic behaviour of the system could cause significant challenges for the existing system, which calls for new monitoring and control strategies. The aim of the project is twofold; firstly, to enhance system stability by deploying Wide Area Monitoring System (WAMS) in power system with a massive share of RES to total electricity generation. Secondly, it focuses on developing and proposing a tool which will improve consultancy in future power grids. A tool developed is Next Generation Grid Operations (NextGen GridOps) Knowledge Framework which is conceptually designed by DNV.

The effectiveness of WAMS applications on system stability improvements and damping enhancements will be evaluated by studying rotor angle stability as well as effect of WAMS on damping of electromechanical oscillations. The response to a disturbance of the remaining synchronous generators will be studied to evaluate the effect of different types of control schemes (grid-following, grid forming control) on the rotor angle stability. Rotor angle stability will be examined to show whether different control structures and WAMS will show enhancements of the overall stability through time domain simulations. WAMS structure in this project consists of Phasor Measurement Units (PMUs) as well as Wide Area Damping Controls (WADCs). While PMUs are sensors deployed in the system to provide synchrophasor measurement, WADCs are damping controllers deployed with an intent of enhancing damping in the system.

This project build upon findings from Horizon 2020 MIGRATE Project. The effectiveness of grid-following control and grid-forming control on stabilizing the grid with massive penetration of PE devices are conducted to set the base case for evaluating the effect of WAMS. Modelling software used in the project is DIgSILENT PowerFactory 2021 SP1 and the PowerFactory Thesis Licence was provided by DIgSILENT GmbH for research and educational purposes. Based on the off-line numerical simulations conducted in IEEE 39 Bus New England test system it was found that WAMS functionality with corresponding PMUs and WADCs can decrease oscillations in the system. It has been verified that grid-following control enables 60% of RES penetration and grid-forming control enables penetration of RES above 80%. There have been two grid-forming controllers used in the system, where Direct Voltage Control (DVC) is able to receive the stabilizing signal while Virtual Synchronous Machine (VSM) grid-forming controller has a supporting role. WAMS and corresponding WADCs deployed on DVCs are able to enhance damping of the low-frequency modes with frequencies below 2.0 Hz, which is supported by time domain simulations and by conducting Prony analysis. Eigenvalue analysis results for some cases with WAMS deployed show no additional enhancements, which is a consequence of newly introduced controllers and interactions among them and existing controllers.

The practical implications of this Master's Thesis study have been modelled in the NextGen GridOps Framework with an intent to make a step towards real world implementation of the findings developed during the project. Framework modelling focused on implementing client maturity classification of WAMS deployments, contributing towards development of WAMS roadmaps and further deployment of WAMS solutions for grid operators as part of the DNV Next Generation Grid Operations advisory services. Work done and information implemented will be valuable for DNV while solving the complex process of future grid operations and at the same time bringing newly developed knowledge into practice. The framework development part of the project ties in with scientific contribution by allowing newly developed information to be further explored.

Effectiveness of WAMS and WADCs on improving selective damping and consequently enhancing system stability has been identified in this project through use of DVCs. It has been proven that VSM control has a better stabilizing effect and would allow even further enhancement of damping critical oscillation modes. Higher damping in the system increases the stability and consequently higher security of energy supply.

Acknowledgements

Contents

List of Figures

List of Tables

List of Abriviations

1

Introduction

The existing power grid is in a desperate need of a thorough transformation, which will provide equal or even better security of supply for electricity consumers. European effort of making energy cleaner and to preserve the environment has caused a significant development in renewable energy technology. European Commission has identified key points, which would enable reaching European climate objectives by decarbonising the European Union (EU)'s energy system. Energy efficiency and development of a system based on RES has been identified as requirements in order to reduce global warming and CO_2 emissions. Goals such as high security of supply in future power grids and can be achieved by developing interconnected EU energy markets [1]. Exploring full potential from offshore and onshore wind energy and cooperation among system operators to share green energy are some of the aspects which will make a transition to European carbon neutrality possible.

A RES generation is increasing significantly in recent years and the trend will increase even further in the future. Nuclear power, hydro power, gas and coal were the main types of electricity generation before year 2010 [2]. Significant increase in wind generation and solar Photovoltaic (PV) generation is observed, while energy produced by coal is becoming less important. Short term predictions for year 2030 is that wind and solar generation will increase even further and electricity generated from coal will start decreasing. Long term prediction for year 2050 shows that coal, oil and gas will contribute to less than a quarter of entire electricity production. Wind and solar power will each contribute to around 25% of overall electricity generation [2] and individual contribution to the overall generation of each source are shown in a figure 1.1. It is also visible from a figure an overall increase in electricity generation, which will balance the predicted increase in electricity demand.

Figure 1.1: World electricity generation by power station type [2].

1

A total share of RES in the power grid will become increasingly more significant in the near future, which makes a correct coupling of these devices to the grid a very important topic for research. PE devices make coupling of RES to the power grid possible, with an ability to adjust the frequency and to couple systems working with Direct Current (DC) to Alternating Current (AC). A benefit of the PE devices is that they have an ability to enhance system stability, when there is just a fraction of PE devices introduced to the grid. Increasing percentage of energy produced from RES becomes an issue for system stability with higher levels of penetration. Horizon 2020 MIGRATE project was developed to research and tackle issues and unknowns that system operators might experience with high share of PE devices.

An objective of MIGRATE Project was to identify the advanced solutions for technical challenges brought to the system with PE devices [3]. Massive integration indicates that RES become a leading contributor to the overall electricity generation, while synchronous generation will become less important in a modern power grid [4]. With that in mind, controllers should be, rather than a kinetic energy stored in the rotating mass of the generators, a dominant force contributing to the overall system stability. Grid-forming control strategy is a feasible option for stabilizing task due to its ability to generate its own reference points. Since it is uneconomical to only install grid-forming control in the system, supplementary control strategy, grid-following control, is also deployed to support the operations in the grid.

Remaining synchronous generators will struggle with continuous active power imbalances while PE devices cannot ensure robust control actions like those delivered by the removed generators. A local control on remaining machines will experience challenges to keep machines in synchronism and match previous levels of rotor angle stability. WAMS has been identified as a possible source of a mitigation implementation since it has an ability of collecting synchrophasor measurements from PMUs. These sensors are able to provide a magnitude and an angle to represent the state of the system and allow grid operators to make correct decision. The time frame of measurements provided by existing Supervisory Control and Data Acquisition (SCADA) does not provide the satisfactory levels of insight required in the modern power grid.

Utilizing the knowledge gained through the extensive research done in the recent years is one of the main focuses of system operators. Leading energy consultant in the Netherlands is Det Norske Veritas - Energy (hereinafter DNV), whose goal is to put information developed through research into practice. DNV has put a lot of effort in developing a tool, which will make them more competitive and more successful in shaping the future grid operations. They call this building the Grid Operations Machine, which will enable real time operations among different vendors and different applications. Next Generation Grid Operations (hereinafter NextGen GridOps) Knowledge Framework is a tool, which considers Next Generations Machine and defines different layers to consider all aspects. This tool will give all DNV employees an easy access to a pool of information, which can be used as knowledge sharing or developing business solutions. An advantage of such a tool is that all information is collected in one place rather than being fragmented in different places. Furthermore, the validity of information is high due to everyone having access to information, which can be easily updated.

2

Problem Formulation

2.1. Problem Statement

Power system should stay in a stable operating condition to provide consumers with constant power supply. Generation of electricity needs to balance the consumption and transmission system needs enough capacity to deliver a required amount from generation plants to the final consumers. With an increasing amount of RES connecting to the power system, it is becoming increasingly challenging to maintain the desired stability in the system. This is because synchronous generation is being replaced by PE devices, to enables coupling of wind turbines and solar PV to the grid. RES have a very stochastic behaviour it is very hard to predict their contribution to the overall electricity generation, meaning that WTs deliver electricity only if there is enough wind to turn the blades on the wind turbine. In case that there is no wind, WTs do not contribute to the overall electricity generation and other sources of generation present in the grid have to balance the load to prevent the instabilities in the grid.

One of the main points of interest for the future power grids is a contribution of an onshore system with a large participation of RES to the overall electricity generation. Contribution of a wind power generation to the overall electricity generation is increasing rapidly and has a potential to reach 70% to 80% and grid-forming control will have to be implemented to ensure stabilizing of the grid following a disturbance. Different grid-forming control strategies will be studied, Direct Voltage Control, Virtual Synchronous Machine, or a combination of strategies, to determined how much of PE penetration has to be grid forming to maintain stability in the system. An objective is to use control strategies that will be able to provide stable operation of RES and to maintain synchronism of synchronous generation in the system.

Consequently, heavy penetration of wind power generation will cause a shift towards 20% to 30% of synchronous generation remaining in the system. Synchronous machines maintained in the grid can experience rotor angle instability in case they are controlled improperly. Rotor angle stability will stay an important aspect of power system stability, even though RES will become a major contributor to the overall electricity generation. Introduction of numerous participating entities will cause an increase in dynamic behaviour of the grid, which will present challenges for synchronous generators to stay in synchronism and to provide continuously power supply. In case that synchronous machines will somehow lose synchronism due to an occurrence of an unplanned event, 20% of generation in the system will be lost. In the worst case scenario, synchronous machines will have to be disconnected from the grid which might lead to a complete blackout of the power grid, leaving many businesses and people without electricity.

Massive penetration of RES will cause an occurrence of low-frequency Oscillation Modes (OMs), which contribute towards system losses and element failure. Monitoring of a fast and dynamic behaviour of the modern power grid will be possible by collecting data of higher quality and accuracy. WAMS takes advantage of PMUs, which provide phasor measurements to increase observability and enable controllability of the grid. Local and inter-area modes of oscillation will be of focus in this thesis project and the impact of WAMS functionality will be studied by Modal and Prony analysis. The occurrence of low and ultra-low frequency oscillations is also expected due to interaction of newly deployed controllers, however such phenomenon is out of the

3

scope of this project. Making use of additional damping controllers, such as WADCs, in combination with local signals will enhance controllability of the system and achieve better damping of critical modes of oscillation.

2.2. State-of-the-art and Scientific Gap

This Master's Thesis Project does not focus on developing and improving local controllers (Automatic Voltage Regulator (AVR), Power System Stabilizer (PSS)), neither on developing grid-forming and grid-following control. In fact, already existing technology and models will be used to perform different studies and evaluate the effectiveness of certain control structures. Grid-forming control concept has been heavily described in literature, due to its ability of generating its own setpoits and by not being influenced by the operational condition of the grid. A concept which has an ability of directly regulating active and reactive power has been researched in [5]. Furthermore, methods with an ability of synchronizing and controlling inverters [6] and an ability of keeping voltage in acceptable limits [7] are also described in literature. Identification of critical OMs has been described in literature as a technique of evaluating the system and investigating parameters such as damping ratio, modes of oscillation and eigenvalues [8].

The effects of using massive penetration of PE interfaced generators on the overall system stability has recently been identified. The impacts of WAMS based mitigation solutions on rotor-angle time stability has not yet been discussed in literature especially in cases with heavily RES penetrated systems. It has not been discussed how one grid-forming control is superior to the other one when large majority of the system stability depends on behaviour on controllers and interaction among them. Previously developed methods for selecting input and output signals have to be modified in order to be able to obtain such information in a power system with mainly power converters. Generator speed has been identified for a state variable when constructing a matrix C in conventional power grids, due to presence of synchronous generators in a conventional power grid [9]. Such state variable is not a feasible option anymore, since only around 20% of total generation buses would be evaluated. Definition of state variables is an important step in constructing observability indices, which will identify buses for deployment of PMUs [9]. Modification of previously developed methodology is required to enable the selection of highest controllability buses and to determine the generators to have the highest damping and stabilising effect.

2.3. Research Goal

The main goal of this project is defined with an intent of observing and studying effectiveness of WAMS on damping of low frequency electromechanical oscillations in the power grid with massive penetration of RES and at the same time developing DNV's knowledge framework to put WAMS technology into practice:

Project aims at investigating how to enhance damping of low frequency oscillation modes by deploying WAMS to improve dynamic behaviour of a power grid with a massive integration of PE devices. Furthermore, it attempts at utilizing methodologies and findings about WAMS applications by implementing modelling steps and maturity level scheme into NextGen GridOps Framework for shaping future grid operations.

The contribution of this project is devoted to a development of WAMS, PMUs and WADC solution strategies for enhancement of damping very low frequency oscillations with distributed sources of energy. Load flow analysis, dynamic simulations, Modal and Prony analysis are performed in DIgSILENT PowerFactory software, where a study model will be modified to include large penetration of RES. Various case studies will be conducted to study the effectiveness of control strategies on the stability of the power system. It will be determined which control system has the best impact and possible what combination of grid strategies achieves best results. The effectiveness of the proposed WAMS structure will be analysed by rotor-angle time simulations.

The system considered for the simulation and study purposes is a IEEE 39 New England test system, which has been modified to enable a study of high penetration of RES. Modified test grid will have an ability to include synchronous generation and 80% WT generation with different controller structures; grid-following and two grid-forming controllers. PMU devices will be linked to buses which will be identified to have the highest observability rather than linking it to every bus, which is done to preserve initial investment. Signal selection method will be used to determine which power plants should receive a stabilizing signals from the controller.

Furthermore, a percentage of grid-forming and grid-following control will be determined experimentally by steadily increasing the percentage of grid-forming before system stabilizes. At the same time, 20% of synchronous generation will remain in the system to support the operation.

Knowledge utilization will be done by taking advantage of knowledge framework developed by DNV. NextGen GridOps Framework is constructed with an idea to support future system operations. Main industry contribution of this Master's Thesis Project is to highlight benefits of using such a framework and to propose how to successfully and efficiently model main findings into a framework.

2.4. Research Questions

1. What modifications are required with respect to a standardized test system to enable a study of different case studies with 80% penetration of RES? How will control models (grid forming and grid following), phasor measurement units and wide area monitoring system (WAMS) be modelled in DIgSILENT PowerFactory?

2. How should a phasor measurement unit be deployed to provide measurements for a wide area damping controller to have the highest observability of the system state?

3. Where should a wide area damping controller be deployed to have the highest impact on controllability of the system? Does deploying wide area damping controller on every power plant bring significant improvements over a case when only a handful of WADCs are deployed on analytically determined bases?

4. What control approach (Direct Voltage Control, Virtual Synchronous Machine or grid following control) or combination of controllers show the highest effectiveness against different disturbances? What control approach or combination of controllers prove to be the most effective as well as realistic for future implementation?

5. What results should be implemented into NextGen GridOps Framework and how should they be modelled to support future system operations?

2.5. Methodological Approach

Steps taken to reach the main goal and to answer research questions are:

1. Selection of a standardized Institute of Electrical and Electronics Engineers (IEEE) test system.

2. Modification of the test system to include WT Type 4, DVC, Space Vector Modulation (SVM) on all generator buses except for buses with generator G01 and G02.

3. Selection of input and output signals for installation of PMUs and supplementary damping controllers.

4. Design of a supplementary damping controller and implementation of such a controller to the existing control structures in PowerFactory.

5. Tuning of damping controller parameters for highest possible damping effect achieved in the system.

6. Performance evaluation through different cases studies of different controllers and different rations between grid-forming and grid-following controllers.

7. NextGen GridOps Framework implementation of information useful for DNV's consultancy.

8. Proposal of the design with a grid-forming control strategy, ratio of controllers and tuned parameters of damping controller for realistic implementation while enhancing overall system stability and offering highest damping of critical modes of oscillation.

2.6. Research Milestones

1. Test system built in DIgSILENT PowerFactory and modified to include PE interfaced generation (grid forming and grid following), phasor measurement units and wide area monitoring system.

2. Root Mean Square (RMS) simulations done in DigSILENT PowerFactory with different control strategies and different combination of strategies to evaluate the system stability.

3. Modal analysis and Prony analysis done to evaluate the improvement in damping critical modes of oscillation with integration of WAMS

4. NextGen GridOps Framework contains results to support system operations in future power grids.

2.7. Thesis Outline

A description of the remaining sections of this Master's Thesis is briefly explained below:

Section 3: Literature Review

Firstly, a background information is given about existing definitions and technologies. A definition of a power system stability is explained with stability categorization as rotor angle, voltage and frequency stability. It is explained why keeping a system in stable operation is more challenging with the massive participation of RES. Furthermore, grid-forming and grid-following control strategies are explained and examples of both strategies are given. WAMS and PMU technologies are explained and its contribution of enhancing controllability of the system is emphasized. The objectives and a motivation behind a development of Next Generation Grid Operations (NextGen GridOps) Framework is explained and its importance to DNV is emphasized.

Section 4: Modelling of the Power Grid with Large Penetration of RES

A description of a standardized test system, adopted for this research, is presented in this section, which is later modified to include massive penetration of PE devices. A single line diagram and a description of the standardized IEEE 39 Bus New England test system is presented as well as modifications made to include Type 4 WTs. A description of a synchronous generator control used in this project is presented with a thorough explanation of individual control components, such as: governor, AVR and PSS. General description is given about working principles of FSCG WT, with a description of different control strategies used in this Master's Thesis. A description about individual components of each control system is given, where a current controller is used as a grid-following control, while Direct Voltage Controller and Virtual Synchronous Machine are used as a grid-forming control.

Section 5: Wide Area Monitoring for Improved Controllability

This chapter demonstrates the structure of WAMS, its components and how they are connected and deployed in the system. It shows what techniques were used in order to identify critical modes of oscillation and explains how Eigenvalue analysis and Prony analysis work as well as provides details about individual scripts used for the analysis. Furthermore, it explains the procedure for a selection of input and output signal and proposes an approach for determining observability and controllability indices in highly RES penetrated systems. Besides, wide area damping controller design has been proposed and associated controller parameters were explained. A parameter tuning approach has been explained and an intent of such tuning is to achieve the desired event of such a controller in the system.

Section 6: Knowledge Utilization: NextGen GridOps Model Framework

A motivation behind developing NextGen GridOps Framework is explained in this section and advantages of using such a tool are highlighted by showing direct benefits during project development. DNV's framework can only be explored to its full potential with correct implementation of information and with consistent implementation. A methodology of structuring that has been developed is explained, where a technique of using drivers, issues, impacts, mitigations, goals and requirements is adopted. Use of the framework also allows categorizing clients based on the maturity level of implementation of a solution in their domain, which enables DNV to adjust their service to client's needs. Maturity level description of WAMS implementation is explained, which also enables to create roadmaps for clients to progress towards the next level.

Section 7: Implementation, Case Studies & Simulation Results

Many case studies have been examined in the project with different combinations of synchronous machines and WT with different combinations of grid-following control and grid-forming control. The effect of WAMS on damping critical modes of oscillations has been studied in each case study and results were compared to the system response when WAMS was disconnected from the system. The final design is proposed, which takes into consideration limitations of the available technology as well as what seems reasonable for real world implementations.

Section 8: Conclusion and Future Work

Last chapter of the thesis project concludes the main findings and answers research questions to even further elaborate on the observations made throughout the project. Lastly, it proposes topics identified during the project execution for future research and which were outside of the scope of the project for future analysis.

3

Literature Review

3.1. Stability Classification and Future Systemic Issues

Conventional Power System

Power system was developed to supply electricity from a source of energy (energy generation) to the consumer (load). Power grid is divided into high voltage level transmission system and low voltage level distribution system. Transmission system is on a much higher voltage level so the losses of the electricity transfer over a large distance can be minimized. Generation is connected to the transmission level with a step up transformer, which means that the voltage level increases. Transmission system is connected to distribution system with a step down transformer, which decreases voltage level to levels which can be safely used in domestic applications.

Supply and demand in power system should be always balanced, which means that the same amount electricity that is produced has to be consumed. An indication of a supply and demand balance is the frequency of the grid, which has to be 50 Hz in European grid and 60 Hz in the United States of America. If frequency increases above 50 Hz it means that there is to much generation and that load does not consume all the electricity produced. On the other hand, if frequency decreases below 50 Hz this means that generation cannot match the consumption, which can eventually lead to load shedding and a possible black out.

Power system is classified as stable when it has an ability to stay in a state of equilibrium in normal operating condition and an ability to return to a state of equilibrium when subjected to a disturbance. Figure 3.1 shows a recent system stability categorisation [4].

Rotor angle stability is associated with an ability of synchronous machines in the interconnected power system to remain in synchronism after being subjected to a disturbance [11]. Rotor angle stability can be further divided into two different categories, which depend on the scale of the disturbance in the system. Transient stability is an ability of synchronous machines to remain in synchronism after being subjected to a large disturbance, such as loss of generation. Mechanical power input of a machine should always match electrical power output, so a synchronous machine stays in synchronism with other machines in a power system. This relationship is represented by a Swing equation 3.1 [11]:

$$\frac{2H}{\omega_0}\frac{d^2\delta}{dt^2} = P_a = P_m - P_e \tag{3.1}$$

where H is inertia with units MW-s/MVA, P_a represents accelerating power (p.u), P_m is mechanical power input (p.u), P_e is electrical power output (p.u), δ is rotor angle (rad) and t is time (s).

In case that mechanical power is larger than electrical power, a rotor of a machine will accelerate, due to accelerating power P_a becoming positive. In instance when electrical power becomes larger than mechanical power, a rotor starts to decelerate since P_a becomes negative. A larger value of Inertia Constant (H) has an ability to decrease the rate of change of δ, which means that it takes a larger disturbance for a synchronous
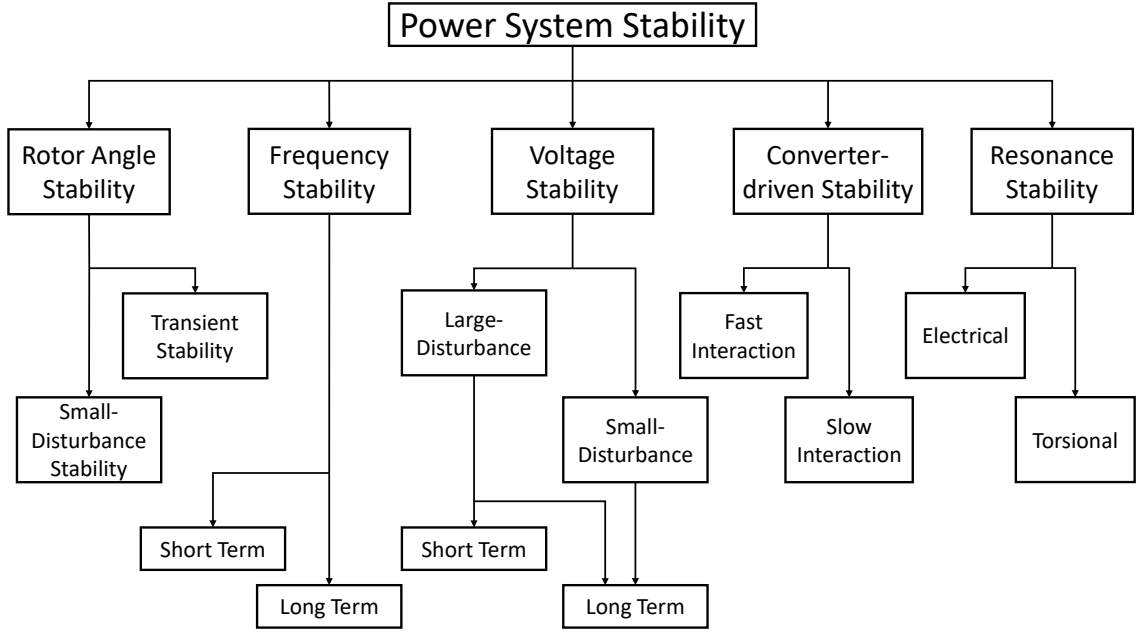
Figure 3.1: The recent and updated stability classification [10]

machine to lose synchronism. Inertia constant is a property of a machine due to kinetic energy that is stored in the rotating mass of the machine. When a machine is directly coupled to the grid it can provide inertial response and increases the stability limits of the power system.

Another aspect of rotor angle stability is when a power system has an ability to stay in synchronism after being subjected to a small disturbance [11]. Several oscillations can occur in PE dominant power systems due to lack of damping torque in the system. These oscillations can occur either locally or globally. The difference is that locally these oscillations occur among a generator and the rest of the system and they are in range of 0.7 Hz to 3.0 Hz. Interarea mode of oscillation occurs when a group of generators in one area oscillates against group of generators in other area and these oscillations are in range of 0.4 Hz and 0.7 Hz [11].

Power Electronically Interfaced Generation

Many aspects of a power system will have to be modified in the future with a transition towards greener energy generation. New solutions will have to be proposed for arising issues, since RES like solar and wind generation cannot be directly coupled to the power grid. PV technology produces DC and in case of wind generation frequency produced does not match with grid frequency, even though that WTs produce AC. RES are connected to the power grid by using PE devices, either with power inverters in case of PV technology or with back-to-back converters in case of WTs. This leads to a realization that PE converters are not able to generate electricity on their own and require a primary energy source or energy storage to behave similar to synchronous generators [12].

PE devices do not consist of any rotating parts where they can store energy, hence they do not provide any inertia to the system. With an increasing penetration of PE devices to the power grid, level of inertia will start to drop significantly and it will become very challenging to keep frequency close to nominal values. PE devices do not have any kinetic energy stored in the rotating mass, however they have energy stored in the capacitor of a DC bus 3.2 [13]. Amount of energy stored is several magnitudes lower compared to energy stored in rotation parts of a synchronous generator.

$$C\frac{dV_{DC}}{dt} = I_{received} - I_{prod} \tag{3.2}$$

where C represents capacitance, $\frac{dV_{DC}}{dt}$ rate of voltage change and I represents current through the capacitor.

Systemic issues associated with PE devices were identified by European Transmission System Operators (TSOs) as part of Massive InteGRATion of power Electronic devices (MIGRATE) Project [4]. Several European

TSOs were asked to firstly list all of the emerging issues that they have either, already experienced during their operation or they are expecting to experience in the future system operation. Secondly they were asked to rank the the most commonly listed issues, which are shown in figure 3.2.
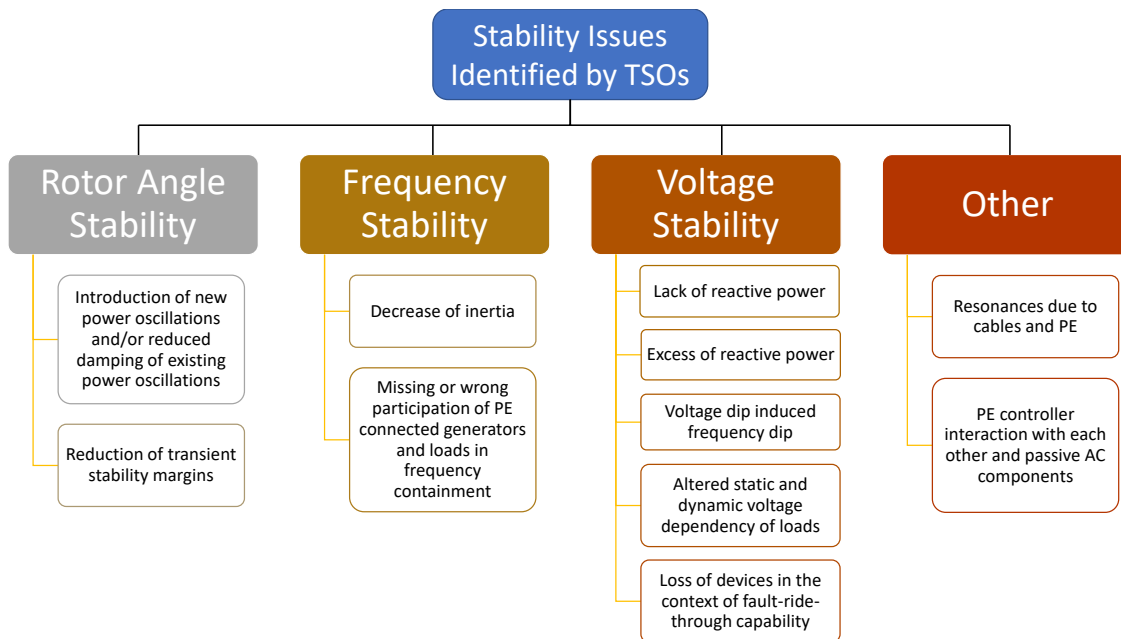
Figure 3.2: Systemic issues identified by European Transmission System Operators [4]

Rotor angle stability will be the main stability focus of this project, hence approaches for improving issues related to decrease of transient stability limits and introduction of new power oscillations will be the main topics in the following chapters. Inertia decrease in the system and participation of controllers were classified as frequency stability issues, while issues associated with reactive power, voltage dip induced frequency dip, load dependency and loss of devices due to inability to withstand disturbances are classified as voltage stability issues. Some issues, such as resonances due to PE devices and PE controller interactions, were not classified in any of the previously mentioned groups, which is why they are listed independently by the European TSOs in MIGRATE project.

One of the reasons why new power oscillations occurred in the power system is due to decommissioning of synchronous generation and associated PSS controllers. This controllers are responsible for damping oscillations in a traditional power grid. However, synchronous generators are replaced by a PE interfaced generation, which introduces new controllers and control algorithms to the system. Interaction between newly introduced controllers and large synchronous machines can cause new oscillation modes in the system [14].

Reports on MIGRATE Project include a proposal of several solutions that have an ability to mitigate the previously mentioned systemic issues. Control structures and schemes that have an ability of improving rotor angle stability will be closely studied. The focus will be on various controllers linked together into a control structure, which will enable linking synchronous generation as well as PE generation and Flexible AC Transmission System (FACTS) devices into a power system. The problem that has risen with distributed power generation is that the behaviour of such technology is much harder to predict. Not only because of stochastic behaviour and unpredictable availability of natural resources, but also because of many smaller capacity generators which are all managed by independent entities. TSO have a hard time predicting whether everyone will decide to feed power produced to the grid or they want to consume it for their own needs. This becomes an even larger problem in remote locations, where the whole load compensation depends on a few stochastic generators. A concept has to be adopted, which can collect measurements from desired locations of the grid and on a very short time scale adjust operations of the power system. Explanation of components needed for a successful linking of different RES (WTs and solar PV) into a power system and still maintaining rotor angle stability is necessary for a completion of the project .

3.2. Wind Turbine Technologies

Distributed Generation (DG) has received a significant attention due to arising ecological issues around the world and increase in electricity demand. A conventional synchronous generation of energy is getting replaced by cleaner and more sustainable sources of energy. A renewable source of energy used in this project is represented by WTs, even though that there are many other sources of renewable energy available on the market, such as solar PV, battery storage and hydrogen technology. Those sources of energy are out of the scope of this project. WTs are the most cost-effective way of electricity generation of any available RES [15], since the rated output power of modern WTs can reach up to 10 MW. With the increasing interest and research in this source of energy, this number can increase significantly in the near future.

Type 1: Fixed speed induction generator (FSIG)-based WTs

WTs can either be a fixed or variable speed. Fixed speed WTs operate at constant speed, where electrical energy is generated by using Squirrel Cage Induction Generator (SCIG) and fed to the power grid through a coupling transformer 3.3 [16]. The downside of this technology is that the WT draws reactive power from the grid, which can be compensated with installation of a capacitor bank. In case that there are no reactive power compensators present, voltage fluctuations occur and line losses in the grid increase. Benefits of this technology are a simple concept and low production cost.
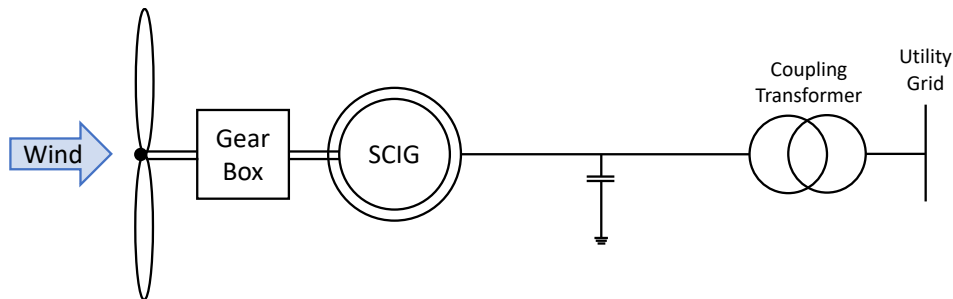
Figure 3.3: A schematic representation of a (FSIG)-based WT [12].

Type 2: Slip ring induction generator (SRIG) with variable rotor resistance-based WTs

This type is a partial or semi variable speed WT which uses a Wound Rotor Induction Generator (WRIG) directly coupled to the grid as shown in 3.4. A capacitor bank present has a function of reactive power compensation, while in series connected resistance with rotor winding of the generator determines the range of the variable speed [15]. A benefit of using a partial variable speed WT over a fixed speed WT is an improvement in energy conversion as well as reducing mechanical stress on turbine components, which lowers maintenance cost of the WT.
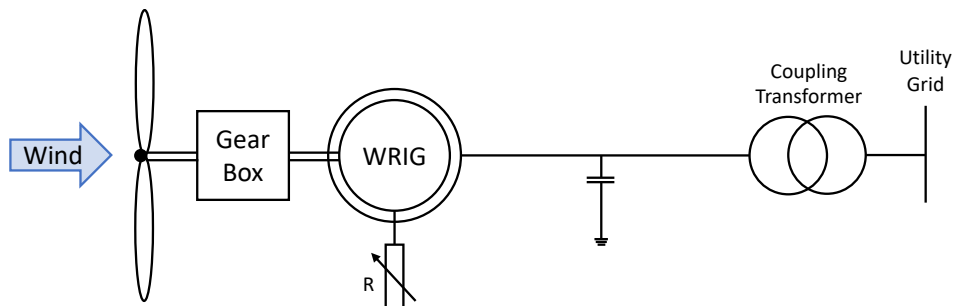
Figure 3.4: A schematic representation of a (SRIG)-based WT [12].

Type 3: Doubly-fed induction generator (DFIG)-based WTs

In Doubly-Fed Induction Generator (DFIG) concept, WT can either be connected directly to the grid through transformer or it can be coupled thought the use of a converter. The structure of the mentioned WT concept is shown in figure 3.5 [15]. Around 30% of nominal generator power can be fed to the grid through the converter and the rest is fed thought the transformer; hence higher power capture compared to fixed or semi variable

speed WTs is observed. Other benefits of using this type of technology is a decrease in mechanical losses, it allows a bidirectional power flow and an ability of islanded operation [16].
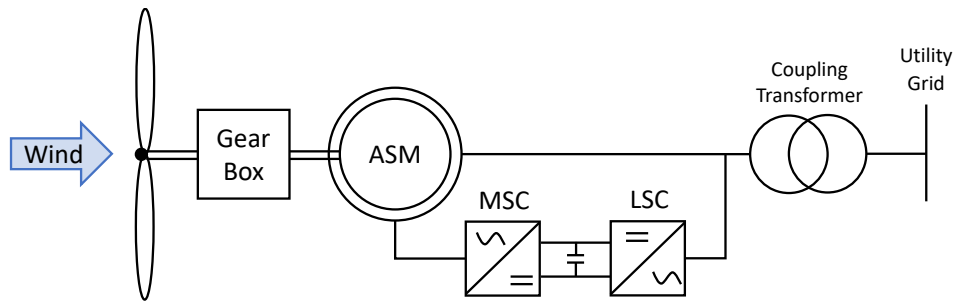
Figure 3.5: A schematic representation of a (DFIG)-based WT [12].

Type 4: Full-scale converter generator (FSCG)-based WTs

Variable speed WTs are a more recent development and are the most interesting concept for this project. They have an ability to capture 15% more energy compared to a constant speed WTs, where extraction of maximum power from the wind is possible by making use of an attached control system [15]. Mechanical power is generated by wind energy turning the blades of the WTs, where the higher wind speed will cause the blades to spin faster and generate more mechanical power. However, at some point the power output has to be limited at the fixed value with an increase in wind speed in order to protect the mechanical components of the WTs. The benefit of the variable speed WTs is that they have an ability to limit their power output by rotating the blades around their axis through pitch control. Mechanical power can then be converted into electrical power through the generator, which is eventually fed into the power grid. A Type 4 WT concept and a structure is shown in figure 3.6 [15]. By using Permanent Magnet Synchronous Generator (PMSG) generator in this concept, the gearbox can be removed from the structure, which will make it a direct-driven WTs. Direct-driven solutions are appropriate for offshore installation due to their benefits of robust and low maintenance WTs [12].
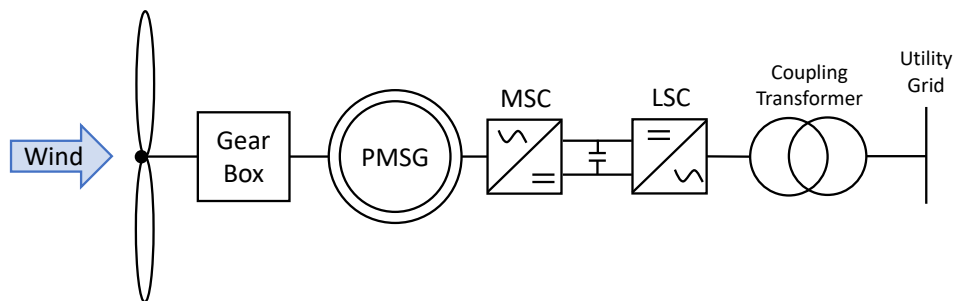
Figure 3.6: A schematic representation of a (FSCG)-based WT [12].

3.3. Control Strategies

A development of a power systems with mainly PE interfaced generation has been done so far in low and medium voltage grids. These systems are often called microgrids, which means that these grids can be isolated from the main grid and still maintain system stability. However, it is more difficult to provide stable operation in high voltage power grids when power is mainly provided by RES. This is due to the power ratings of the system, since they are much higher and behaviour is hardly predictable in case of any large disturbances [13]. In this project use of PE devices will be adopted in high voltage transmission grid, where synchronous generation is replaced by control strategies, more specifically grid-forming control and grid-following control. An advantage of a grid-forming controller is an ability to generate its own frequency and voltage, rather than observing parameter set points from the grid.

3.3.1. Voltage Source Converter Technology

Voltage Source Converter (VSC) behaves as a grid-forming controller in the system and it can be applied to High Voltage Direct Current (HVDC) systems, FACTS, solar PV and WTs. Voltage and current are both sinusoidal waves, which have to be transformed into a dg-reference frame for making control process possible. Typical control schemes in the system use Proportional Integral (PI) controllers, which have difficulties regulating sinusoidal waves from a VSC [17]. Transformation from a three-phase sinusoidal frame towards the dq-reference frame is done to make an effective use of vector control, which allows a controller to know the exact position of the rotor [18].

Clark Transformation

In AC power system, current and voltage have three phases (a, b and c), which are separated by 120°. Three phase current can be separated into two different and orthogonal currents, torque (i_α) and flux (i_β) current [18]. This transformation is useful since it eliminates one phase, however torque (i_α) and flux (i_β) components are still sinusoidal and PI controllers will still have difficulties controlling these variables. This transformation is called Clark Transformation. Current transformation equation is shown in 3.3 and voltage transformation is shown in 3.4 [17].

$$\begin{bmatrix} i_\alpha \\ i_\beta \end{bmatrix} = \frac{2}{3} \begin{bmatrix} 1 & -\frac{1}{2} & -\frac{1}{2} \\ 0 & -\sqrt{\frac{3}{2}} & \frac{\sqrt{3}}{2} \end{bmatrix} \begin{bmatrix} i_a \\ i_b \\ i_c \end{bmatrix} \tag{3.3}$$

$$\begin{bmatrix} v_\alpha \\ v_\beta \end{bmatrix} = \frac{2}{3} \begin{bmatrix} 1 & -\frac{1}{2} & -\frac{1}{2} \\ 0 & -\sqrt{\frac{3}{2}} & \frac{\sqrt{3}}{2} \end{bmatrix} \begin{bmatrix} v_a \\ v_b \\ v_c \end{bmatrix} \tag{3.4}$$

Park Transformation

Park transformation is applied to remove the AC part from the previously generated $\alpha\beta$ system, which is done through the use of a rotating reference frame, where a controller experiences the rotor's point of view. On the other hand, a controller would experience a rotating reference frame if looking from a stator side. A transformation is shown by an equation 3.5, while the matrices used in the equation are shown by an equation 3.6 [17]. A signal is converted into a DC signal, which allows controllers to effectively control PI and Proportional Integral Derivative (PID) control loops.

$$\begin{bmatrix} u_s^d \\ u_s^q \end{bmatrix} = \begin{bmatrix} T_{dq} \end{bmatrix} \begin{bmatrix} u_\alpha \\ u_\beta \end{bmatrix} = \begin{bmatrix} T_\theta \end{bmatrix} \begin{bmatrix} u_a \\ u_b \\ u_c \end{bmatrix} \tag{3.5}$$

$$\begin{bmatrix} T_{dq} \end{bmatrix} = \begin{bmatrix} cos(\theta) & sin(\theta) \\ -sin(\theta) & cos(\theta) \end{bmatrix}; \begin{bmatrix} T_\theta \end{bmatrix} = \frac{2}{3} \begin{bmatrix} cos(\theta) & cos(\theta - \frac{2\pi}{3}) & cos(\theta + \frac{2\pi}{3}) \\ -sin(\theta) & -sin(\theta - \frac{2\pi}{3}) & -sin(\theta + \frac{2\pi}{3}) \end{bmatrix} \tag{3.6}$$

The whole process of Clark-Park transformation is shown in 3.7, from a three phase system to ($i\alpha$) ($i\beta$) stationary reference frame and then to dq-rotating reference frame. Generated output signal then needs to be converted back to three phase signal, which is done by inverse Park and inverse Clark transformations.
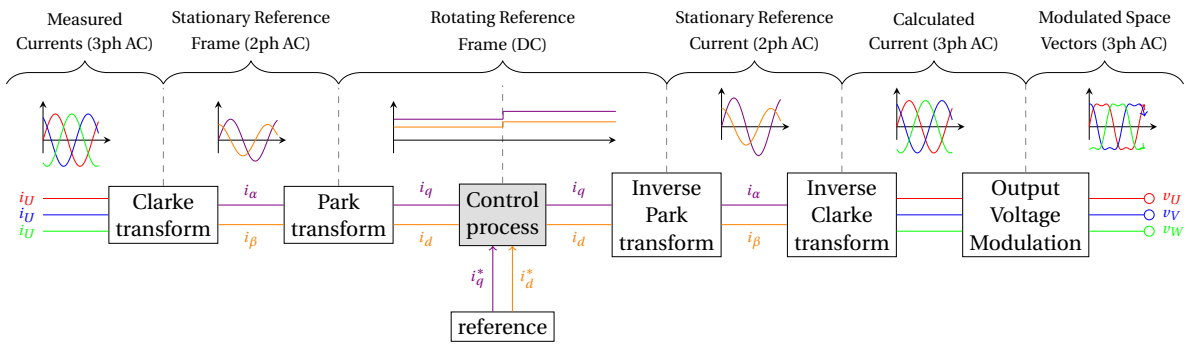
Figure 3.7: Clark-Park transformation [18]

3.3.2. Grid-Following Control

Grid-following control strategy is developed in a dg-reference frame, which allows decoupling of active and reactive current control [5]. This type of inverter controls the current injection based on voltage measurements at the terminal to meet the power set points. Power can be injected independent of voltage or frequency deviation at the terminal, which means that this strategy can also be a grid-feeding control [19]. Grid-feeding control is represented as an ideal current source in parallel with high impedance as shown in figure 3.8. Grid-supporting inverters can either be voltage source based or current source based and their task is to deliver active and reactive power setpoints to contribute to grid frequency and voltage.
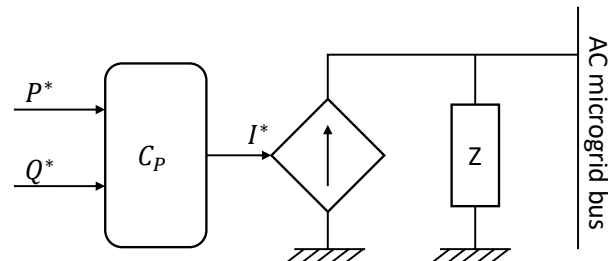
Figure 3.8: Grid-feeding control strategy [20].

Current Control

A conventional method applied in the power grid with high penetration of PE interfaced generation is current control. This method is classified as a grid-following control, since like mentioned before it receives set points from the grid. Unlike in some grid-forming controls, current controller indirectly regulates active and reactive power through current components of a dq-reference frame [5]. PI controller is used to regulate the decoupled currents and performance highly depends on PI parameters as well as tuning of controller parameters. Current controller takes advantage of Phase-Locked Loop (PLL) strategy, which could be a source of stability issues in the system. Some grid-forming control techniques explained later will eliminate the use of PLL to prevent an occurrence of related issues.

This kind of control is usually implemented with conventional Type 4 WTs or it was at least previously implemented. There was no reason to implement grid-forming technology with WTs when there was just a fraction of PE penetration in the grid. WTs using this type of control have a supporting role in the grid and they are not able to operate in a stand alone operation. This control is required to operate with some other generation source, which have some sort of stabilizing effect on the system. It can either provide inertia from rotating masses or some other stabilizing effect provided by control functions. Those kind of control functions will be examined under grid-forming control strategies.

3.3.3. Grid-Forming Control

Grid-forming control has an ability of forming constant frequency and voltage, independent of the system set points. When more grid-forming controllers are present in the grid, a synchronizing signal provided by a central controller is required in order for the controllers not to work against each other. Signals are synchronized by making use of Global Positioning System (GPS) system, which stamps signals according to when the event happened rather than when the signal was received. GPS helps reducing the effect of time delay on accuracy of signals and mitigates issues that might occur with making use of PMUs. If measurements provided by PMUs are not stamped correctly, an introduction of new oscillations can occur in the system and even further reduction of stability limits. A grid-forming control strategy is shown in figure 3.9 [20]. From this figure is visible that an ideal voltage source with low-output impedance represent the controller with forming ability.

Direct Power Control

Direct Power Control (DPC) is a concept with forming ability, which directly regulates the active and reactive power [5]. Sliding Mode Control (SMC) scheme can enhance DPC strategy by calculating the converter voltage, which eliminates active and reactive power errors. Furthermore, transient performance of a controller is enhanced by controller simplified system design. SVM enables constant switching frequency and benefits of using such technology is that transformations are not needed. This enhances transient performance even further as well as steady-state current harmonic spectra [21]. Another method of improving DPC
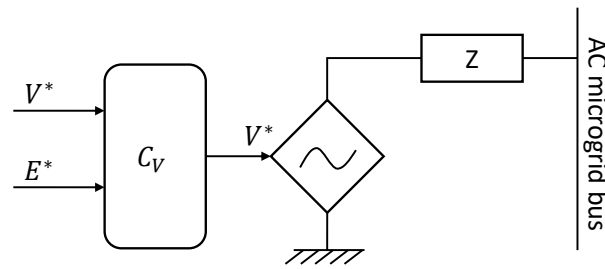
Figure 3.9: Grid-forming control strategy [20].

is by eliminating the PLL and benefits of doing so were already discussed for a current controller. A virtual phase angle adopts functionality of a PLL, which is synchronization of generators and converters in the power grid and accurate phase and frequency detection [22]. The stability of Voltage Source Inverter (VSI) can be compromised due to a negative slope of resistance where increase in voltage causes decrease in current flowing through the inverter. Effect on stability can be improved by decreasing the bandwidth of the PLL, however a dynamic performance could be compromised. Furthermore, weak grids present another stability challenge for VSI, since rated real power can be injected to a weak grid only by VSI injecting reactive power.

Virtual Oscillator Control

Main goal of implementing Virtual Oscillator Control (VOC) is to synchronize and control inverters in the power system to mimic the dynamics of a nonlinear oscillator [6]. This is especially beneficial in microgrids and distributed AC highly RES penetrated power systems. Control system does not require communication to synchronize voltage output for inverters and sharing of load power proportional to their power ratings. Besides being robust, VOC is also a modular control strategy, which means that it is independent of the number of inverters. Furthermore, this method enhances the stability independent of load variations [6], which makes it a very appealing option for designing a grid with primarily renewable sources of energy.

Direct Voltage Control

DVC can act as a voltage source and can cover a demand as long as it is within wind turbine's rated power capacity limits [7]. This control method is especially superior in islanded operation, because it has an ability of keeping transient overvoltages in acceptable limits. Besides, this methods is becoming significantly appealing in grids with high penetration of RES. Overvoltage can cause severe damage to other components in the system. Directly controlling voltage ensures that levels stay in acceptable limits [23], rather than controlling voltage through reactive current injection.

Voltage control can be decoupled, where voltage injected in d-axis has an impact on voltage of the grid and voltage injected in q-axis controls active power flow [23]. A conventional circuit voltage control applied to WT control is Maximum Power Point Tracking (MPPT), however such control cannot be used in islanded power systems. Alternative option of a speed-power controller is used to enhance blackstart and restoration capability [7], however this solution will not be pursued further in the project.

Virtual Synchronous Machine

With European initiative to increase penetration of RES above 50% of overall power generation, the existing control strategies are not able to provide stable operating condition. VSM method can be implemented in cases of more than 50% penetration due to similar behaviour to conventional synchronous machines. This control technique integrates swing equation similar to the one described for a synchronous machine. Swing equation is integrated into a control loops of the inverter and imitates the power angle relationship [5]. Similarly to a synchronous machines, this method enhances system inertia, which is visible in a system Rate of Change of Frequency (ROCOF). Mathematical representation of ROCOF is $\frac{df}{dt}$, which tells how much system frequency drops over a certain period of time. The larger drop of frequency over a shorter period of time suggests poor system inertia and consequently system stability might be difficult to maintain.

This method can also provide synchronizing power and voltage reference to other VSMs and generators, however it can introduce new oscillatory modes to the system. This method will be further explored in this project and its abilities will be tested in the grid with 80% penetration of PE devices.

3.4. Wide Area Monitoring for Improved Controllability

Rapid development of new sources of electricity and a higher participation of prosumers in the power grid has a significant technological and economical effect. Lack of transmission capacity, transfer of large amount of power, number of dispersed electricity producers and consequently more dynamic market are just some of the challenges that occurred recently with new developments. Increasing a transfer capacity with an installation of more transmission lines might not be the most feasible option, which is calling for technologically more advanced solutions. Flow of electricity used to be unidirectional, where power flow occurred from a large generation plant via transmission and distribution towards large and domestic consumers. In contrary to unidirectional, a power flow has become bidirectional in modern power girds with installation of RES. Energy can flow from a small prosumer to the grid and is consumed by a large factory. A prosumer is defined as someone who participates in consumption as well as production of electrical energy. Bidirectional power flow introduces new challenges to the system control and protection and forces power system to operate closer to their stability limits [24].

The overall demand can be predicted by system operators by following previous patterns and by compensating demand dictated by day-ahead market. In case that system operators observe that a large amount of power will be required at a different location as usual, they can prepare in advance to cover that specific load. Looking from the other perspective, costumers can buy a certain amount of energy in day-ahead market which will balance their demand in the next day. This has a positive effect on reducing the possibility of any congestion occurrence in transmission or distribution grid. Talking about fundamental energy market processes, bidding in intraday market happens on a shorter time scale, which further helps with dedicating power towards highly loaded areas. In case of surplus of electricity in the system, price of energy decreases which motivates consumers to buy electricity. On the other hand, when there is lack of power in the system, price increases and motivates consumers not to use extra power. This is how market participation and price variation can help with stabilizing the system with increasing amount of producers and consumers.

Low frequency oscillations are gaining attention in the modern power grid with massive integration of RES sources. Small-signal stability problems can cause significant issues due to poorly damped oscillations in the system. There is a significant increase in implementation of power electronic devices to the power grid due to high penetration of renewable energy sources, since PE devices make coupling to the grid possible. Large percentage of PE devices in the system create low-frequency oscillations, which can in the worst case lead to a system split or even a blackout [8]. Interarea oscillations are a global phenomena, which is a reason why local control like PSS does not have an effect in damping these oscillations.

There has been a rising interest in technology, which will enable a successful damping of critical OMs. A mitigation proposed and recently heavily researched is WAMS since it has an ability of collecting signals from different parts of the system to improve the overall grid stability. Signals are obtained from synchrophasor measurements provided by PMU, which are strategically dispersed around the power grid and located on generator busses [25]. It is required that all measurements are time stamped, which is achieved by synchronising all phasors using GPS. Signals provided by PMUs have to guarantee a certain degree of observability, which means that internal state of the system is well represented. Number of PMUs installed in the system should be minimized to preserve the investment cost and keeping the amount of data low, while not jeopardizing the observability of the system. WAMS replaces the existing SCADA system, since it provides better insight in highly dynamic behaviour in the power system. Furthermore, PMU devices provide more accurate signals for easier detection of power oscillations, which is very beneficial for designing damping controllers.

Small signal stability can be enhanced using either quasi-decentralized, centralized or hierarchical control structure [26] [27]. Decentralized control is where only local control is applied. A local controller receives and sends a signal to the same subsystem. Similarly, quasi-decentralized control receives some signals from other subsystems, but majority of signals are still controlled locally. This system does perform better than a decentralized control in damping interarea oscillations, however a use of a centralized control is necessary for an effective damping. Centralized control takes advantage of WAMS; this control strategy collects input signal from remote locations and feeds signals to other most appropriate generators. This is an effective strategy, however this technique does not consider local controllers like PSS and AVR. Another disadvantage of a centralized control strategy is that in case of communication failure, control strategy cannot receive and send signals anymore, which might lead to cascading outages. Hierarchical control scheme uses WAMS characteristics and combines it with local controllers. In this strategy, signal are collected from remote locations and combined with local signals.

3.4.1. Identification of Oscillation Modes

This analysis is performed to either evaluate the state of the uncontrolled system or evaluate an effectiveness of control methods on stabilizing the grid. The analyses can determine dominant modes of oscillation, damping ratio and eigenvalues. These methods allow evaluating and comparing the effects of control methods in the system. It can be determined whether a control strategy was able to only damp the desired OM and to enhance the stability or it causes new issues in the system and brings it even closer to its stability limits. Identification techniques mentioned in the literature will be listed and explained in this section, even though they will not all be used while identifying modes of oscillation during the projects. It is important to know all the existing options, so the most applicable technique can be chosen for an individual projects.

Modal Analysis (Eigenvalue Analysis)

A state space representation of a power system is defined in (3.7) [28].

$$\Delta \dot{x} = A\Delta x + B\Delta u \tag{3.7}$$
$$\Delta y = C\Delta x$$

where $A \in R^{nxn}$ is state matrix, $B \in R^{nxm}$ is input matrix and $C \in R^{pxn}$ is an output matrix. Eigenvalues representing different modes of oscillations are computed from a matrix A.

Modal analysis is a very useful method of identifying modes of oscillation and finding critical OMs [8]. Those modes are crucial for identifying the stability limits of the system. Poorly damped modes of oscillation represent either local oscillations or inter-area oscillations, which can explain the behaviour of the system or individual generators. Eigenvalues, defined in 3.8 determine the relationship between modes and system parameters [11].

$$\lambda_k = \sigma_k \pm j\omega_k \tag{3.8}$$

where σ_k is a real part and ω_k is an imaginary part.

Frequency with which a specific mode is oscillating is derived from the imaginary part of the eigenvalue as shown by equation 3.9 [11]:

$$f = \frac{\omega_k}{2\pi} \tag{3.9}$$

where ω_k is the imaginary part of the eigenvalue described in 3.8.

A system is classified as unstable in case one of the modes has a positive real part (σ_k). Systems which have all eigenvalues with only negative real part (σ_k) are classified as asymptotically stable. Damping ratio is computed using 3.10 [11].

$$\zeta_k = \frac{-\sigma_k}{\sqrt{(\sigma_k)^2 + (\omega_k)^2}}; \zeta_k \leq \zeta_{th} \tag{3.10}$$

Right eigenvector (ϕ) associated to λ_k shows the activity of the state variables. The magnitude shows the extent of the activity, while the angle shows the phase displacement; great way of visualizing different modes of oscillation. The left eigenvector (ψ) associated to λ_k can be weighted by the right eigenvector (ϕ), which is called a participation factor, shown in 3.11 [11]. This allows getting a value independent of unit and scaling, where a larger number of the participation factor (value close to a number one) indicates a parameter, which is a good a candidate to be controlled to enhance stability.

$$p_{ki} = \phi_{ki}\psi_{ik} \tag{3.11}$$

Prony Analysis

Prony analysis is another method for estimating frequency, damping ratio and phase of a signal. Prony analysis is performed on results obtained from time-domain simulations and only a specific time window of a signal is applicable for analysis. Appropriate time window is after the disturbance occurs and before oscillations stabilize, which is called a ring-down period. The analysis can also be done in the ring-up period and those are the only two scenarios which would give correct results. Since the analysis is done on the time-domain simulations, no additional information is required for a successful implementation [8]. Information

is read from a signal output labeled as $y(k)$ in equation 3.12 [29]:

$$y(k) = \sum_{i=1}^{L} A_i e^{\sigma_i t} cos(2\pi f_i t + \theta_i) \qquad k = 0, 1, 2, ..., N-1 \tag{3.12}$$

Parameters identified by Prony analysis are amplitude (A_i), phase (θ), frequency (f) and damping ratio (σ) and they should not very within the time window examined to obtain reliable results. Previously shown equation can be rewritten as shown by 3.13 by applying Euler's rule, where k is the sample index and L is the model order [29]:

$$y(k) = \sum_{i=1}^{L} A_i e^{\sigma_i t} e^{\lambda_i k} \qquad k = 0, 1, 2, ..., N-1 \tag{3.13}$$

There should be as little noise as possible in the signal output in order to obtain accurate previously mentioned parameters. Presence of a noise might compromise the accuracy of this method, which is why an analysis called Kalman filter has been proposed in the literature. This is due to its ability to bridge main drawbacks of Prony analysis and its able to deliver accurate results even with presence of strong noises in the signal.

Kalman Filter (KF)

Online estimation of electromechanical oscillations can be done by using Kalman filter (KF). A benefit of this technique is that feasible results are delivered even when strong noise is present in measurements [8]. It has an ability of giving very accurate predictions in very short time, which is why it is getting increasingly used in wide-area damping systems.

A model used for applying Kalman filter is formulated by equation 3.14 [29], with L number of time-varying coefficients a_i:

$$\hat{y}(k|k-1) = \sum_{i=1}^{L} a_i(k) y(k-1) \tag{3.14}$$

where $\hat{y}(k|k-1)$ is the predicted value of the output signal $y(k)$. Like mentioned before, in many cases the output signal $y(k)$ contains measurement noise, which is added to the formulation as shown in equation 3.15. This noise is presented as an error $\epsilon(k)$ defined by equation 3.16:

$$y(k|k-1) = \sum_{i=1}^{L} a_i(k) Y(k-1) - \epsilon(k) \tag{3.15}$$

$$\epsilon(k) = \hat{y}(k|k-1) - y(k) \tag{3.16}$$

The Kalman filter is then used in order to optimize the coefficients to minimize the sum of the squared prediction error, which is defined by the equation 3.17:

$$J = \min_{a_i} \sum \epsilon^T \epsilon = \min_{a_i} (\hat{y}(k|k-1) - y(k))^2 \tag{3.17}$$

This section gives an explanation about what is the main idea of the Kalman filter and what is this method trying to accomplish, however more details about this method can be fund in the reference paper [29], where a summary of detailed Kalman filter equations and a list of variable definitions is further explained.

3.4.2. Input and Output Signal Selection

Controllability/Observability Measure

Signals should be selected appropriately to have an ability to damp oscillation modes, which occur due to high penetration of PE devices. A state space representation of a power system is defined in (3.7) [28]. A first method of control loops selection is based on geometric measures of controllability and observability [30] [31]. The matrix A has n eigenvalues λ_i for $i = 1, 2, ..., n$). Right eigenvector e_i and left eigenvector f_i are associated with previously mentioned eigenvalues. Left and right eigenvectors are orthogonal $(e_i f_i = 1)$, so the

geometric measure of controllability m_{ci} is defined in (3.18). Similarly, geometric measure of observability m_{oi} is defined in (3.19).

$$m_{ci}(k) = cos(\alpha(f_i, b_k)) = \frac{|b_k^T f_i|}{\|f_i\| \|b_k\|} \tag{3.18}$$

$$m_{oi}(l) = cos(\theta(c_l^T, e_i)) = \frac{|c_l e_i|}{\|e_i\| \|c_l\|} \tag{3.19}$$

where b_k is kth column of B, c_l is ith row of C, $\alpha(f_i, b_k)$ is angle between the output vector b_k and the right eigenvector f_i and $\alpha(c_l, e_i)$ is angle between the output vector c_l and the right eigenvector e_i.

The joint measure is shown in (3.20), and the closer the angle between observability and controllability is to 90°, less controllable or observable is the mode. Furthermore, the larger the joint measure ($m_{coi}(k, l)$) - closer to 1, control loop is more effective in damping a specific mode [32].

$$m_{coi}(k, l) = m_{ci}(k) m_{co}(l) \tag{3.20}$$

Residues Method

This method is appropriate for selecting signals from remote locations. A transfer function associated to 3.7 is represented in 3.21.

$$G(S) = \frac{y(s)}{u(s)} = C(sI - A)^{-1} B = \sum_{i=1}^{n} \frac{R_i}{s - \lambda_i} \tag{3.21}$$

$$R_i = C e_i f_i^H B \tag{3.22}$$

where R_i is a residue matrix, C is an output matrix, B is an input matrix, e_i is a right eigenvector and f_i^H is the complex conjugate of the left eigenvector [31].

Residue consists of a magnitude and phase angle, while only magnitude is considered when selecting the best signal. Maximum value of a residue has the best ability to damp the desired oscillation mode.

$$m_{coi} = |\delta_i| \|R_i\|_F = |\delta_i| \|C e_i f_i^H B\|_F \tag{3.23}$$

$$\delta_i = \sum_{j=1}^{n} (\lambda_i - \lambda_j)$$

Controllability measure m_{ci} (3.24) and observability measure m_{oi} (3.25) are deducted from a joint controllability/observability measure m_{coi} given in 3.23 [28].

$$m_{ci} = |\delta_i| (f_i^H B B^T f_i)^{1/2} \tag{3.24}$$

$$m_{oi} = |\delta_i| (e_i^H C^T C e_i)^{1/2} \tag{3.25}$$

Hankel Singular Value (HSV) Method

Equation 3.7 can also be represented by Lyapunov equations: (3.26 and 3.27) [32]

$$AP + PA^T + BB^T = 0 \tag{3.26}$$

$$A^T Q + QA + C^T C = 0 \tag{3.27}$$

are such that P = Q = diag $(\sigma_1, \sigma_2, ..., \sigma_n)$ where $\sigma_1 \geq \sigma_2 \geq, ..., \geq \sigma_n$ and P and Q represent the controllability and observability Gramians [31].

Interactions between specific modes and input-output control loop are determined by Hankel Singular Values (σi). The highest value of Hankel Singular Value (HSV) is preferred, since high measures provide the best signal to damp the oscillation modes [31]. On the other hand, when using a wide-area loop, large joint controllability and observability measures are needed for some modes and minimal controllability and observability measures for the remaining ones [32].

After the HSV values are found for individual inputs and outputs, the total contribution for a specific mode is determined by using equation 3.28 [31]. Highest value of the signal has been considered as potential feedback signal.

$$C_k = \sum_{i=1}^{n} \sigma_i^2 p_i(\lambda_k) \tag{3.28}$$

where σ_i is a Hankel value calculated for the state variable, p_i is the participation factor and λ_k is the desired mode k.

3.4.3. Central Controller Design of Hierarchical Control

This section explains possible methods or approaches of designing a central controller in WAMS. Central controller receives a signal from PMUs, which are providing synchrophasor measurements to a controller. These signals are then adjusted in a controller and created outputs are combined with other local controllers, such as PSS and AVR, before being fed to the generators. Hierarchical control strategy has a benefit of collecting signals from remote buses and combining them with local control to effectively stabilize the system as well as damping interarea oscillations in the power grid.

Important to note is that the method that will be used for input and output signal selection in this project will be the controllability and observability measure. In the following section, there will be different approaches explained with the design of a damping controller and inputs and outputs will be only determined with one method. Out of all damping controller approaches explained in the following section, only the wide-are supplementary damping controller will be used in this project, however it is important to list and explain some alternatives. One can by reading this section notice that the design of all proposed techniques is very similar and every approach includes a washout filter, one or more lead/ lag compensators and a gain. The design of the damping controller will be in details explained in Chapter 5.

Linear Quadratic Regulator (LQR)

Linear Quadratic Regulator (LQR) method in one of the techniques used to develop a centralized controller to damp interarea oscillations. LQR is connected to the system similarly to WASDC, which is shown in 3.10. The only difference among these two techniques is the overall structure of the controller, but not the way that the output signal is combined with local signals. It is worth noticing that remote signals provided by PMUs serve as an input to a central controller and an output of the central controller is then combined with local controllers. In the conventional power grid, PSS controllers focused only on stability of the local modes. Presence of LQR in the system improves damping of the interarea oscillation compared to only having local (PSS) control in the system [33]. Furthermore, highest damping in the system is achieved when more generators receive signals form LQR controller. The damping ratio achieved by controlling more generators with highest geometric measures of controllability is much higher compared to when only a few generators are controlled by LQR [33]. LQR method is able to improve damping in the system even when common disturbances occur, which shows an improvement over local controllers.

A way of assessing the effect of having a LQR central controller in the system is achieved by modal analysis. Eigenvalues, frequency and damping ratio results should be improved over results where only local control was deployed. A performance of a central controller is most effective in the operating condition, which was used for designing a controller [33]. When various events, such as faults or line tripping, are introduced, the damping is not as successful anymore. Common events that can occur in the system should be considered while designing a controller to maintain high efficiency in case of a disturbance.

Wide-Area Supplementary Damping Controller (WASDC)
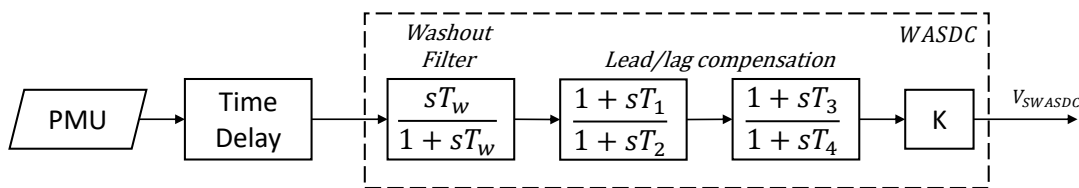
Figure 3.10: Block diagram of a WASDC [34].

WASDC is another approach of damping interarea oscillations and a controller consist of a washout filter, load/lag compensation and a gain block as shown in figure 3.10. Besides providing a damping control to synchronous generators, this approach can provide supplementary damping control to HVDC links, FACTS devices or any RES. Configuration of a controller used in WADC is shown in figure 3.11 [34] and WASDC with respect to PSS and AVR.
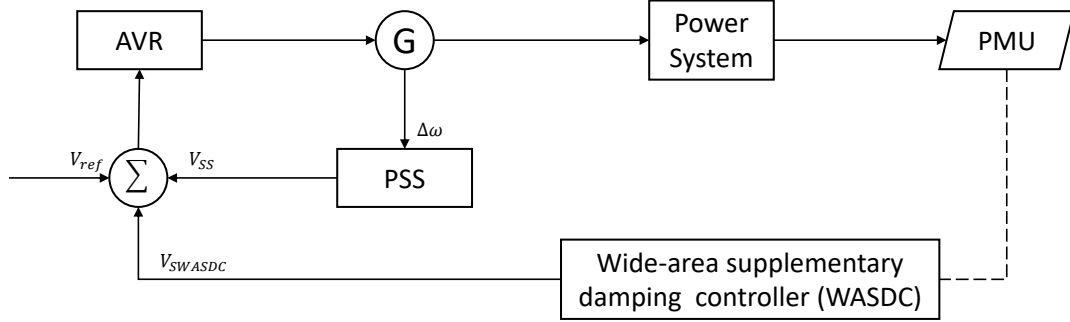
Figure 3.11: Implementation of a (WADC) to a control structure of a generator [34].

A performance of WASDC method can be further enhanced by installing a wind power plant to the power system. There is a possibility to directly control wind power plants with signals from centralized controllers or having an independent controller on a wind power plant. Wind turbines are a useful source of energy, which can improve damping in the system with increasing their power input. In case that the wind turbine power park is not directly controlled by WASDC, damping of a critical oscillation mode improves slightly, however a probability of poorly damped oscillations is still very high [34]. An improvement in damping of critical oscillation modes can be achieved when input signals and a location of WASDC were determined based on observability and controllability indexes. An improvement in damping ratio can be expected for all penetration levels of wind turbine power output, even when a wind turbine park is not controlled directly [34]. These findings makes such a solution very interesting for this project, where 80% of generation will be from wind energy instead of a single WT.

Power Oscillator Damping
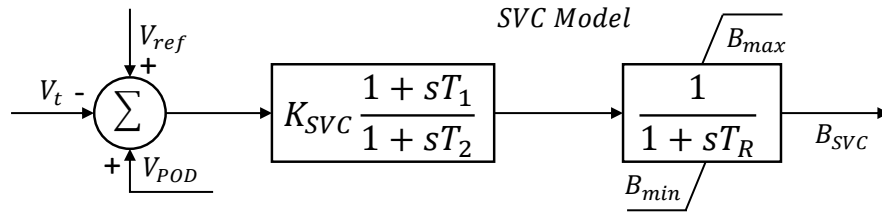
Figure 3.12: Static VAR Compensator (SVC) model [31].

Static VAR Compensator (SVC) model is shown in 3.12, where V_{pod} signal is received from Power Oscillation Damping (POD) model shown in 3.13 and combined with a reference voltage signal and V_t.

Installation of FACTS devices in a modern power grid has become a feasible option for damping interarea oscillations. These devices can be combined with POD controllers, which have an ability of damping low-frequency modes [31]. In this case, a POD serves as a central controller, which sends their signal to FACTS devices and a structure of POD connected to SVC is shown in figures 3.12 and 3.13 [31]. Instead of a FACTS device, a signal from a POD can be fed into a synchronous generator or a source of renewable energy. A controller consists of a gain, washout block and lead/lag block as represented by equation 3.29.

$$H(s) = K_w \left(\frac{sT_w}{sT_w + 1} \right) \left(\frac{sT_{lead} + 1}{sT_{lag} + 1} \right)^m \tag{3.29}$$

A washout block is present to guarantee a zero POD output in a steady-state, while gain dictates the amount of damping by POD. To make POD more effective and less likely to experience any failures, appropriate signal should be selected for the input [35]. It is recommended to only use a local signal, so the communication costs

or delays could be avoided. Most importantly, a balance has to be found between saving communication costs and receiving appropriate signals.

$$POD\ Model$$

$$\text{Stabilizing Signal} \longrightarrow \boxed{K_{POD} \times \frac{sT_w}{1 + sT_w} \times \left(\frac{1 + sT_{lead}}{1 + sT_{lag}}\right)^m \times \frac{1}{1 + sT_m}} \longrightarrow V_{POD}$$
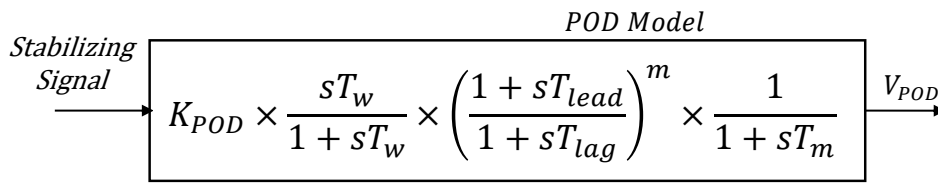
Figure 3.13: Power Oscillator Damping (POD) model [31].

3.4.4. Hardware Means of Oscillation Damping

Controlling synchronous generators and sources of renewable energy in a power grid is a strategy that can help stabilizing grid and damp low-frequency oscillations. However, there are other hardware means and approaches which can help with mitigating oscillation issues in the system. More precisely, these approaches are FACTS devices and HVDC systems. A decision to add additional hardware to the system has to be properly justified, because adding new components and installing new lines is a significant financial investment.

Flexible AC Transmission Systems (FACTS)

FACTS consist of controllers, which are able to control parameters to increase stability in the system. These devices can either be stand alone or they can be controlled in a similar manner as synchronous generators or RES [36]. They can be either classified as shunt, series or shunt-series FACTS. Shunt FACTS devices have the ability to supply or consume reactive power by injecting current to the system and they are able to supply or consume reactive power in case whn injected current and line voltage are in phase. Examples of shunt FACTS devices are the SVC and the Static Synchronous Compensator (STATCOM).

On the other hand, series FACTS can provide or consume reactive power in case injected voltage is in phase with line current. Some of the series controllers listed are the Thyristor Controlled Series Capacitor (TCSC) and the Static Synchronous Series Compensator (SSSC). Shunt-series FACTS consists of series and shunt controllers and are able to compensate reactive power and controlled active power flow interchange. An example of a combined controller is Unified Power Flow Controller (UPFC).

The STATCOM is able to more efficiently provide voltage support compared to SVC [36]. Reactive power generation or consumption is done within the STATCOM itself, which enables a generation of synchronous voltage at its terminals. Since it can generate voltage on its own, it has an ability of controlling its capacitive and inductive current. Reactive power is injected by STATCOM, when bus voltage drops below the predefined value. In that case the STATCOM absorbs leading current and is able to increase voltage; acts as a capacitor. Inductive behaviour is observed when voltage is above the reference and the STATCOM has to consume the lagging current; hence reactive power is consumed from the grid.

$$u \longrightarrow \sum \longrightarrow \boxed{\frac{K_r}{1 + sT_r}} \longrightarrow i_{SH}$$
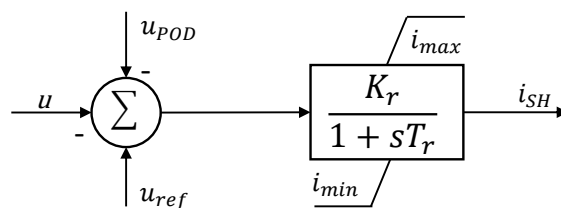
Figure 3.14: Static Synchronous Compensator (STATCOM) model [36].

The TCSC is able to compensate transmission line impedance since it operates as a series controlled resistance. A benefit of having a TCSC in the system is its ability to compensate a larger load due to fast switching of the controller. Another important aspect is its ability to increase damping and in case of contingency it can also make power flow adjustments. With those adjustments it can keep the power flow inside the physical limits [36]. This device can also control active power flow, it can enhance the rotor angle stability and it can limit the short-circuit current.
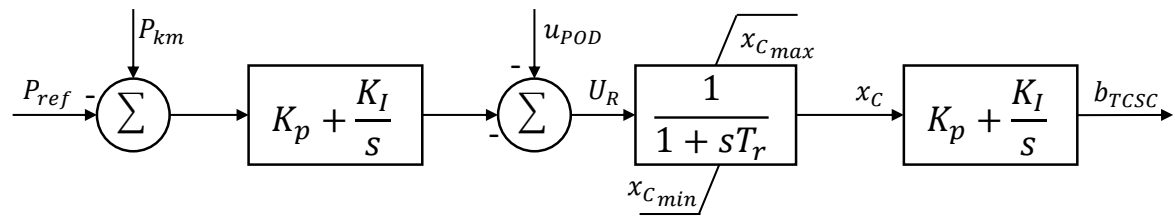
Figure 3.15: Thyristor Controlled Series Capacitor (TCSC) model [36].

High Voltage Direct Current (HVDC) Transmission

HVDC links can further improve damping of oscillation modes in the power grid. This technique enhances small signal stability in the system with massive integration of WTs to the power grid. Advantages of connecting a WT farm to the power grid with the HVDC transmission are the ability of keeping the rated power very high, minimizing voltage drops and minimizing the cost of reactive power supply [37]. There are different types of WTs commonly used in the power system, which can be connected to the grid with HVDC links. Possible WTs used in a modern power grid are DFIG, SCIG and PMSG, which are coupled to the grid via High Voltage Alternating Current (HVAC) or HVDC transmission. Which WT technology in combination with HVDC provides the best damping control to the grid can be determined based on eigenvalue analysis and time domain analysis. Which WT technology is used for a design depends on its advantages and drawbacks.

PMSG WT has the highest ability of enhancing system stability based on its damping potential; PMSG has the highest damping among all WT technologies when using HVAC or when couple to the grid with power electronic devices. The occurrence of oscillatory modes is less likely when PMSG is connected to the grid. On the other hand, when using DFIG method, there is a possibility that a frequency below 3% will occur, which indicates a local mode of oscillation. When SCIG is used, a low-frequency oscillation can occur (below 0.7%), which can indicate an occurrence of a global mode of oscillation. DFIG and PMSG have a high ability of recovering voltage back to there nominal values shortly after the disturbance, while SCIG has more difficulties controlling voltage drop in case of an event [37]. This can occur due to limitations of this method in providing reactive power support in the system. This drawback can be solved by means of connecting a capacitor bank before a step-up transformer.

Performance of WT technologies can be improved by replacing HVAC transmission with previously mentioned HVDC transmission, which should improve damping of critical modes. Some other advantages of HVDC are its ability of keeping high rated power of the converter, minimizing the voltage drop and minimizing the cost of a reactive power supply [37]. However, connecting a large wind turbine park can causes an occurrence of new OMs in the system. Nevertheless, HVDC link is able to enhance small-signal stability and it offers a possible solution for future power trends.

3.5. NextGen GridOps Knowledge Framework

This section gives an introduction about NextGen GridOps Framework and a more detailed description will be given in the section about knowledge utilization. The main connection of such a framework to this project is to enable a real world implementation of information developed throughout an extensive research in the field of massive penetration of RES. Findings that will allow integration of RES devices to the existing grid as well as techniques that will satisfy stability limits of the grid with 100% PE interfaced generation have to be eventually put in practice to justify the effort. These technologies and solutions, developed in response to the introduction of new regulations, have been proposed with an intend of preserving the environment for future generation and not compromising the security of supply. DNV came to a conclusion that due to a complexity of the problem it would be beneficial to create a knowledge framework, which will allow to put such information into fruition and it will also enable better consulting to their clients. It will make them stand out due to incorporation of modern solutions as well as helping society by developing best possible solutions.

There has been a lot of research done about the impacts of renewable sources on the power grid in recent years, however knowledge gained is fragmented and scattered among different sources. When a specific piece of information is needed, it is hard to find required information, difficult to know whether this solutions has already been developed, is information found up to date or how valuable is a certain piece of information.

All these issues are solved by storing and collecting information in a knowledge pool, such as a framework proposed by DNV. For the framework to be exploited to the fullest, employees have to be motivated to use it and to update previously implemented information. NextGen GridOps Framework will also serve as an overview of what has already been researched and developed regarding the future grid operations, which will motivate a development of new services or solutions for any identified gaps. It will allow DNV to propose new solutions in areas, where clients didn't even think they needed an improvement.

Objective of the framework is twofold. Firstly, the proposed framework can serve as a learning loop and knowledge sharing among colleagues in the company. The intent of a framework is to have all recent developments and regulations already stored in the framework, so DNV employees have access to organized information with corresponding links to other relevant information. Secondly, this framework serves as a project accelerator for any business related developments. The framework will allow much faster and more efficient consultancy, which will increase DNV's value on the market. More information implemented will make work easier, since information necessary for project development will be found in the framework.
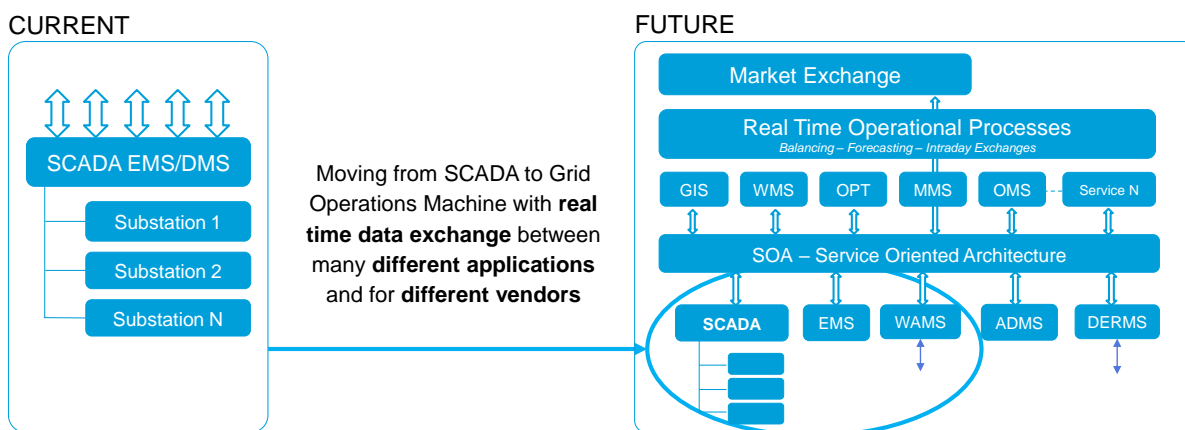
Figure 3.16: Overview of complexity of future system operations.

An overview of complexity of future grid operations is illustrated in 3.16. An intent of showing this figure is to highlight the complexity of the future grid operations and to serve as a motivator for developing a tool like NextGen GridOps Framework. A figure shows a collection of applications which will have to be considered in the future operations and an increase in complexity and amount of data exchanged is expected. NextGen GridOps Framework therefore serves as a collection of information, procedures, implementation methodologies, roadmaps, regulations, standards and it is developed to tackle future grid operations. Development of this framework has been identified by DNV is one of the priorities of their development plan, taking into consideration that the existing way of thinking and operating the grid will not satisfy the future needs and expectations of the society. NextGen GridOps Framework will play a vital role in developing solutions on larger scales, such as considering many applications and organizing data among them in real time. On the other hand, the framework can also help with applying very specific and technical methodologies, such as damping of low-frequency oscillations which will prove useful during development of new projects and solutions.

A figure 3.16 represents the transition which will happen in the near future from grid operations point of view. An existing SCADA and associated Energy Management System (EMS) will become a small part of more complex structure, with participation of many other applications and one of them is also WAMS. Current system operation is done by help of SCADA and EMS, which perform monitoring, controlling and protection of the existing power grid. SCADA collects measurement in the seconds time domain, which was in the conventional power grid enough to provide satisfactory insight about stability of the system. However, SCADA is no longer able to provide required insight into the power grid due highly dynamic processes and new actors in the power grid. It is becoming very challenging for system operators to successfully monitor and control the evolving power grid with existing solutions.

The transition towards more renewable generation of electrical energy requires a transition from SCADA and EMS towards Grid Operations Machine, shown in figure 3.16. DNV identified a structure of Service Oriented Architecture (SOA), which includes applications, processes and market exchange in the future grid operations. The biggest challenge for the framework will be the real time data exchange between many different

applications and for different vendors. There will be an increase in data and complexity with addition of newly developed applications, multi-vendors and multi-contracts. Seamless interaction between grid operation applications will have to be provided with near-real time data exchanges within the IT for OT grid operations system architecture.

3.6. Scientific Contribution

The main focus of this Master's Thesis Project is investigating whether the current practice of selective damping control is an effective method in power system with share of PE devices above 50%. It has been proven that WAMS with corresponding PMUs and WADCs have been a successful method in conventional power system with mainly synchronous generators. It will be studied whether the current practices of wide-area damping control with a single output are still effective in highly penetrated system with 80% of RES. Furthermore, three input of the WADCs will be considered proved by three PMUs deployed in the system. A locating of PMU and WADC deployment will be determined by a modified methodology for selection of input and out signal which was developed for the conventional system.

Analysis will be done by taking into account different types of the inverter, gird-following and grid-forming. The only inverter type that has an ability of receiving the remote signal is a DVC, hence this grid-forming controller has to be present in every case scenario. Additional grid-forming control that will be added to the simulation is a VSM and an effect of having multiple grid-forming controllers in the system will be studied. Effect of deploying grid-following control in the system as a partial replacement of grid-forming control will be studied to mimic a more realistic scenario. Different scenarios with different types of inverters will enable to determine the effect of a selective damping method. This will be evaluated by an Eigenvalue analysis and Prony analysis, which will then be verified by a time domain signal response of the remaining generators in the system.

4

Modelling of the Power Grid with Large Penetration of RES

Software used during this Master's Thesis Project is DIgSILENT PowerFactory 2021 SP1 (hereinafter Power-Factory) and the licence (PowerFactory Thesis Licence) was provided by DIgSILENT GmbH for research and educational purposes.

4.1. Standardized Test System

A test system used in this Master's Thesis Project is a standardized test system IEEE 39-Bus New England System (hereinafter IEEE 39 Bus). A line diagram of the standardized IEEE 39-Bus system is shown in figure 4.1. A standardized test system was used during this research and the goal was to modify the test system to include PE devices and WAMS functionality with PMUs and WADC. This particular test system was chosen based on the research done about the most appropriate test systems for stability analysis. It was found that IEEE 39-Bus is a very strong candidate for stability analysis and it also has a great potential for planning of future expansions or modifications [38]. It is also a feasible option due to presence of 10 generation units, which could be replaced by RES. The nominal frequency of the system is 60 Hz, since the model is from the United States grid.

The standardized test grid includes the following elements [39]:

- **Ten (10) generators** - Generator G01 represents the extension of the US grid, Generator G02 is a reference machine with voltage magnitude of 0.982 p.u. and voltage angle of 0.0 degrees. Generators G02 to G09 are considered as steam turbines and Generator G10 is considered as hydro turbine.
- **Thirty-four (34) lines** - The length of the transmission lines is calculated based on the assumption that reactance per length is 0.3 Ω/km. Line data was calculated based on nominal voltage of 345 kV and nominal frequency of 60 Hz. The line current is assumed to be 1 kA.
- **Thirty-nine (39) buses** - The main grid voltage is 345 kV with Bus 12 at 138 kV, Bus 20 at 230 kV and Buses 30 to Bus 38 at 16.5 kV.
- **Twelve (12) transformers** - All transformers have YNy0 vector group connection.
- **Nineteen (19) loads** - They are modelled as constant active and reactive power demand and are not voltage-dependent.

Standardized IEEE 39-Bus system has been described, however the test grid has to be modified for the purpose of this study; evaluation of the WAMS control with massive integration of PE devices. A massive integration of PE means that there will be 20% of synchronous generation remaining in the system and the other 80% will be replaced by WTs. The stability of the entire system can only be guaranteed if the remainder of SGs stay in synchronism, which will be evaluated by transient and small signal stability analysis. It was decided that Generator G01 and Generator G02 should be the two generators that will be kept in the system, due to their characteristics. All the other generators will be replaced by WT technology and the scope of this project is to use a concept of FSCG WTs. In this case the generator is connected to the grid through the full-
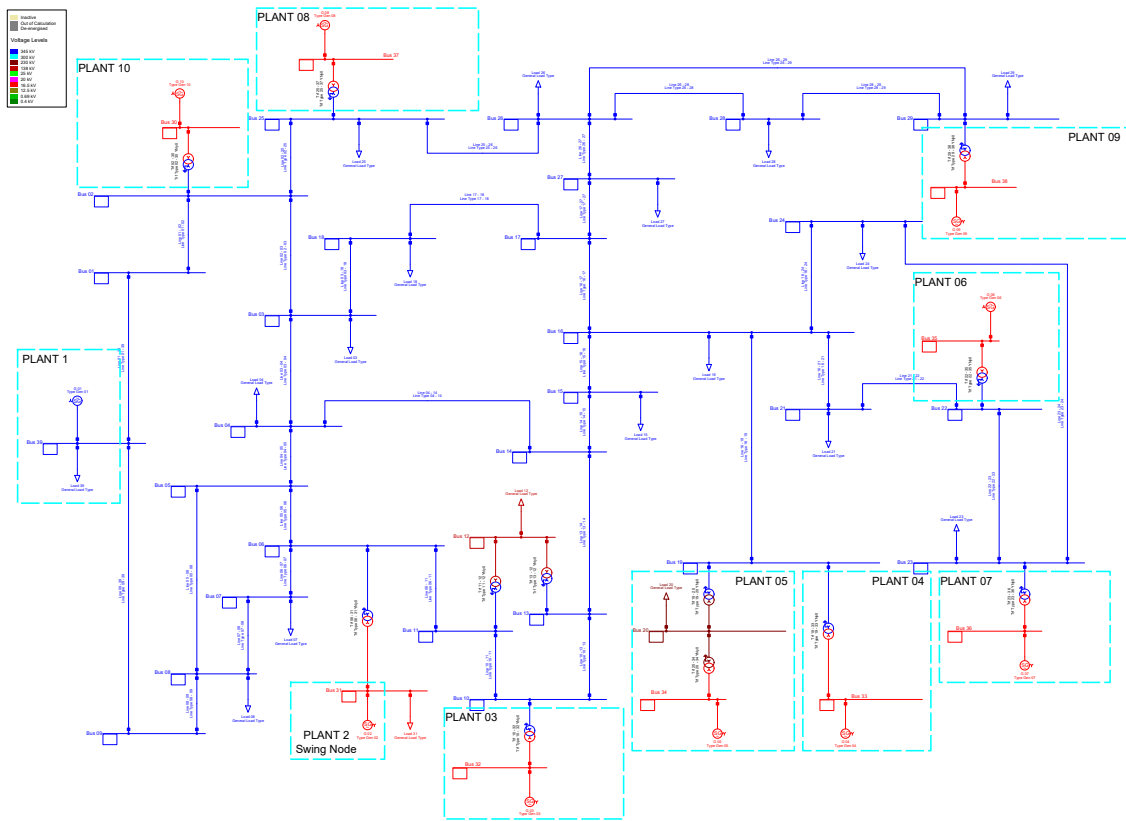
Figure 4.1: One Line diagram of IEEE 39-Bus New England Test System.

scale converter. A control of the Type 4 WT will either be modelled as a standard current control or a form of grid-forming control strategy.

The location of WTs with either current control or grid-forming control will be determined based on the analysis. Grid-forming control strategies implemented and studied in this project are VSM and DVC, which will be studied and compared to evaluate which strategy requires smaller fraction of grid-forming control in the system to guarantee stability. A study system has been modified to include both grid-forming control strategies as well as a grid-following control on every generation bus. This enables construction of different network variations for later analysis. The test system has been model to include Vector Current Control (VCC), DVC and VSM strategies connected to every generation bus, except for buses with synchronous machines connected to them. A closer look to Plant 05, Plant 04 and Plant 07 has been shown in figure 4.2 for easier visualization of modifications made in the test system.
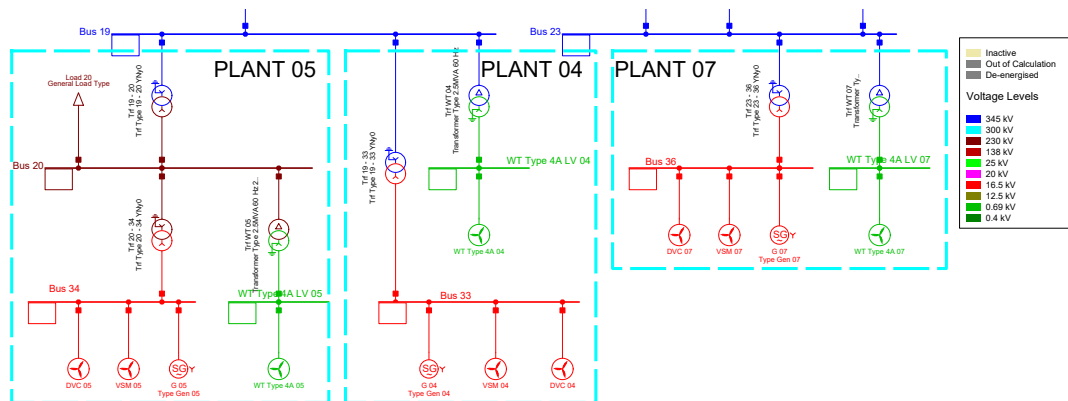
Figure 4.2: Plants 05, 04 and 07 with Vector Current Control, DVC and VSM control for wind turbines.

WT using grid-forming control strategies DVC and VSM are placed by connecting to the same bus as the already existing synchronous machines. There was no need to introduce new transformers to the system in order to successfully connect WT with grid-forming control. On the other hand, implementation of a WT Type 4 with VCC strategy required an associated transformer to make a connection to the grid possible. A vector group of an associated three phase transformer is Dyn5, while a vector group of a three phase transformer used for grid-forming control is YNy0.

Power plants present in the system require a control strategy, which allows a dynamic analysis of the test system. Proper implementation of the associated control strategies is required for the correct response of the power plants after an introduction of disturbances to the system. Different type of a generators requires a different associated control system and they differ in its purpose and its response to the disturbance.

4.2. Synchronous Generator Control

Synchronous generation will not remain a major contributor of electrical energy in the test grid, however the control that allows a smooth operation is highly important. Furthermore, with predictions of moving towards low carbon energy generation, the existing control strategies might not be enough anymore to enforce system stability. Even though that a transition towards green energy is underway, a complete replacement of synchronous generation with RES will not happen in a near future. This is a reason why analysis and investigation of the power grid with a fraction of synchronous generation is currently highly researched topic.

Taking a closer look to the control structure associated with synchronous machines in the system is crucial when talking about system stability, even though that only a fraction of energy will come from this source of electricity. Making sure that the remainder of synchronous machines stay in synchronism is necessary when talking about preserving system stability and enforcing high security of supply. Rotor angle stability of a modern power grids will stay as important as it was in the conventional power grids and it will stay an important requirement when designing a "green" power system.

4.2.1. Governor

Electrical energy is generated by a synchronous machine, which comes from a prime mover generating mechanical energy. A primary speed control is performed by an associated governor at individual power plant and its main objective is to maintain power exchanged among different parts of the system. An indication about active power control in the system is frequency, which will be held at the constant value if governor is working properly.

Figure 4.3 shows a steam turbine and associated governor control [40]. A governor model used in this project for nine power plants is classified as a steam turbine IEEE Type G1. For a unit number 10, a hydro turbine is used, which is classified as a IEEE Type G3. The governor or a primary control used in this project works by observing the speed deviation of the turbine and it adjust the steam input. Since it serves as a primary control, the frequency is not adjusted back to its nominal value and frequency stabilizes around a new value.
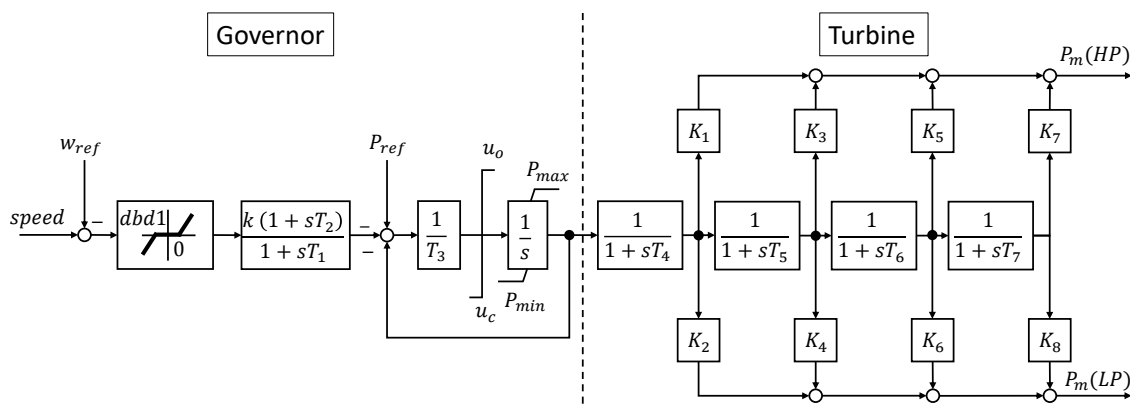
Figure 4.3: Governor and a steam turbine [40].

Values for the parameters used in a governor model for generators G02 to G09 in this project are presented in table 4.1, while values and parameters for the generator G10 are presented in table 4.2.

Symbol	Value	Symbol	Value
K [pu]	5	K4 [pu]	0
T1 [s]	0.2	K5 [pu]	0.3
T2 [s]	1	K6 [pu]	0
T3 [s]	0.6	K7 [pu]	0.15
T4 [s]	0.6	K8 [pu]	0
T5 [s]	0.5	PNhp [MW]	0
T6 [s]	0.8	PNlp [MW]	0
T7 [s]	1	Uc [pu/s]	-0.3
K1 [pu]	0.3	Pmin [pu]	0
K2 [pu]	0	Uo [pu/s]	0.3
K3 [pu]	0.25	Pmax [pu]	1

Table 4.1: Governor values and parameters for generators G02 to G09.

Symbol	Value	Symbol	Value
Tg [s]	0.05	a23 [pu]	1
Tp [s]	0.04	Tw [s]	0.75
Sigma [pu]	0.04	PN [MW]	0
Delta [pu]	0.2	Uc [pu/s]	-0.1
Tr [s]	10	Pmin [pu]	0
a11 [pu]	0.5	Uo [pu/s]	0.1
a13 [pu]	1	Pmax [pu]	1
a21 [pu]	1.5	-	-

Table 4.2: Governor values and parameters for generator G10.

The governor model used for controlling synchronous machines in this project does not include droop control, which would enable a proper load sharing among all machines in the system. Droop or speed regulation is used to increase the power output of the turbine with an decrease in frequency of the system. Different generators in the system might have different droop characteristics associated, which in reality means that in case of decrease in frequency, generators with less capacity will be assigned to pick up smaller load compared to machines with higher capacity. This way machines in the system get assigned proportionally similar value of load.

Lack of secondary control will be visible when load-event simulations will be performed. Frequency will stabilize shortly after an event, however at a different value than a nominal frequency. When performing an analysis, such as short-circuit event, the frequency will stabilize at the nominal value when synchronous generators will be a dominant source of energy. However, the response of the system with high penetration of WTs will be slightly different and it will need an advanced solution in order for the system to stabilize.

4.2.2. Automatic Voltage Regulator

Excitation provides machine field winding with direct current and controls field voltage and current [11]. Furthermore, the reactive power flow is controlled through control of voltage to enhance the system stability. It also has an ability to respond to large rotor angle disturbances with field forcing, which is a part of protection that exciter is able to provide [11].

An excitation model used in this project is excitation system model Type DC1A or an AVR model IEEE T1, which is shown in figure 4.4 [41]. This type of excitation is not commonly used in modern applications, however it is used for simulations due to its simplicity. AVR type IEEE T1 represents field-current DC commutator exciter with continually acting voltage regulators [41].

The main input of the AVR is V_c, while stabilizing power signal input V_s represents many inputs as shown
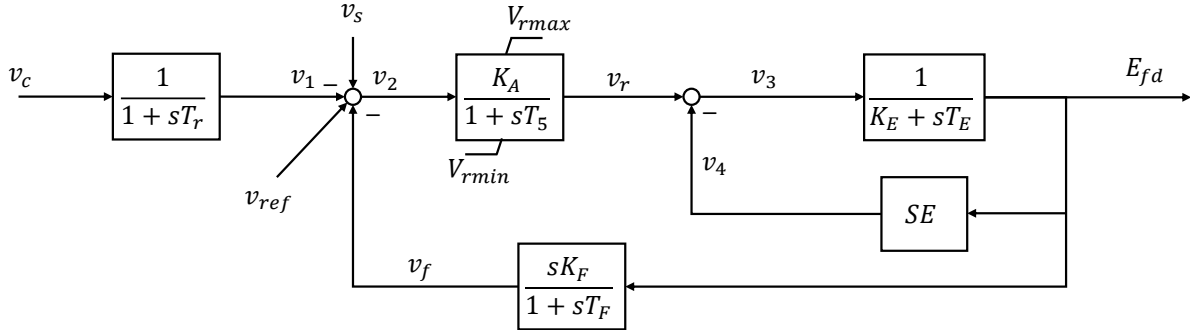
Figure 4.4: Automatic Voltage Regulator [41].

in equation 4.1:

$$V_s = V_{pss} + V_{uel} + V_{oel} \tag{4.1}$$

where V_{pss} represents the output from PSS, V_{uel} represents output from under-excitation limiter and V_{oel} represents output from over-excitation limiter.

The control structure of the synchronous machines used in this project does not include under-excitation limiter and over-excitation limiter, which means that those inputs are zero and they can be neglected. Stabilizing signal V_f is used at the summation point to generate the error signal. SE block is a nonlinear function and it represents the saturation block, where output is the product of the block and the input E_{fd} [41]. The output of the exciter block is E_{fd}, which is fed into a synchronous machine. Only other input for the synchronous machine is p_t, which comes from a governor control.

Values for the parameters used in AVR model for every generator in this project are presented in table 4.3. It can be noticed from the table that AVR for every generator has different values for the parameters unlike in governor model, where values for the governor of the same type were the same.

Symbol	G02	G03	G04	G05	G06	G07	G08	G09	G10
Tr [s]	0	0	0	0	0	0	0	0	0
Ka [pu]	6.2	5	5	40	5	40	5	40	5
Ta [s]	0.05	0.06	0.06	0.02	0.02	0.02	0.02	0.02	0.06
Ke [pu]	-0.633	-0.0198	-0.0525	1	-0.0419	1	-0.047	1	-0.0485
Te [s]	0.405	0.5	0.5	0.785	0.471	0.73	0.528	1.4	0.25
Kf [pu]	0.057	0.08	0.08	0.03	0.0754	0.03	0.0854	0.03	0.04
Tf [s]	0.5	1	1	1	1.246	1	1.26	1	1
E1 [pu]	3.0364	2.3423	2.8681	3.9267	3.5868	2.8017	3.1915	4.25676	3.5461
Se1 [pu]	0.66	0.13	0.08	0.07	0.064	0.53	0.072	0.62	0.08
E2 [pu]	4.0486	3.1231	3.8241	5.2356	4.7824	3.7356	4.2553	5.6757	4.7281
Se2 [pu]	0.88	0.34	0.314	0.91	0.251	0.74	0.282	0.85	0.26
Vrmin [pu]	-1	-1	-1	-10	-1	-6.5	-1	-10.5	-1
Vrmax [pu]	1	1	1	10	1	6.5	1	10.5	1

Table 4.3: Automatic Voltage regulator values and parameters for every generator.

4.2.3. Power System Stabilizer

PSS block is added to the control structure to enhance damping of system oscillations, which is done by producing electrical torque in phase with speed deviations [11]. A structure of a PSS is shown in 4.5, where it is visible that the input signal is a shaft speed deviation (rotor speed deviation). PSS is designed to damp local as well as global modes of oscillation, which means that it should have an ability of damping a range of frequencies to cover many oscillatory modes.

The signal in a PSS controller first passes through a gain block, where the amount of damping is set and assigned to the signal. The effect of increasing the value of gain should be examined, where a high value
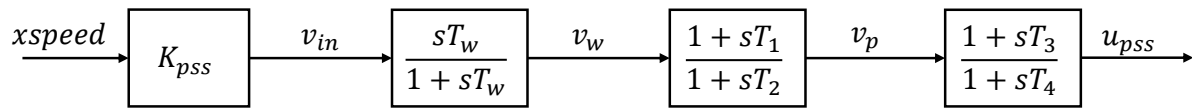
Figure 4.5: Power System Stabilizer [11].

improves the transient stability of the system. However, the PSS should be designed in such a way to have a positive effect on the whole system stability rather than just on large disturbance stability.

Washout block used in a PSS design serves as a high-pass filter, which prevents modifications of the field voltage. A washout time constant is an important design consideration, since the value will determine what signals will pass through the filter unchanged. The lower time limit of the filter should be positioned not to block the stabilizing signals at the desired frequencies. A value of a higher time limit should be low enough not to cause voltage excursions [11]. More specifically, a higher-time constant for a filter is necessary when dealing with low-frequency oscillations, which prevents an occurrence of phase lead during low frequencies. Reduction of synchronizing torque at lower frequencies can occur if appropriate attention is not given to this issue.

PSS design used in this project is composed of two phase-lead compensation blocks. This blocks are developed with an intent to deal with an occurring leg between exciter input and electrical torque. More phase-lead compensation blocks are used in a design to achieve the desired phase compensation. In some cases, under-compensation can increase the synchronizing torque in addition to increase in damping torque. The last block shown in a PSS structure is a limitation block, which has a relatively large value for the positive output limit and a slightly lower value for the negative limit. Larger value of the positive limit allows a high contribution during large swings and a smaller lower limit allows an appropriate transient response.

Values for the parameters used in PSS model for every generator in this project are presented in table 4.4. It can be noticed from the table that PSS for every generator has different values for the parameters; hence parameters for every generator are listed in the table.

Symbol	G02	G03	G04	G05	G06	G07	G08	G09	G10
Kpss [pu]	0.5	0.5	2	1	4	7.5	2	2	1
Tw [s]	10	10	10	10	10	10	10	10	10
T1 [s]	5	3	1	1.5	0.5	0.2	1	1	1
T2 [s]	0.4	0.2	0.1	0.2	0.1	0.02	0.2	0.5	0.05
T3 [s]	1	2	1	1	0.5	0.5	1	2	3
T4 [s]	0.1	0.2	0.3	0.1	0.05	0.1	0.1	0.1	0.5
Vmin [pu]	-0.2	-0.2	-0.2	-0.2	-0.2	-0.2	-0.2	-0.2	-0.2
Vmax [pu]	0.2	0.2	0.2	0.2	0.2	0.2	0.2	0.2	0.2

Table 4.4: Power system stabilizer values and parameters for every generator.

4.3. Wind Turbine Control Strategies

A simplified model of a FSCG WT is shown in figure 4.6, where Machine Side Converter (MSC) and WT generator parts are neglected. This is because this parts are not relevant when performing a dynamic assessment of the system, which means that close attention is payed to Line Side Converter (LSC) [12]. It is visible from a figure that the constant active power is injected into a DC circuit, which also consists of a DC chopper. A DC chopper is included as a PE converter protection, which limits the DC voltage when the value rises above the threshold.

A number of parallel units that each WT is composed of in the test system is shown in table 4.5. Every WT independent of control structure has a rated apparent power of is 2.5 MVA and active power dispatch of 2 MW. An active power dispatch of an individual WT is multiplied by the number of parallel units to obtain a power dispatch of the whole power plant. Furthermore, figure indicates the bus that either a power, voltage, current or PLL measurements are observed from and used for generating inputs for any WT control. There is also a remote bus measurement, which is initially used for remote voltage measurement for DVC.

The test system composed of ten synchronous generators represents a stable test system with reliable sup-
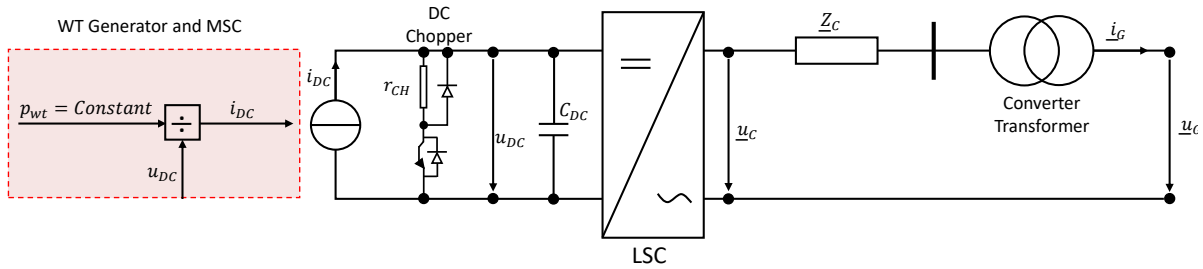
Figure 4.6: A schematic representation of a FSCG-based Type IV WT [12] [42].

Plant	WT 01	WT 02	WT 03	WT 04	WT 05	WT 06	WT 07	WT 08	WT 09	WT 10
No of Units	-	-	325	316	254	325	280	270	415	125
Bus	-	-	32	33	34	35	36	37	38	30
Remote Bus	-	-	10	19	20	22	23	25	29	2

Table 4.5: Number of WT parallel units and a bus for power, voltage, current and Phase-Locked Loop measurements.

ply of electricity. The control structure connected to synchronous generators is able to defy different kinds of events, such as load event or short-circuit event. However, due to European initiative of migration towards greener energy, the transition towards DG involves introduction of many PE devices to the grid. Different control structures available for controlling WTs will be described, where some have grid-following functionality while some have grid-forming ability.

Grid-forming control strategies used in this project are DVC and VSM. DVC was based on the literature review a preferred option for grid-forming tasks, however there is no PowerFactory built-in template for this kind of control structure. DVC technology was found in another PowerFactory project, where it was created as a template and imported into this project. VSM is already included in PowerFactory as a template, which is modelled as a static generator with already associated control structure.

4.3.1. Current Control

Current control is represented as an ideal current source and it behaves as a grid-following control. WTs with current control are not able to stabilize the system following the disturbance in highly penetrated RES systems. Since a behaviour of the system with massive integration of PE in the system is of interest in this project, current control will have to be complimented with grid-forming control strategies.

The base WT control model is generated according to European Standard Wind energy generation system - Part 27-1: Electrical simulation models - Generic Models (IEC 61400-27-1:2020) [43]. Control of Type 4 WT can either be modelled to include the mechanical part of the turbine and to take the aerodynamics into account when performing a dynamic simulation or it can be modelled by ignoring the mechanical part. For this project Type 4A WT was chosen, where model only includes the generator control and grid protection, without including a mechanical module. While generator control will be closely examined, the grid protection will be ignored since protection is out of the scope of the project. This is visible in figure 4.7, where only generator control is illustrated and protection was excluded from the original structure.
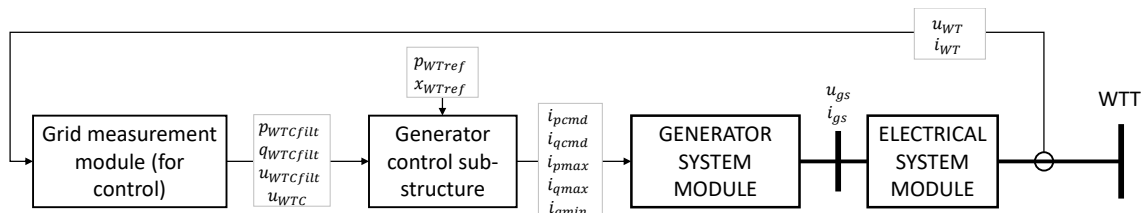
Figure 4.7: Modular structure of the WT Type 4A without protection [43].

Voltage measurement and current measurement blocks - represented by a Grid measurement module - provide input data for the generator control sub-structure. Wind power plant controller provides active

power reference as well as reactive power reference/ delta voltage reference, which both serve as an input for the generator control sub-structure. However, in this case there is no wind power plant controller installed, which means that the input signals are initialized as constant values.

Current control is used in the system as a grid-following control, which means that this control strategy is applicable only to the system with only a small penetration of RES. In a project, where the large majority of power generation comes from WT, this control is no longer applicable and it has to be replaced with a form of grid-forming control. In other words, grid-following control obtains set points from the system and "follows" the grid, rather than create set point to form the grid.

Since the grid-forming control is superior to grid-following control, some might think that installation of only grid-forming control will solve an issues. In reality, it is far more complicated due to already present wind power plants with a current. An option to replace control on every WT might not be feasible and expensive. Hence, simulation will be performed with grid-forming control in a combination with grid-following control. This will be a more realistic representation of the future development and system response to any disturbances with mainly RES connected to the grid.

4.3.2. Direct Voltage Control

DVC is implemented in power grids with a high participation of PE interfaced generation due to its ability of ensuring a stable dynamic operation without a presence of inertia provided by large rotating machines. Details of individual block structure implemented in PowerFactory can be found in appendix B.

Reactive Power Control

Active power control structure implemented in DVC is represented by figure 4.8. Slow global Var control's response time is in range of couple of seconds and up to 30 seconds [42], while VQ droop block is used to set a reactive power reference signal as an input for a PI block to generate the voltage signal.
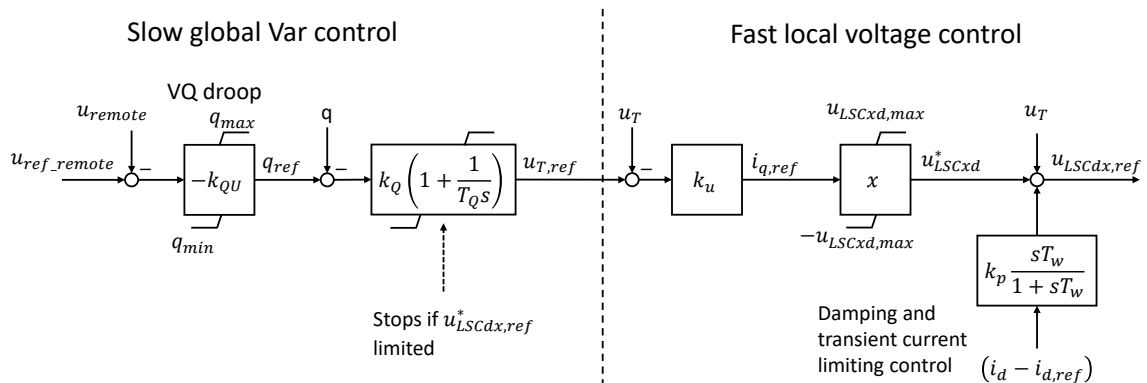
Figure 4.8: DVC reactive power control [12] [42].

A fast local voltage control with proportional characteristics takes action for events that require a faster response. The implementation of limiting control allows a selective damping and replaces the proportional component [42]. D-component is determined after an addition of controlled terminal voltage and the reactive current is therefore removed from a control scheme. This eliminates a possibility of integrator windup during an event, which causes a split of the system [42].

Active Power Control

The amount of energy produced from RES is not constant due to stochastic behaviour of natural resources. In case of WTs this natural resource of energy is wind and energy produced by WT is only possible when wind spins the blades on a WT. The amount of wind energy and availability of wind energy can only be predicted to some extent, which makes simulations of real behaviour of the system very challenging. An assumption made in this project is that there is a constant active power available with the set rating of the unit [44].

The active power injected into the network is represented by a calculation 4.2 [42].

$$p = u_T \cdot i_P = -u_T \frac{u_{Cq}}{x} \tag{4.2}$$

where p represents active power, u_T represents terminal voltage, u_{Cq} represents q-component of the converter voltage and x represents the reactance. Figure 4.9 indicates active power control structure [42].
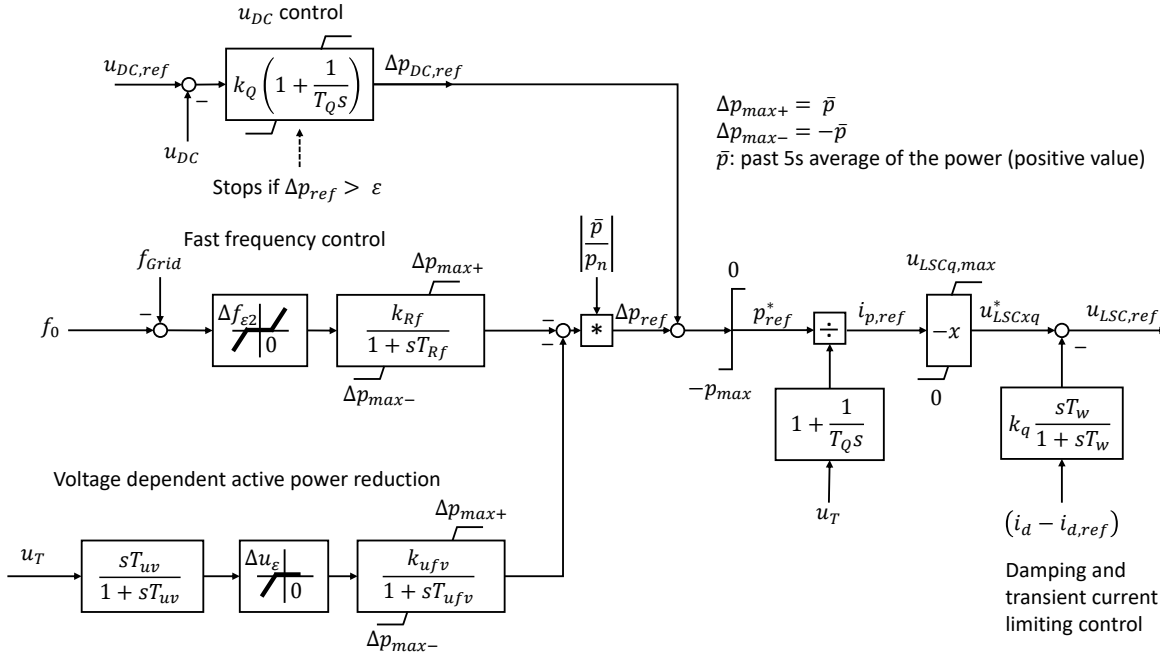
Figure 4.9: DVC active power control [12] [42].

Figure 4.9 shows an active power control structure with corresponding elements. The function of a fast frequency control is set to react when frequency crosses the threshold value [42]. Voltage dependent active power reduction is used to improve the transient stability [12]. The power reference power set point is lowered during the fault, which compensates converter's inability to inject reactive power into the system. The power injected is adjusted based on the terminal voltage of the converter. Values for the parameters used in DVC model for converters DVC03 to DVC10 in this project are presented in table 4.6. Parameters listed in the table are combined for previously explained reactive power control, active power control and current limitation.

Symbol	Value	Symbol	Value
k_ir [-]	1.2	Tud [s]	5
Kdc [-]	4	T [s]	60
Tdc [s]	0.03	db_voltage_VDACR [pu]	0.1
UdcN [kV]	1.276	KuVDAPR [-]	2
Ku [-]	0.2	TuVDAPR [s]	0.005
Kqu [-]	6.6	Tp_aver [s]	5
Kq_remote [-]	0.002	id_max [pu]	-0.95
Tq_remote [s]	15	uset_min [pu]	-0.5
T_rate_limit_freq [s]	0.2	id_min [pu]	0
imax [pu]	1	qmax [pu]	0.31
l [pu]	0.1	uset_max [pu]	0.5

Table 4.6: Direct voltage control values and parameters for converters DVC 03 to DVC 10.

Current Limitation

Current limitation is used to prevent any damages on Insulated-Gate Bipolar transistors (IGBTs), which could be caused by overcurrent. The task of a current limiter is to block the PE converter in case of an overcurrent, which helps preserve the health of IGBTs [12]. The general current limitation in VSC is shown in detail in figure 4.10 and it compares cases with i_P priority, i_Q priority and no priority set. Figure 4.10 shows that

a magnitude will be limited in case with no predefined priority, while active current priority will limit reactive current and vice versa. The priority can be changed during the operation and it is based on the voltage support set points [12]. The current limitation logic of the DVC using in this project is depicted in figure 4.11.
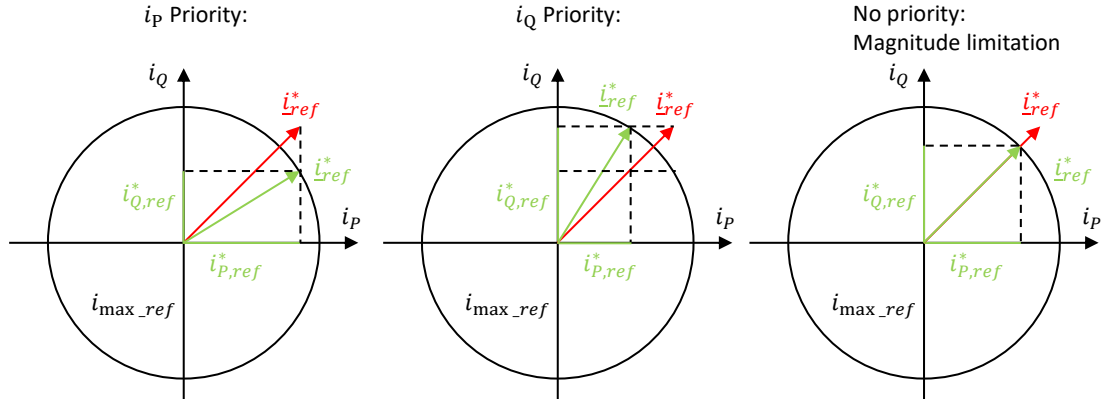
Figure 4.10: Current limitation VSC [12].
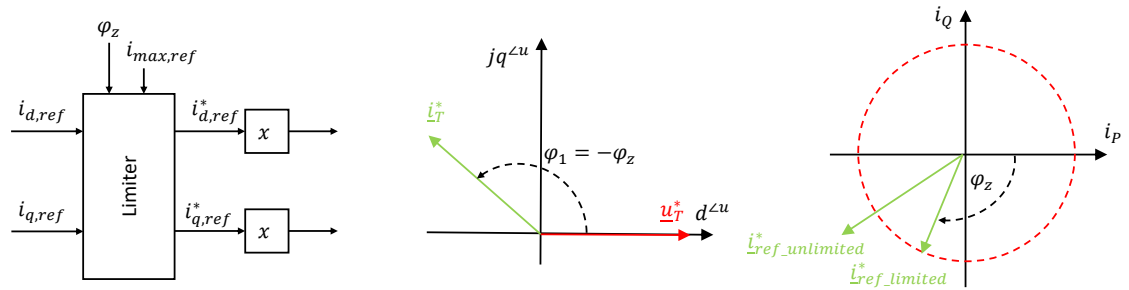
Figure 4.11: Converter current limitation method [12] [42].

When the maximum value of the current is exceeded by an actual converter current, then a new maximum current is calculated as represented by calculation 4.3. In figure 4.11 it is represented how an impedance angle and new maximum reference current are used in a limiter block.

$$(|i_d + j i_q| - i_{ref\_max0}) > 0 \rightarrow i_{ref\_max} = i_{ref\_max0} - k_{red} \cdot (|i_d + j i_q| - i_{ref\_max0}) \tag{4.3}$$

In case that reference current is not limited, then voltage is calculated based on equation 4.4.

$$u_{LSCdx,max} = u_{LSCqx,max} = x \cdot i_{max,ref} \tag{4.4}$$

however if reference current is limited, voltage is calculated based on new maximum reference current as shown in equations 4.5 and 4.6.

$$u_{LSCdx,max} = x \cdot i^*_{Q,ref} \tag{4.5}$$

$$u_{LSCqx,max} = x \cdot i^*_{P,ref} \tag{4.6}$$

Converter can provide the best possible voltage support since it has an ability of changing the reference current based on the impedance it sees [12].

4.3.3. Virtual Synchronous Machine

Virtual synchronous machine has an ability to provide virtual inertia and mimic the behaviour of a synchronous machine. Mechanical inertia is emulated and can be represented by a swing equation [45]. This kind of control will be highly valuable in the future power grids with decentralized power generation and high penetration of PE devices. This type of control was used in this project due to its characteristics. Behaviour of the controller will be compared to DVC, another form of grid-forming controller.

An internal dynamics and behaviour of a VSM can be represented by a SG per unit balance in the Laplace domain, represented by equation 4.7 [45]:

$$T_a \cdot s \cdot \omega_{VSM} \approx p_0 - p_{el} - D_p(\omega_{VSM} - \omega_g) \tag{4.7}$$

where a time constant T_a represents the rotor angle; hence it can also be written as $2H$, p_0 and p_{el} represented the power reference and power output respectively, and D_p is a damping coefficient.

Equation 4.7 also represents rotating speed of VSM, ω_{VSM} and grid frequency, ω_g. Since this controller is mainly used in weak grids, the grid frequency ω_g will become a frequency reference provided by an additional controller. VSM provides a voltage angle θ_v as an output, however the voltage amplitude has to be provided by a separate reactive power controller. The block diagram of a grid-forming part of a VSM controller is shown in figure 4.12 [46].
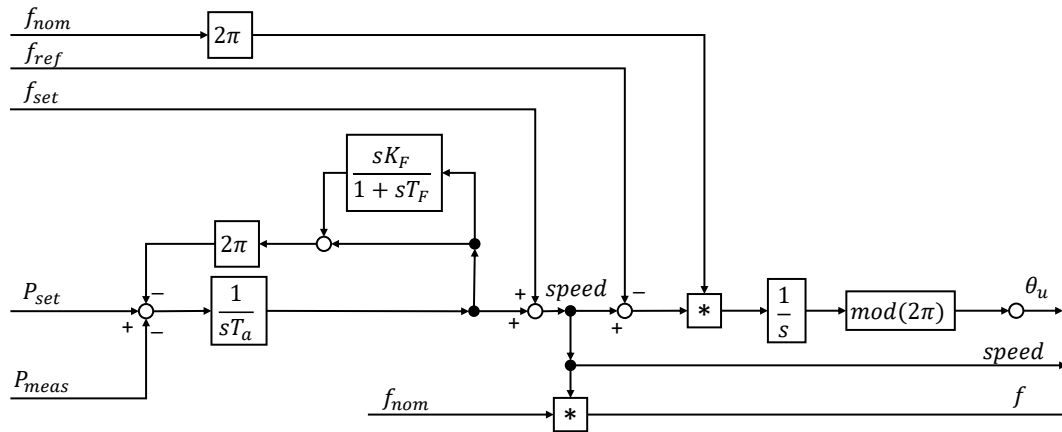
Figure 4.12: Grid-forming block of the virtual synchronous machine [46].

The overall structure of the VSM controller implemented in the PowerFactory consist of voltage control, power calculation, virtual impedance and output voltage calculation besides the grid-forming controller, where a VSM structure explained is located. The measurements that serve as an input to the controller, are voltage and current measurement. The VSM controller attempts at stabilizing the grid based on the values that are provided from the grid.

5

Wide Area Monitoring for Improved Controllability

5.1. Overview of Wide Area Monitoring System Structure

The proposed WAMS structure used in this project is demonstrated in figure 5.1, where locations of PMUs are illustrated for demonstration purposes. The exact locations of signal will be determined with the analysis and the methodology of determining those locations will be explained in the following sections. This section will allow us to answer one of the objective questions of this project, which will show a methodology of using WAMS to enhance damping of very low frequency oscillations.
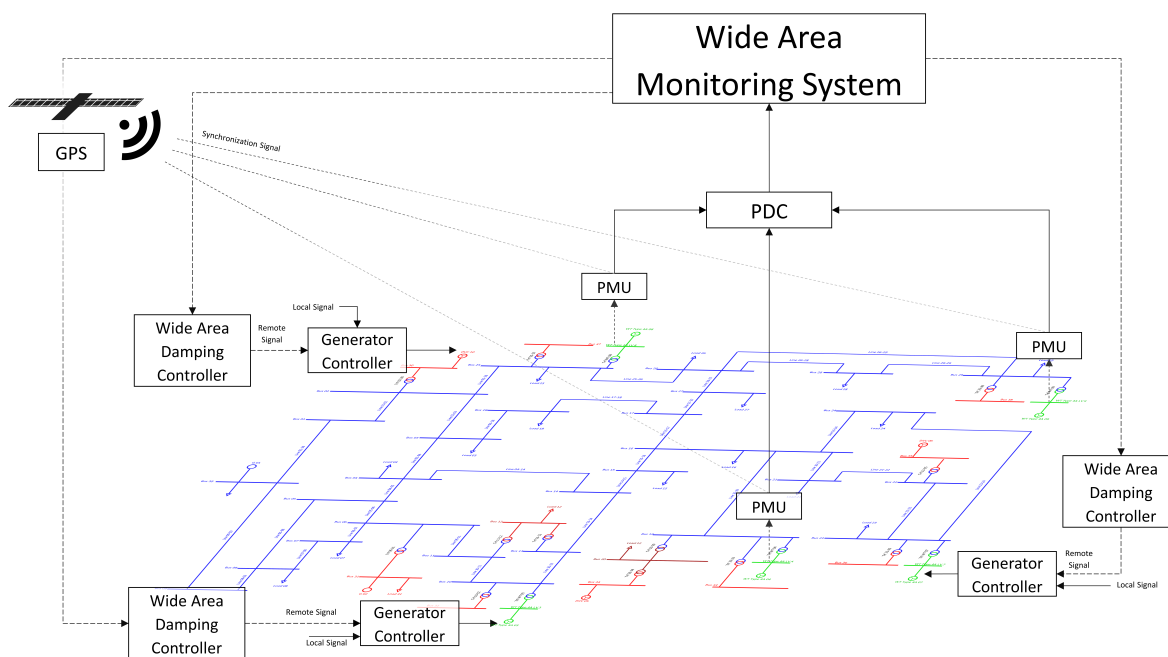
Figure 5.1: WAMS structure with implemented PMUs and WADC.

The main idea taken into account when proposing a structure was to deploy three PMU devices on generator buses with highest observability index. This will guarantee that measurements observed from those buses well represent the state of the whole system. It was assumed and even desired that it is not necessary to install PMUs on every generator bus to preserve the initial and maintenance cost. This was done with keeping in mind a real world scenario where it will not be feasible to install sensors (in this case PMU devices) on all

generator buses. It will be tested whether this kind of PMU deployment is feasible for damping critical modes of oscillation. It is important to point out that those signals are synchronized by making use of GPS, in order to stamp signal at the source and achieve higher effectiveness of the system.

The second part of the WAMS structure focuses on the deployment of supplementary damping controllers. These are deployed with an intent to add additional damping to critical modes of oscillation. Signals from the supplementary damping controller will be fed to generators or WTs connected to generator buses with the highest controllability index. In reality it means that controllers located on those buses will have the highest impact on overall damping. The output of the damping controller will be combined with the existing local control associated with synchronous generators or wind power plants.

5.2. Identification of Critical Modes

The main technique for determining critical modes, damping rations and frequencies will be Modal or Eigenvalue analysis. It will additionally be used for input and output signal selection while determining locations of PMUs and WADCs. Furthermore, the analysis based on the time-domain signal will also be carried out, which will serve as a comparison for results obtained by Modal analysis.

5.2.1. Modal Analysis

The theory behind eigenvalue and eigenvector dependency on matrix A is represented by equations 5.1 and 5.2 [9]:

$$(A - \lambda_i I)v_i = 0 \tag{5.1}$$

$$\omega_i^T(A - \lambda_i I) = 0 \tag{5.2}$$

where v_i represent the right eigenvectors and ω_i represent the left eigenvectors associated with the eigenvalue λ_i and A is a matrix A, which depend on system parameters.

In order to obtain the expression which is useful for this project, the previous equation 5.1 has to be differentiated with respect to parameter K and the obtained expression then needs to be multiplied by left eigenvector ω_i^T. An assumption taken into consideration is that the left and right eigenvectors are orthogonal ($\omega_i^T v_i = 1$) as already explained when introducing an equation 3.7. The final expression 5.3 is then observed:

$$\frac{\partial \lambda_i}{\partial K} = \omega_i^T \frac{\partial A}{\partial K} v_i \tag{5.3}$$

Modal analysis can either be done manually in PowerFactory or it can be done by executing a DIgSILENT Programming Language (DPL) script, where the following output files are generated:
- **Amat.mtl** - System matrix A
- **Evals.mtl** - System eigenvalues
- **lEV.mtl** - Left eigenvectors
- **rEV.mtl** - Right eigenvectors
- **Jacobian.mtl** - Jacobian matrix J
- **M.mtl** - M matrix
- **PartFacs.mtl** - Participation factors
- **VariableToIdx_Jacobian.txt** - rows and columns description for matrix J
- **VariableToIdx_Amat.txt** - rows and columns description for matrix A

5.2.2. Prony Analysis

Prony analysis is based on the input signal able to determine eigenvalues, damping ratio, frequencies, reconstructed signal, amplitudes and phase angles. Prony analysis will be performed in MATLAB with an intent of verifying and validating results observed prom Eigenvalue analysis. It will be studied whether results from Modal analysis give accurate results for further analysis of input and output signal selection. Eigenvalue and Prony analysis sometimes do not produce the same result or the magnitude of values due to additional control loops present in the controller structures.

5.3. Input and Output Signal Selection

A controllability index (CI) is expressed as 5.4 and an observability index (OI) is expressed as 5.5. Controllability and observability indices are obtained by normalizing the mode controllability (MC) and mode observability (MO), respectively [9], which is represented by 5.6.

$$CI_l = \frac{MC_l}{\max_{l \in L} MC_l} \tag{5.4}$$

$$OI_\delta = \frac{MO_\delta}{\max_{\delta \in \Delta} MO_\delta} \tag{5.5}$$

where CI is a controllability index, MC is the mode controllability, OI is an observability index and MO is the mode observability.

$$|\lambda_i'| = |\omega_i^T B_a| \cdot |H(\lambda_i)'| \cdot |C_a v_i| \tag{5.6}$$

where $|\omega_i^T B_a|$ represent the mode controllability (MC) of mode i and $|C_a v_i|$ represent the mode observability (MO) of mode i. More details about the derivation can be found in the reference [9].

Controllability index is calculated with an intent of identifying (generator) buses in the system for installation of additional damping controllers. It is assumed that less controllers will be needed in the grid if they are deployed on buses where the highest impact can be guaranteed. Similarly, observability index will be used to identify (generator) buses for installation of PMUs, where a goal is to collect measurements that will correctly represent the state of the whole system. In addition to damping controllers, it is assumed that only a handful of PMUs is needed in the system to collect important information if they are placed according to analysis.
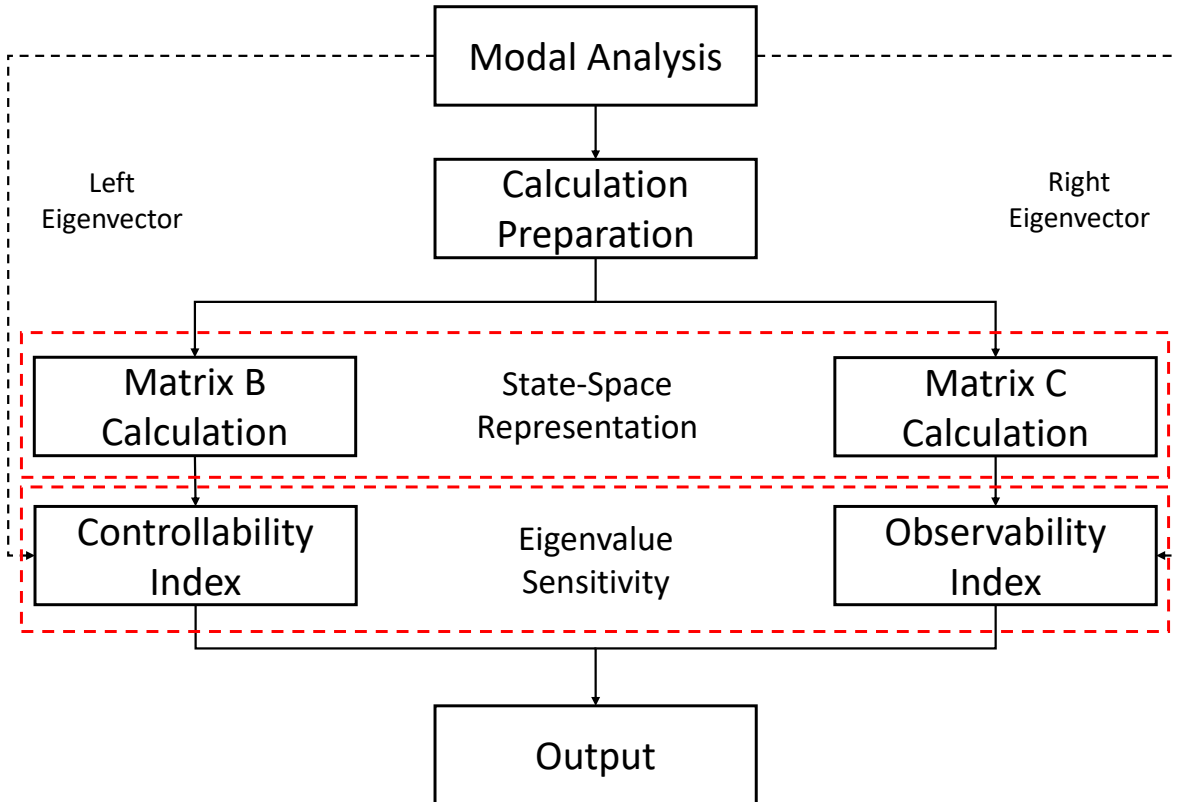
Figure 5.2: Flow chart of determining buses with highest observability and highest controllability [9].

Important to point out is that matrix A is like mentioned before available as an output of the Modal analysis; either by performing a Modal analysis in PowerFactory or as an output file exported to the target folder by running the before mentioned script. Unfortunately, matrix B, matrix C and matrix D are not available as the output of Modal analysis, because they depend on user definition.

A flow chart which was followed to determine best locations for PMUs and WADCs, which is shown in figure 5.2. This flow chart is executed in PowerFactory by two different scripts. Main objective of the first script is to perform Modal analysis and to write the outputs to the desired path. The second script on the other hand is more complex and it performs all the other steps mentioned in the figure and the process is in detail described below.

5.3.1. Determination of Matrix B and Matrix C

Figure 5.3 shows the flow chart of matrix B (left) and matrix C (right) construction. An explanation for construction of both matrices is given below with details and differences in the process are highlighted.
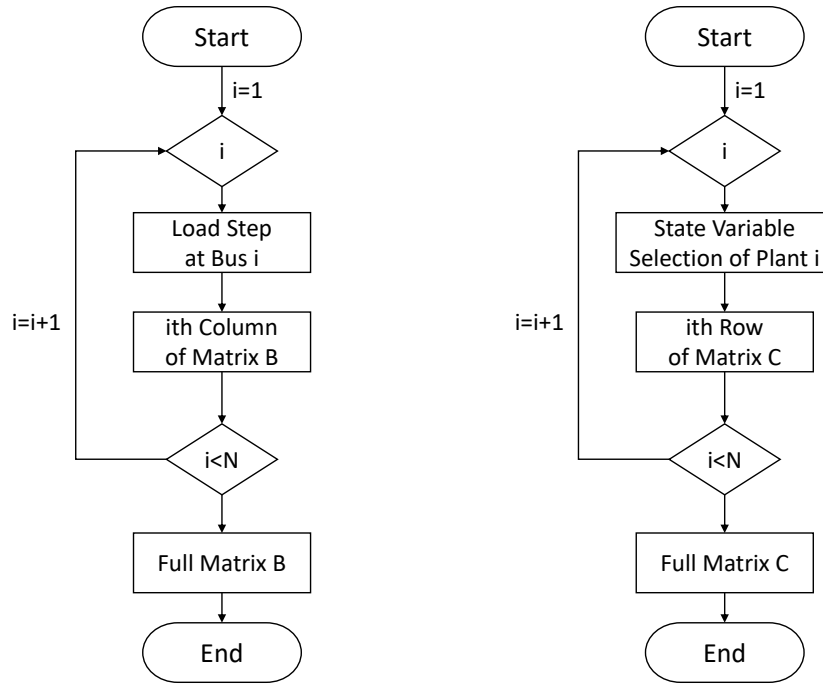
Figure 5.3: The flow chart of Matrix B and Matrix C construction [9]

Matrix B Calculation

A column in matrix B is constructed by introducing a mobile load and connecting it to every generator bus in the system. Every time a mobile load is introduced to a new generator bus, a new column in a matrix B is written. Important to point out is that the constructed column is an estimation and the time step should be very small in order to minimize the error of the Forward Euler formula. In this case the time step is set to be 0.0001 s, which means that the time final "tf" = 0.0001 s [9]. Manually generated switch event enables to perform a load step on every bus done by a mobile load. Mobile load is modelled as a constant active power output of 100 MW, which is the same as the base power of the system.

The task is executed by firstly assigning the mobile load to the first bus in general selection by creating a node and a breaker. Mobile load is associated with the previously created node and manually generated switch event is triggered. After the Mobile load is connected to the desired bus, RMS simulation is executed by calculating initial conditions and executing the simulation. Like mentioned, the simulation time is set to a very small value of 0.0001 s to minimize the errors [9]. Appropriate column of the matrix B is constructed every time a mobile load is assigned to a different bus until there are as many column in the matrix as there are buses assigned. Coefficients obtained from simulations done by introducing Mobile load to generator buses construct a complete matrix B.

Matrix C Calculation

Matrix C is just like a matrix B constructed based on the information defined by the user. The output variable of the power plant can be defined as any of the state variables available from a specific power plant. In case of a synchronous machine, a state variable studied is a speed of the machine [9]. Large amount

of different controllers in the project do not have any rotating parts associated with them. In that case, a definition of a different state variable is required to give feasible results of the analysis.

A task of constructing a matrix C works by identifying a location of a state variable in each row associated with the defined option [9]. The associated term in the specific row will then get assigned a value of "1" and the other terms, which are not the selected state variable, will be zero. The same procedure will be done for all other rows of the matrix C. At the end there will be as many rows in the matrix C as there were state variable terms recorded. In practice it means that there will be as many rows of the matrix C as there are power plants with the desired state variable. Furthermore, a txt file is generated which allows easier identification of the output values.

5.3.2. Observability and Controllability Indices

Figure 5.4 shows a flow chart of the controllability matrix and observability matrix construction. The previous step had some differences between constructing matrix B and matrix C, however in this case the procedure is exactly the same with considering different inputs. A process will be explained in the following section.
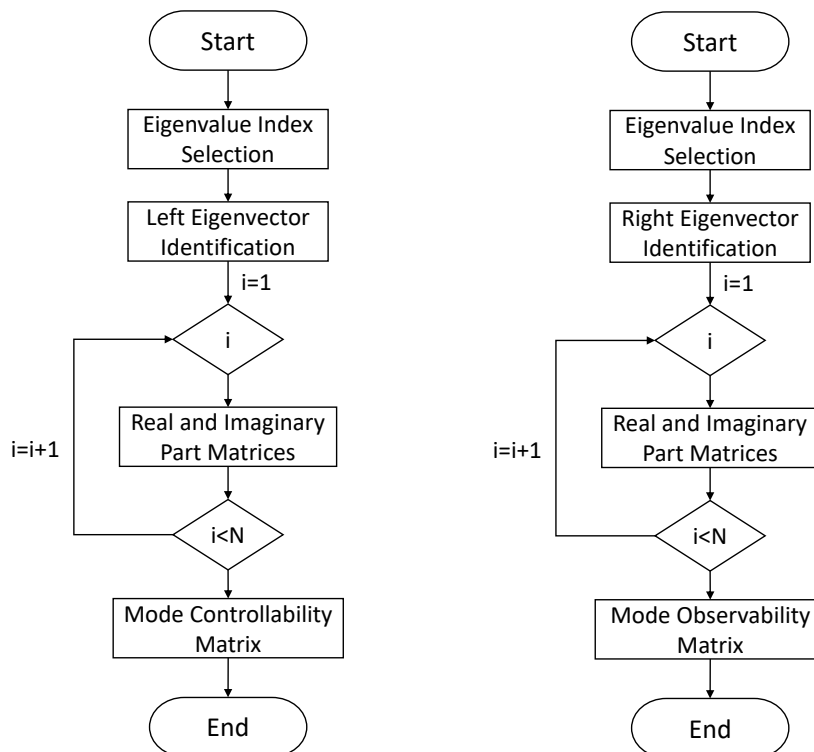
Figure 5.4: The flow chart of Controllability Matrix and Observability Matrix construction [9]

Controllability Index

Controllability indices are obtained by taking into account matrix B and left eigenvector associated with previously selected eigenvalue. This procedure is illustrated in a figure 5.2. Eigenvalue of interest for this project is the one associated with inter-area mode of oscillation, which can be found in "Evals" file generated by Modal analysis [9]. Task is executed by locating the desired eigenvalue based on a manual setting of the range of the imaginary part. The desired eigenvalue should be located between the defined minimum and maximum value. A range should be defined in a way that only one mode is identified. Real and imaginary part of the left eigenvector are used to get the magnitude of the mode controllability, which are further normalized by equation 5.4 in order to get controllability indices exported in the csv file.

Observability Index

Observability indices are obtained similarly to controllability indices, except this time matrix C and the right eigenvector are taken into account. The difference from the procedure explained before is that in this case there is only one output generated per row when matrix C is multiplied with the right eigenvector [9].

This is due to a matrix C only having one nonzero value per row, which is the only one that will give the nonzero output. The output values are observability modes, which are normalized by equation 5.6 to obtain observability indices exported in the *csv* file.

5.4. Wide Area Damping Controller

Modelling of PMUs in this project do not get much attention and they are modelled as voltage measurements that collect voltage magnitude from a desired system bus and feed the signal to wide area damping controller. On the other hand, a WADC is designed to have an ability to collect measurement information from multiple PMUs placed around the system. WADC feeds the generated output value to the main controller of the grid-forming controller of a WT.

The blocks and their corresponding parameters that were used in the WADC are shown in the table 5.1. Initial values assigned to the paraemters are also listed in the table. This values will eventually be adjusted with optimization problem called Particle Swarm Optimization (PSO) to have the highest effect on damping.

Symbol	Value	Symbol	Value
Kpss1 [pu]	1	T1 [s]	5
Kpss2 [pu]	1	T2 [s]	0.4
Kpss3 [pu]	1	T3 [s]	1
Tw [s]	10	T4 [s]	0.1

Table 5.1: Wide area damping controller parameters and initially assigned values.

5.4.1. Controller Design
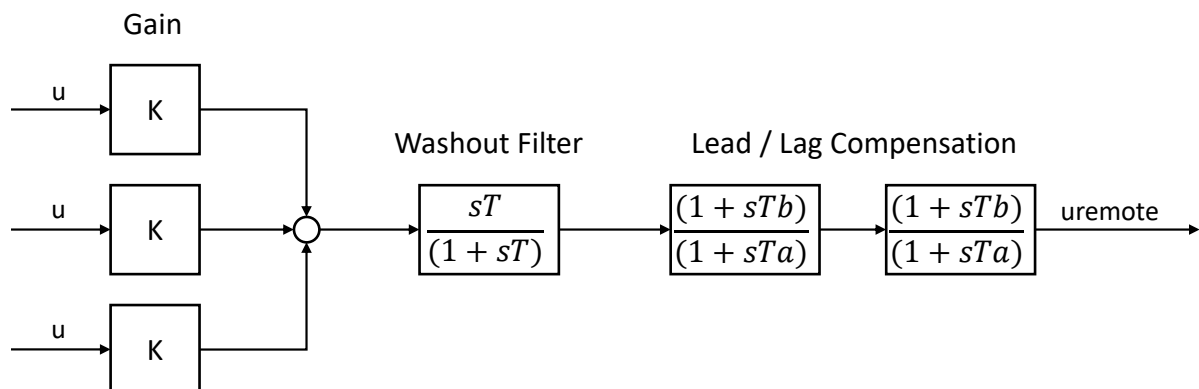
Figure 5.5: Blocks used in designing the wide area damping controller.

The design of a WADC is shown in figure 5.5 and it has a similar design as a PSS block, since they both have damping objectives. WADC implementation into control structure of DVC in Power factory (C.1) and a model of the block (C.2) are located in appendix C. There are three inputs to the wide area damping controller, which are measurements collected by PMUs from the previously defined buses. Locations of those buses are determined based on the input and output signal selection analysis described in the previous section.

Every measurement signals have a corresponding gain block, which are all modelled to have the same initial value. Three measurements imitate three PMUs deployed on generator buses determined by the previously explained methodology. Every signal firstly passes through the gain block so the optimization algorithm can dedicate the appropriate value of gain to the specific input. Such approach enables the option to dedicate higher gain to a specific signal. All three signals are then combined and a signal passes though a washout filter and two lead/ lag compensation blocks. The main intent of the washout filter is to filter out the undesired low-frequency inputs. The main intent of the lead/ lag compensation blocks is to improve the frequency response.

5.4.2. Implementation of the Controller to the Existing Control Structures

WADC is designed to receive synchrophasor measurements from analytically determined locations and has an ability to feed the stabilizing signal to grid-forming controller, more precisely to DVC. Which power plants receive the stabilizing signal is determined by the previously explained method based on the highest controllability method. The obtained value generated by WADC is subtracted from the reference voltage signal in DVC controller, which has a stabilizing effect in the system.

5.5. Tuning of Damping Controller Parameters

Values initially assigned to WADC parameters are not determined based on any analysis. They are implemented in a range of numbers that return a feasible output, however to obtain the desired output these values should be tuned. This means that the software based on a criteria defined by the user tries to find values of the parameters in a defined range to get as close as possible to the desired result.

5.5.1. Optimization Problem Formulation

The optimization problem conducted in this project is a bound constrained signal objective optimization problem with an objective function defined with an equation 5.7 [47]:

$$e = \int_{t0}^{tmax} \sum_{n=1}^{n} \left| (m_i(t) - c_i(t)) w_i \right|^p dt \qquad (5.7)$$

where m_i is a measured response, c_i is a simulated response, w_i is a weighting factor and p is a power.

The bound constraints with initial values are shown in table 5.2. This bounds are set up to limit the possibilities available for determining parameter values. It serves as a pool of available parameters which optimization tool can use to find the overall best solution. The inequality defining the bound constants is shown in 5.8:

$$x_{min} < \mathbf{x} < x_{max} \qquad (5.8)$$

where $\mathbf{x}$ is a vector containing the optimization/ decision variables.

Such bounds were determined based standard limit range of the parameters for PSS found in literature [48] and adjusted for the initial values of the parameters. Experimental work was done to determine the impact of the parameters when the values are moved out of the range and it has been identified that these bounds return a feasible result.

Symbol	Initial Value	Lower Limit	Upper Limit	Symbol	Initial Value	Lower Limit	Upper Limit
Kpss1 [pu]	1	0	5	T1 [s]	5	3	10
Kpss2 [pu]	1	0	5	T2 [s]	0.4	0	1.2
Kpss3 [pu]	1	0	5	T3 [s]	1	0.5	2
Tw [s]	10	5	14	T4 [s]	0.1	0	0.5

Table 5.2: Wide area damping controller parameters and initially assigned values.

5.5.2. Particle Swarm Optimization

PSO algorithm was executed from the inbuilt function in PowerFactory. This option was considered for this project because it produces desired results. However, developing an optimization technique in python and running a script might give better results which could be done in the future. The maximum number of iterations has been set to 1000 iterations and the number of particles has been set to be automatic. PSO is the optimization method selected for this project due to being a robust option for finding the best solution from the set of available solutions. Like the name is suggesting, this algorithm uses a set of particles that behave as a swarm to find a best solution. These particles do not move randomly in the space, since their movement is influenced by the current velocity, previously found best locations and locations found by other particles they are in contact with [36].

The optimization problem is this project has been defined to minimize the oscillations of the remainder of the synchronous generators against each other. The idea was to minimize the difference of generators' speed for them to stop swinging against each other, which would mean that oscillations would damp out in the system. It is important to point out that the optimization process does not effect the results of the Modal analysis. It does on the other hand effect results of the time-domain simulations and consequently results of the Prony analysis.

Three different communication methods between particles for PSO method are possible. The first possibility is the ring strategy, where a particle forms a cyclic topology with the two neighbouring particles. This strategy allows each particle to only communicate with two other particles, which is not the case in a stochastic star communications strategy. In this strategy, every particle communicates with every other particle particle moving in the space. This does not mean that every iteration particle communicates with every other particle, however particle decides randomly whether the communication signal will be received or not. The last communication strategy possible is a done via the reference set, where the set of locations is defined and maintained [36]. It has been decided that for this project the stochastic star strategy is the most appropriate one.
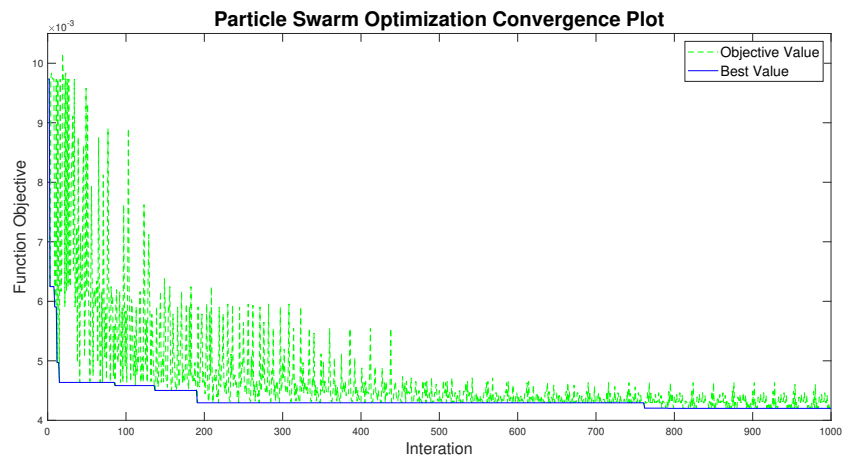
Figure 5.6: Particle Swarm Optimization convergence plot showing the objective plot and the best solution for 1000 iterations.

Figure 5.6 shows the convergence plot of the PSO algorithm for one of the study cases analysed in the results section. More specifically the figure shown is for the study case 7.6, where the green line show the objective values of individual iterations and these values do not improve with iterations. On the other hand, the best value is shown with the blue line and this values either improve or stay the same with the proceeding iteration.
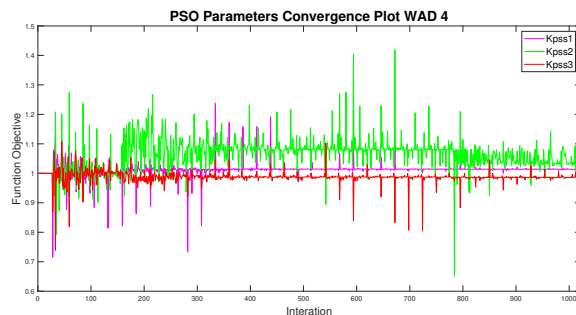
Figure 5.7: Particle Swarm Optimization gain parameters convergence plot for WADC 4.
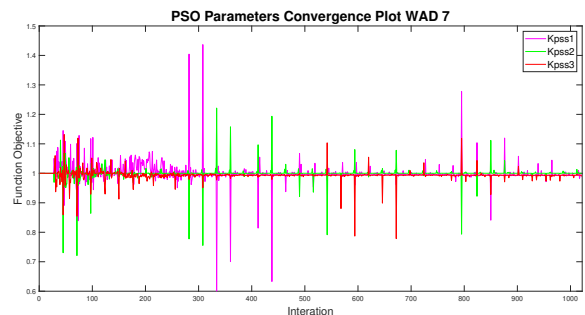
Figure 5.8: Particle Swarm Optimization gain parameters convergence plot for WADC 7.

Figures 5.7 and 5.8 show a parameter convergence plot for gains Kpss1, Kpss2 and Kpss3 for WADC 03 and WADC 07. Converge plot for other WADC parameters is not shown, due to a similar behaviour. Plots shown indicate the values of individual parameters while the PSO algorithm attempts at finding the best overall value as shown in figure 5.6. First part of the figures 5.7 and 5.8 show the initial values of the parameters (1.0) and

then they show value of each parameter determined for every iteration. Important to point out is that the value of parameters during the last iteration is not necessary the value of the best solution, since the best solution might have been found in earlier iterations.

Figure 5.7 shows that during the optimization process it has been determined that gain Kpss 2 should be larger than initial and that gain Kpss3 should be lower than initial. This is all done with an objective of finding the overall best function objective. On the other hand, figure 5.8 highlights the attempt of an algorithm to find the best solution by changing the values of the parameters of the gain. It can be visible that the best objective function has been found with values of the gain parameters of WADC 07 close to its initial value.

Knowledge Utilization: NextGen GridOps Knowledge Framework

NextGen GridOps Knowledge Framework built by DNV, one of the leading energy consultancy companies in Europe, is constructed in Enterprise Architect. The modelling language used for a clear representation and illustration is ArchiMate 3.0. Due to confidentiality of the NextGen GridOps Framework structure, only a limited amount of the framework structure will be explained here; enough for making a clear story-line and highlighting the importance of such a tool.
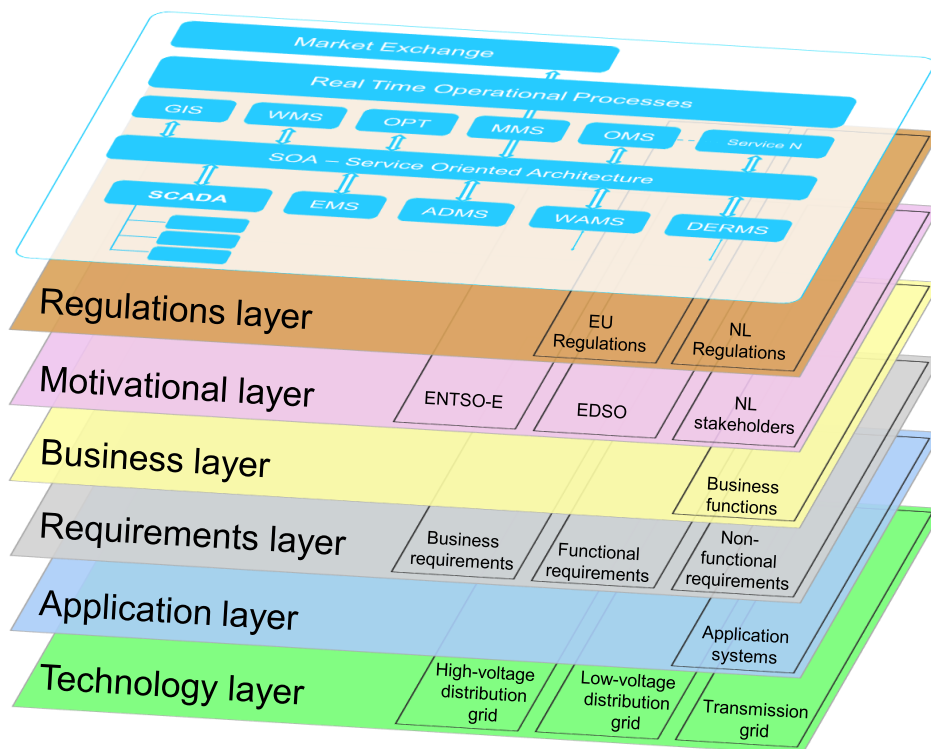
Figure 6.1: NextGen GridOps Framework structure.

Figure 6.1 shows the layers defined in the NextGen GridOps Knowledge Framework. Each layers consists of corresponding information and the whole process of future grid operations can be created by combining information from each layer. One layer collects recent and historic regulations, next layer indicates all stakeholders, another layer defines technical and non-technical requirements. Information implemented in

the framework collects knowledge gained through European projects, published regulations, lists of vendors with corresponding evaluations and individually developed processes valuable for future implementations. Work done in this thesis project mainly focuses on the bottom three layers; requirements, application and technology layer. Knowledge gained was focused on the transmission grid, where individual and a group of applications of the Grid Operations Machine were studied based on predefined requirements.

6.1. Motivation

NextGen GridOps Framework is important from two very different perspectives. This framework allows putting all of the recently researched and developed solutions into practice, which is very important from technological point of view. However, we should not forget that this tool is developed by DNV to allow them next generation of consulting. It allows DNV to provide the most complete solutions to their clients by taking an advanced approach when developing projects; referring to a pool of high quality information of previous projects, updated standards and corresponding linked information. This does not only allow solving a problem but also foreseeing some of the issues that might be raised in the future.

A goal for DNV is to gain interest of their current and new clients about consultancy they are able to provide due to a framework they have developed. A framework would be their internal tool for accelerated process and higher quality result, without any intentions of selling the framework itself. Words of their development and marketing team is that they are trying to sell themselves and not a framework. Framework would position them a step ahead of the competition, for their own benefit and also for benefit of the society.

Looking from a broader picture, this framework can contribute to a smoother transition towards a green energy generation and reduction of CO_2 emissions. This tool can enable putting developed solutions into a real-world, since DNV, an energy consultant, will be using framework during project development. This point brings us to the most important aspect of the framework, which is that in order to exploit the potential of the framework to the fullest this framework needs to be used regularly by DNV employees.

6.2. NextGen GridOps Framework for Project Development
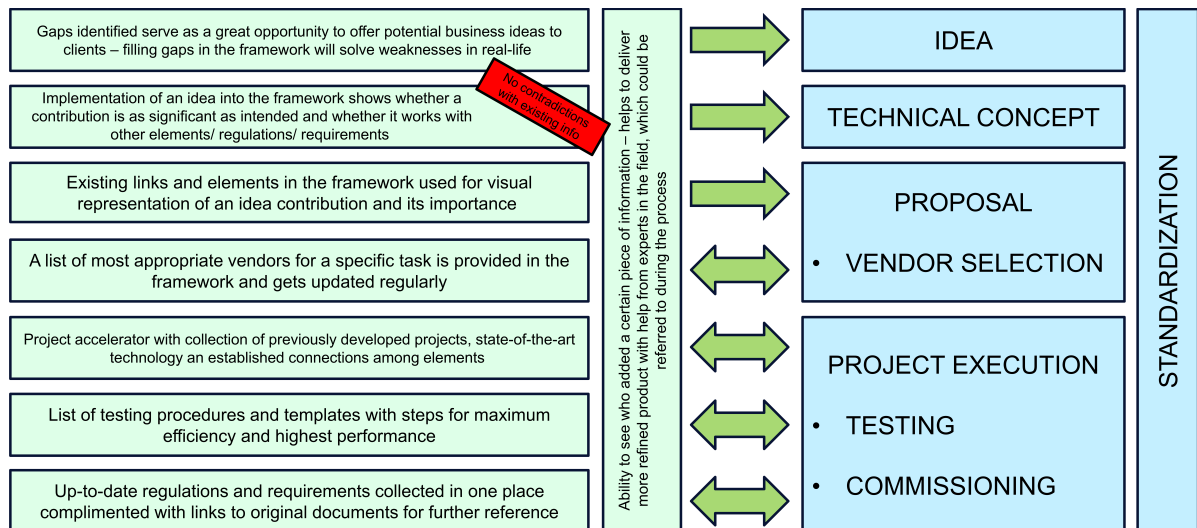
Figure 6.2: Benefits of using NextGen GridOps Framework during project development.

The easiest way to show and explain benefits of NextGen GridOps Framework is by showing how it will improve and accelerate projects done by DNV. The following table 6.2 was generated in an attempt to demonstrate benefits of the framework during every step of developing a project. Green boxes on the left part of the figure indicate benefits brought by the framework for the steps of the project development collected in blue boxes on the right side. Note that arrows pointing from left to right indicate how information from the framework is used for development of a specific project step. While arrows pointing in both directions represent that a framework also consists of information that can be referred to and such information can later be ap-

plied to a project.

A complexity of projects developed by DNV has been the main motivator for development of the NextGen GridOps Framework and benefits of such a structure are outlined with a link to some concrete steps of the process. One of the biggest benefits of the framework is a clear indication who implemented a certain piece of information to the framework. It is assumed a person is an expert in a topic and such a person can be consulted in case of any delays or arising challenges on the way. It also enables a verification of implemented information in cases when additional explanation and potential modifications are required.

An **Idea** born and presented to clients can be based on gaps identified in the NextGen GridOps Framework, where a collection of information in the framework illustrates which areas of future grid operations would require improvements or updates. Gaps or areas of improvement are identified based on an assumption that the framework represents a complete knowledge pool with every project and each piece of information implemented in the framework. Note that it is hard to implement every piece of information developed, which means that proposed ideas have to be checked before presented to management or clients.

A **Technical Concept** can be constructed with implementing newly constructed idea into the framework and observing the impacts such modification has in the framework. When an idea is implemented to the existing structure it becomes clear whether an idea will have an intended effect on issues and impacts previously indicated. It is important to realize whether solutions are compatible with other technology and regulations and they do not contradict with other information. However, due to the nature of framework this task can be accelerated due to the existing information and connection between elements.

Existing elements, links among them and implementation of a new solution can highlight an importance while writing a **Proposal**. Structure in Enterprise Architect enables a clear visual representation, which enables higher quality and more effective documents. NextGen GridOps Framework also consists of a vendors list with corresponding indication which vendors are most appropriate for a specific tasks. This is highly beneficial during **Vendor Selection** process, since it allows fast, efficient and effective selection of most appropriate vendors. It is important for DNV employees to update lists of vendors regularly, so this process can be further optimized with better criteria for selection process. DNV should conduct vendor benchmark analysis for different applications to have the information pool prepared once they are asked for their recommendations.

Another benefits of DNV's knowledge framework is to serve as a project accelerator, which means that the **Project Execution** is faster and more efficient. It is important to keep in mind that using such a tool dos not compromise the quality of a product and it should increase the quality of service. This is possible due to a large amount of previously developed information implemented in the framework in a structured way, so developed information can be recalled when needed. **Testing** can be done with higher efficiency when using the framework, due to implemented testing procedures. This procedures offer guidance and in advance prepared templates with defined steps that are advised to be followed for maximum efficiency. An access to up-to-date collection of regulations is significantly valuable for **Commissioning** of the project and it provides a clients with trust in projects supervised by DNV. The framework does not only contain requirements implemented in the framework but also links to original documents for further reference. **Standardization** is done throughout the whole process of project development, to enable even more efficient process in the future. If the full potential of the whole procedure explained will come into fruition only depends on the extent of DNV employees using the tool.

6.3. MIGRATE Implementation in NextGen GridOps Framework

The main intent of implementing information from various different projects to DNV's framework is to put the developed solutions into practice. It would allow DNV to base their business on innovative solutions developed in projects. It can be explained as collecting public information and developments, placing and organizing them in the framework and later use them when conducting business. With successful implementation of information from many projects, the organization and structure of such information will play a crucial role in exploiting framework to the fullest and all its benefits. There might be many different strategies in organizing and structuring information, so that it can later be recalled and used. A methodology developed throughout this project is shown in figure 6.3, where a top to bottom approach is adopted. It is important to clarify that there is no universal solution to what is a correct way of implementing information, since the

framework and an idea is still in its early development. Figures highlighting implementation of MIGRATE results related to stability issues are shown in appendix A.
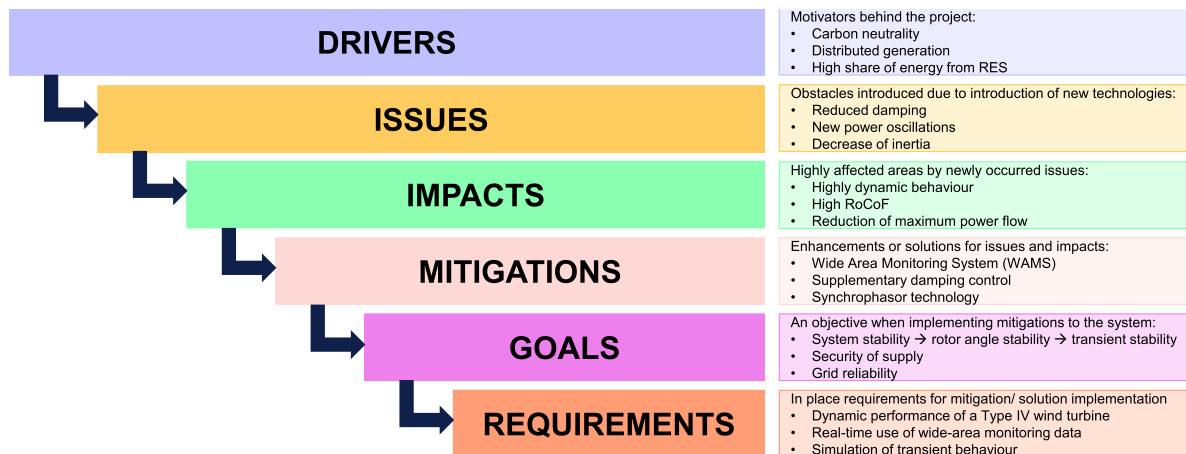
Figure 6.3: Steps of modelling information into NextGen GridOps Framework.

Drivers

The first step of implementing information in this specific methodology begins with the top layer where drivers are located. It provides a clear motivation for conducting a specific project. This level identifies ideas, concerns and initiatives, which were pointed out and proposed for accomplishing an improvement in society. The effects of such an idea as well as specific technical solutions are unknown while proposing new trends. It serves as a clearly defined scope of the project, since it points out what initiatives were taken into consideration when solutions were developed for newly raised issues.

The most important driver behind a MIGRATE Project is an intent to eliminate sources of CO_2 emissions and to become carbon neutral in the near future. Other drivers identified, which are all dictated by carbon neutrality, are decommissioning of large fossil fuel power plants and replacing such generation loss with high penetration of RES. RES like wind energy and solar energy are currently energy sources that draw high attention due to its low running costs. This means that large centralized power plant would be replaced by smaller capacity decentralized energy generators, which would also be able to balance an anticipated increase in energy demand and prevent any congestions that might follow in the existing power grid infrastructure.

Issues

Anticipated as well as unanticipated issues are usually risen due to newly proposed initiative and modifications made to the existing power grid. These issues can be explained as obstacles that occur while making necessary modifications towards fulfilling motivators explained in the previous level. They prevent a smooth integration of desired technology and research is needed to implement proposed technology into a real world. Issues do not occur with every single initiative and modification made, however in those cases there is no need for additional research and project development. A framework is crucial in instances when issues do occur and feasible mitigations have been developed. A framework is useful where significant amount of information has been developed during a project and knowledge can later be applied in some other projects.

Linking this step to MIGRATE project, a conventional power grid is designed to transfer power from a massive power generators, over transmission and distribution infrastructure to energy consumers. Even though this concept has been working for a very long time, it will not be able to comprehend the transition towards green energy generation. The existing power grid will have to be modified by making use of advanced and smart solutions to make use of distributed energy generation. Reduced damping and lack of inertia will be some of the issues that will follow after a large majority of synchronous generators will be decommissioned. Distributed power generators will cause an introduction of new power oscillations, where inter-area oscillations have a significant impact on characteristics of the power grid.

Impacts

This layer gives a final assessment of the impacts that were introduced to the grid with an implementation of new technologies. Elements modelled has an impact on a specific characteristic of the grid, which may

cause significant financial or technical challenges to system operators. It is indicated where biggest loses and challenges in a physical domain will occur and which areas will need the most attention. In simplified terms, system operators will be able to identify issues in their grid by paying attention to indicators listed in this section. These indicators will enable operators to take correct actions in order to mitigate any issues that might have risen in the grid. A description of this layer will become more clear with an explanation of the following example.

Issues presented before are an occurrence of new power oscillations and reduced ability to damp these oscillations by implementing PE interfaced generation. A system operator will observe this issues by examining the impact of those issues on some basic characteristics of the grid, such as frequency, voltage and power flow. New oscillations will cause a reduction of a maximum power flow and system operators will be looking for possible explanation for these losses. Another example is that a high ROCOF will identify a lack of inertia in the system and that emulated inertia has to be introduced to the grid.

Mitigations

Information implemented and explained up to this point summarizes what was decided that the future trends will look like and then what will occur as a consequence of linking such technology in the power grid. Presence of solutions explained in this section will eventually allow the deployment of intended progress by mitigating issues that hinder the overall system stability. These mitigations might either be a new device that can be implemented in the grid, it can be a new control structure, proposed physical modifications or enhancement of the existing grid. It might be taking advantage of new communication technologies or technologies that enable a better understanding of what is happening in the grid and what is system's state. Every process, technology and idea enhancing system stability is eventually grouped in this section. Methodology followed thus far serves for mitigating very specific issues that were identified during development of a particular project, however a challenging part is how to use this well developed solutions for future applications. In this particular strategy of knowledge implementation this is done by determining goals. Those goals can later be linked to requirements, which can recall implemented mitigations for future purposes.

In context of MIGRATE project, an occurrence of inter-area oscillations with integration of RES is identified as the main issue. Such complex problems are difficult to completely solve, which is why solutions proposed are classified as mitigations. During MIGRATE project it has been identified that WAMS and making use of PMUs with synchrophasor technology is able to significantly improve this issues with improving observability and controllability of the test system. Another mitigation proposed which is able to tackle an issue of reduced damping is implementation of a supplementary damping controller, which is able to produce a stabilizing signal which in combination with a local signal reduces the occurrence of critical OMs.

Goals

Elements modelled as goals serve as an objective for implementing mitigations to the system, meaning that a specific mitigation is implemented with a intent to achieve a certain goal. These goals are defined as a global system objectives and they are motivated by how should an ideal system behave. It is important to note that perfect and ideal will never be achieved in real world, but well designed solutions can help bring a system closer to such objectives. Elements in this layer are modelled as if these solutions were actually achieved, where an intent is to emphasize a goal achieved by introducing proposed mitigations.

Solutions based on WAMS an PMU technology are developed throughout this project with an intent to enhance system stability, more precisely rotor-angle stability. Both aspects of a rotor angle stability, transient stability as well as small-signal stability are enhanced by using WAMS. Consequently, security of supply was also enhanced with such technology, since a power grid enhanced with such solutions is less prone towards blackouts and system splitting. Similarly, grid reliability is also affected by similar solutions, which was identified based on making use of DNV's framework. This goal is listed even though that mitigations researched in this project were not developed specifically for this goal.

Requirements

This layers consist of requirements defined by regulatory institutions; during this project the focus was on requirements defined by European Commission and those requirements might not be relevant in other parts of the world. NextGen GridOps Framework consisted of network codes for different requirements and corresponding articles were implemented as a reference. These individual elements can be linked to requirements specified under each project implemented and with an ability to display relationship it is possible to

later recall projects with similar requirements. This strategy allows locating mitigations compliant with requirements of interest from different parts of the framework and it allows to categorize and trace solutions appropriate for new applications. This way not only mitigations are traced to specific requirements, but also desired goals as well as any possible issues and impacts that might occur without a proper attention.

Requirements identified and applicable for this projects are the ones that deal with goals mentioned before and with generation technology applied in this project. An important requirement was a dynamic performance of the Type 4 WT, since they are heavily implemented in this project. Furthermore, significant attention was on requirements associated with WAMS and real-time use of wide-area monitoring data. Unfortunately, not every requirement identified in this project was able to be linked to an article of network codes, due to a novice nature of technology and some of the recent technologies have not yet been implemented.

6.4. Maturity Level of WAMS Application and Roadmap Planning

During the process of implementing findings of Horizon 2020 MIGRATE Project it has been identified that one of the main mitigations/ solutions for issues and impacts raised with implementation of new technologies is WAMS; hence the empirical study has been done on the test system to show the benefits of taking advantage of such a solution. A successful implementation and noticeable improvements with implementation of WAMS technology calls for a real world implementation; a main reason behind conduction such a study. NextGen GridOps Framework makes such an implementation possible, with motivating DNV employees to start conducting business based on WAMS technology.

There is a broad range of clients that are taking advantage of DNV's services, meaning that every client will be looking for services that fit their level of development and level of developed infrastructure. More precisely, some costumers would need to make very specific modifications or expansions to their domain and those will be listed for them in the framework in advance. In some instances, clients are ready to make a step forward, however the infrastructure around them is not ready for an implementation of advanced technology. In that instance, a roadmap for the future can be made for them, with a clear vision and requirement that would make an implementation possible.

A five level maturity level structure was developed, which will enable maturity level identification of different clients and different levels of WAMS implementation during massive integration of PE devices. Level 0 identifies a client who is very novice to WAMS technology implementation, while Level 4 identifies a client with very advanced WAMS functionalities implemented in their domain. Information about each level is summarized in a table 6.1 and each level is described in detail below.

PHASE	INITIATED	PILOTED	DEPLOYED	INTEGRATED	OPTIMIZED
	Level 0	Level 1	Level 2	Level 3	Level 4
Identification parameters for effective classification	• No PMUs installed • No WAMS architecture • No signal exchange – WAMS context • No damping controller • No communication channels • No communication protocols	• Random/ experimental implementation of PMUs • Use of WAMS + SCADA and EMS • Supplementary role of WAMS • Communication infrastructure in place	• Signals provided by PMUs • PMUs located on analytically determined buses • Signals fed to mainly to synchronous generators • No use of supplementary damping controller	• Damping controller • Analytically determined location of controllers • Damping controller signal combined with a local signal • Advanced communication infrastructure	• Damping controller parameters tuned • Damping controller affects a desired mode • Preserving CAPEX and OPEX with placement of PMUs and controllers • Effective observability and controllability

Requirements for progression – roadmap definition	• Implementation of test PMUs
	• Introduction of protocol:
	  • IEEE C37.118,
	  • IEEE C37.242,
	  • IEEE C37.244
	• Signal synchronization based on GPS
		• Identification of oscillation modes (Modal, Prony)
		• Input/ output signal selection (GOCM)
		• Installation of fiber optic infrastructure → long distance communication
			• Damping controller design
			• Installation of satellite communication infrastructure
			• Installation of wireless communication infrastructure
				• Use of optimization techniques → controller parameters tuning
				• Optimal PMU placement based on cost-effectiveness analysis
					• Further optimization and cost-reduction
					• Ability to adapt WAMS to grid expansions
					• Ability to adapt WAMS to new regulations and protocols

Table 6.1: Stages of WAMS implementation.

Level 0

When a client is interested to make a first step towards WAMS technology, they are identified as Level 0. It means that this specific client is using an existing SCADA system and in order for a client to cope with recent

technological developments they are required to begin with implementation of some basic WAMS elements. A client is categorized into this category if there are no PMUs implemented on any buses in their power grid and there is no WAMS architecture in place. Consequently, there is no signal exchange in WAMS context and there are no communication channels and protocols implemented for this technology. Furthermore, supplementary damping controllers are not introduced in addition to local controllers located on synchronous generators to damp local or inter-area oscillation.

There are a certain requirements for a client to follow in order to proceed from a level 0 to Level 1 and DNV can suggest next steps based on the scheme modelled in NextGen GridOps Framework. A first step should be for a client to implement a couple of test PMUs to the system, to get familiar with the procedure and implement basic requirements for a working WAMS infrastructure. During this process there is a collection of protocols that should be followed and some of them are IEEE C37.118, IEEE C37.242 and IEEE C37.244 [49]. IEEE C37.118 is responsible for transformation of data to phasors and data sampling synchronization. IEEE C37.242 standard is a guide for testing and implementation of PMUs, while IEEE C37.244 standard is responsible for Phasor Data Concentrator (PDC) communications and requirements. Another important aspect of this transition is to make sure that infrastructure for signal synchronization via GPS is in place for future applications.

Level 1

A client is categorized in this level if there are already some PMUs in a power system, however a nature of such implementation is more random or in sense experimental. WAMS system used is not a standalone system yet and it is more of a supplementary system to support convectional SCADA and EMS. Some of the signals received from PMUs installed on some of the buses may be used as a reference to support the accuracy of the existing conventional monitoring systems in place. Data transfer from PMUs to PDCs is done via Power Line Communication (PLC), however this technology can only be used for small data transfer and not over a very long distance. Once a client has a more developed WAMS technology, there should be some other means of data transfer in place.

Services offered to a client to move to another level become more advanced, where the first task is identification of oscillations modes. This can be done by methods such as Modal analysis and Prony analysis and these are able to identify eigenvalues, damping ratio and frequency. These methods determine the stability of the system and how well some of the critical modes of oscillations are damped. Similarly, input and output signal selection should not be random anymore and proposed methods should rather be followed. A highly used method for signal selection is Observability/ Controllability Method, however there are also some other techniques available. Furthermore, an investment towards a fiber optic infrastructure should be made, which would make large data transfer and long distance communication more affordable.

Level 2

Clients, whose WAMS infrastructure is developed to the extend where SCADA and conventional monitoring system for system operations are not needed anymore, are labeled as level 2. Such development allows a use of PMUs to provide signals which allow fast dynamic analysis of the system. In addition to experimental buses implemented in the early steps, PMUs have to be installed on all critical buses, where the highest level of observability is available. There might also be some extra PMUs installed in the system, which would serve as a back up since clients would rather make a higher investment to prevent any potential blind spots in the system. Signals from WAMS are fed to synchronous generators rather than to RES, even though there are already some RES implemented in the power grid. Furthermore, there is no supplementary damping controller in place and signals from WAMS are directly fed into the generators. This stage could also be labeled as taking advantage of a signal from a remote or critical buses.

This kind of wide-are monitoring structure is already able to stabilize the system and damp some of the oscillations, however WAMS can offer more than was explored up to this point. The first large improvement made in this case can be implementation of an additional controller, whose duty is to damp critical oscillation modes and further stabilize the system. Another possible improvement might be an installation of satellite or wireless communication, which would allow exchange of data from different parts of the world and exchange of data from different system operators. Countries in European power grid are connected to each other, which allows power to flow to different countries and reduces possibilities of congestion occurrence. That is the reason why also data should be exchanged among different parties, so system operators know what is happening in the neighboring power grids.

Level 3

A supplementary damping controller implemented is able to enhance damping of poorly damped low frequency oscillation modes, which means that low-frequency oscillations will be less dominant in the system. This has been verified by performing Modal analysis and Prony analysis for different case scenarios with different network variations. It has been also verified by running time domain simulations for generator speed of the remainder of generators. A stabilizing global signal provided by a damping controller is combined with local controllers such as PSS and AVR and this combination is much more effective then just local control signals. In this case the damping signal from WAMS structure is not only feed to synchronous machines, but to whichever power plant is decided to have the best stabilizing ability. Advanced communication infrastructure allows exchange of data among different system operators, which helps finding a cause of certain oscillations in the system. Oscillations that occur at a certain point in the system can travel in the network and cause issues in a completely different area. That is why it is important to have a transparent system and have an insight into other parts of the network even if they are operated by a different entity.

A damping controller can be fully exploited by tuning parameters, so the effect of damping the desired OMs can be maximized. It is desired for a supplementary damping controller to only have an effect on a desired critical modes of oscillation and at the same time should not have any impact on other modes. Stable modes should not be affected by a controller, otherwise there are some issues in the process of damping oscillations. Signals provided by PMUs distributed around the grid accurately represent the state of the system, however not every PMU in the grid might be required in order for a system operator to have a clear representation of the system's internal condition. Having a larger number of PMUs in the grid requires high initial and running costs and at the same time having more chances of failure. At the same time, in case of a failure there might be good to have some extra PMUs in the grid to prevent any black spots.

Level 4

Most advanced level of WAMS applications is reserved for clients with the entire WAMS infrastructure in place, with tuned controllers and cost-efficient number of PMUs. Block parameters of a supplementary damping controller such as lead-lag, washout and gain block are tuned according to highest damping achieved of desired OMs while not affecting any other modes in the system. Furthermore, PMUs are installed on buses with highest observability and no additional PMUs are installed. Signals provided to WAMS and signals fed to damping controllers allow observability as well as controllability of the system, which means that system operators see in heart bit of the system in real time. They would have an ability to control the grid to compensate for any events that might cause stability or some other issues in the grid.

Even though this is the highest of maturity levels of WAMS implementation, there is always room for improvements. This goes for optimizing daily operation or implementation of new technologies that will be developed in the near future. Furthermore, system operators should always have an infrastructure prepared to quickly adapt to any possible grid expansions or other modifications done to the grid. Even further improvements of WAMS strategy can occur in case that a future power grid will be viewed as a whole rather than each system operator taking care of its own domain.

7

Case Studies & Simulation Results

The outline of this chapter is structured to guide a reader from the existing standardized IEEE 39 Bus New England system towards the proposed solution of the future power grid with massive penetration of RES. First four study cases are shown to demonstrate the base case and what has been proposed during MIGRATE project. The intent is to show level of RES penetration with only grid-following control and penetration of RES with two different grid-forming controllers.

Dynamic Behaviour of Different Network Variations:

1. **Section 7.2** - Study Case 1: Dynamic Behaviour of 10 Synchronous Generators

2. **Section 7.3** - Study Case 2: Dynamic Behaviour of 4 Synchronous Generators and 6 WT with Grid-Following Control

3. **Section 7.4** - Study Case 3: Dynamic Behaviour of 2 Synchronous Generators and 8 DVC

4. **Section 7.5** - Study Case 4: Dynamic Behaviour of 2 Synchronous Generators and 8 VSM

Secondly, study cases are presented with an intention to show the behaviour of the modified system with grid-forming controllers on all WT connected to the system with associated WADCs. Furthermore, study system is modified with an intent to mimic more realistic behaviour with different grid-forming and grid-following control structures.

Dynamic Behaviour of Different Network Variations with WAMS:

1. **Section 7.6** - Case Study 5: WAMS with 2 Synchronous Generators and 8 DVC with 8 WADC

2. **Section 7.7** - Case Study 6: WAMS with 2 Synchronous Generators and 8 DVC with 3 WADC

3. **Section 7.8** - Case Study 7: WAMS with 2 Synchronous Generators, 4 DVC and 4 WT with Grid-Following Control

4. **Section 7.9** - Case Study 8: WAMS with 2 Synchronous Generators, 3 DVC, 1VSM and 4 WT with Grid-Following Control

NOTE: It is important to note that whenever talking about the number of WTs implemented, those actually represent the WTs with current control and whenever WTs have grid-forming control they are indicated by the name of the grid-forming controller (either DVC or VSM).

7.1. Load Flow Analysis of Standardized and Modified IEEE 39-Bus New England Test System

A load flow analysis is performed to evaluate the flow of active power (P) and reactive power (Q) in the power system in a steady-state condition. Furthermore, bus voltages (V) and their phase angles (θ) are determined during such an analysis [50]. This is an important step for investigating the operational state of the system under a given loading and the limits of the system can be highlighted by conducing such an analysis. The classification of buses present in the system is as follows: Generator Bus (P-V bus), Load Bus (P-Q bus) and

Slack bus, which is a reference bus in the system [47]. A load flow method used in PowerFactory is a Newton-Raphson method, which is a method suitable for an analysis of larger power systems. A dispatch of individual power plants of the test system as well as voltages are summarized in table 7.1.

Gen	1	2	3	4	5	6	7	8	9	10
P (MW)	1000	-	650	632	508	650	560	540	830	250
V (p.u.)	1.03	0.982	0.9831	0.9972	1.0123	1.0493	1.0635	1.0278	1.0265	1.0475

Table 7.1: Generator dispatch and voltages.

Performing a load flow analysis before studying the dynamic behaviour ensures that the elements in the grid are connected correctly and their initial properties satisfy the load balance. Load flow analysis determines whether generation is able to match the system demand and indicates whether the lines and transformers present in the system are modelled correctly to be able to withstand the loading. Voltage levels on all system buses are identified, which might identify possible issues in the system. Making sure that the load flow converges is the first step in successfully modelling and modifying the test grid and later focus can be towards the dynamic properties and control structures associated to the power plants connected.

7.1.1. 10 Synchronous Generators

One line diagram of 10 synchronous generators connected in the system is shown in figure 7.1, where 100% of electricity is generated by synchronous machines. This represents the base case model built according to standardized test system. Each machine is modelled according to reference provided by DIgSILENT PowerFactory [39], where generators G02 to G09 are considered as steam turbines and generator G10 is considered as a hydro turbine. Generator G01 is modelled as an extension of the power grid, which is not modelled in detail. Figure 7.1 indicates the voltage levels in the system, ranging from 16.5 kV on generator buses to 345 kV on the majority of other buses in the system. There are some other buses in the system with other voltage levels as indicated in the legend.
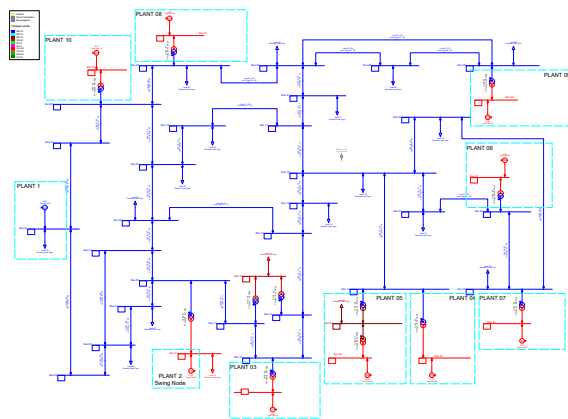
Figure 7.1: One line diagram of a test system with 10 SGs.
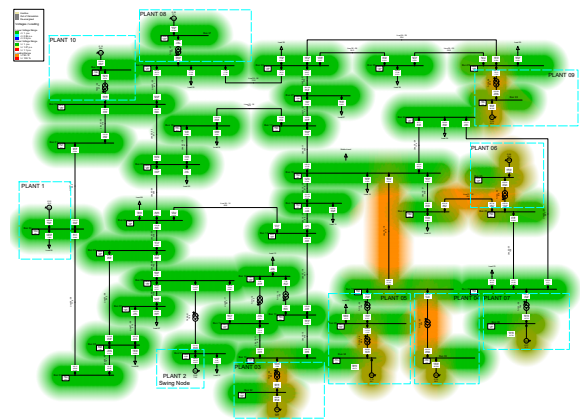
Figure 7.2: Load flow of a test system with 10 SGs.

A heatmap of the load flow analysis of the standardized test system with 10 synchronous generators is shown in figure 7.2, where is visible that the load flow converges and that the test system is well balanced. There are no congestions in the system, however there are some lines and transformers that are heavily loaded. Heavily loaded lines and transformers are working close to their limits in order to balance the demand in the system. Right part of the system might be working closer to their operational limits, as indicated with orange colors for Line 16 - 19 and Line 21 - 22 and transformers associated with generators G03, G04, G05, G06 and G09.

7.1.2. 4 Synchronous Generators and 6 Grid Following Control

One line diagram of the system with 4 SGs and with 6 WTs with grid following control is presented in figure 7.3. Horizon 2020 MIGRATE Project has determined that 60% penetration of RES can be connected to the grid with

grid-following control [51]. Such network topology was studied to verify results from MIGRATE Project and later case studies demonstrate the ability of grid forming control to surpass the 60% penetration and show better stabilizing ability of grid forming control.
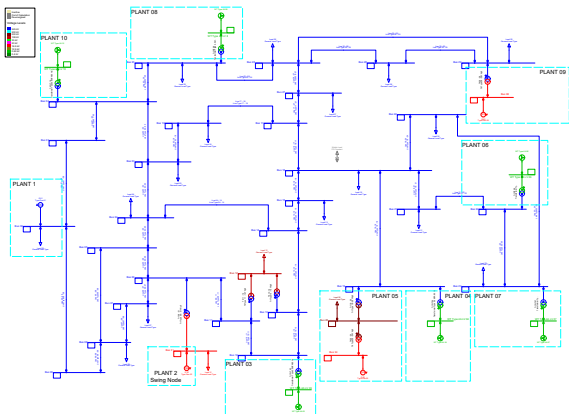
Figure 7.3: One line diagram of a test system with 4 SGs and with 6 wind turbines with grid following control.
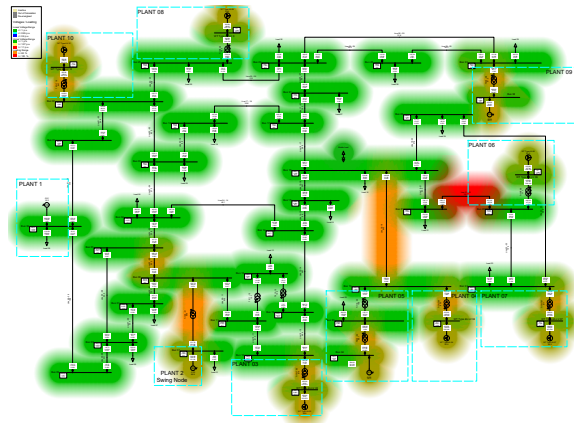
Figure 7.4: Load flow of a test system with 4 SGs and with 6 wind turbines with grid following control.

Figure 7.4 show the heatmap of such system, where high loading is visible in Line 21-22. It is visible that the limit of the line is exceeded by 1.9%, however the load flow was able to converge and no additional modifications were made to the system to decrease the loading of the line.

7.1.3. 2 Synchronous Generators and 8 Direct Voltage Controllers

One line diagram of the test system with 80% penetration of RES is shown in figure 7.5, where eight power plants are represented by WTs instead of synchronous machines. The power output of each power plant is equal as before and the voltages levels are equal as described for the previous case. Furthermore, the load flow of the system is able to converge despite the modifications made to the system, which indicates that demand is satisfied by the power produced by synchronous machines and WTs.

The output power of each wind turbine park was modelled to have the constant power output, since it is out of the scope of this project to study the effects of stochastic availability of natural resources on system stability. There is the possibility to model the output of wind turbines based on the speed of the wind, which could be a topic for further research in the area of massive penetration of PE devices.
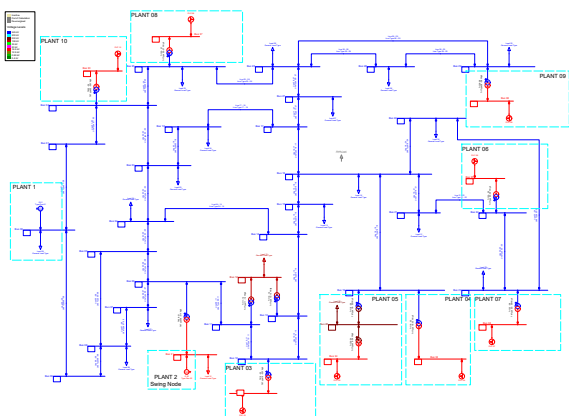
Figure 7.5: One line diagram of a test system with 2 SGs and with 8 wind turbines with DVC.

Figure 7.6: Load flow of a test system with 2 SGs and with 8 wind turbines with DVC.

There are no congestions in the system and the same lines are heavily loaded as indicated in the base case as visible from in heatmap 7.6. Line 21-22, connecting bus 21 and bus 22, operates closest to its limits out of all the lines in the system with a value of 99.1%. A transformer connecting bus 20 and bus 34, is loaded 88.0%,

which is more than any other transformer in the system. Such steady-state behaviour of the test system is reasonable and no adjustments are required to improve the behaviour.

7.1.4. 2 Synchronous Generators, 4 Direct Voltage Controllers and 4 Wind Turbines with Current Control

Figure 7.7 shows a one line diagram of the system with presence of synchronous generators and WTs with grid-forming voltage control and grid-following current control. Synchronous generators are connected to the same buses as in the previous cases, however four DVC were replaced with WT with current control as it can be seen in the figure. This case is oriented towards more realistic implementation of RES to the power grid, where not every wind power park will have a grid-forming control associated. This goes specifically towards WTs already implemented with current control and it would be cost inefficient to replace existing controllers on WTs.
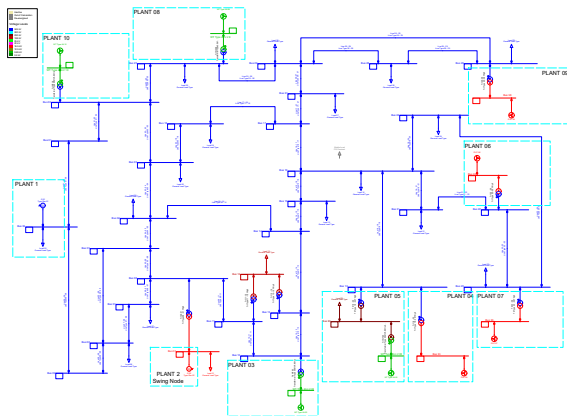
Figure 7.7: One line diagram of a test system with 2 SGs, 4 wind turbines with DVC and 4 wind turbines with current control.
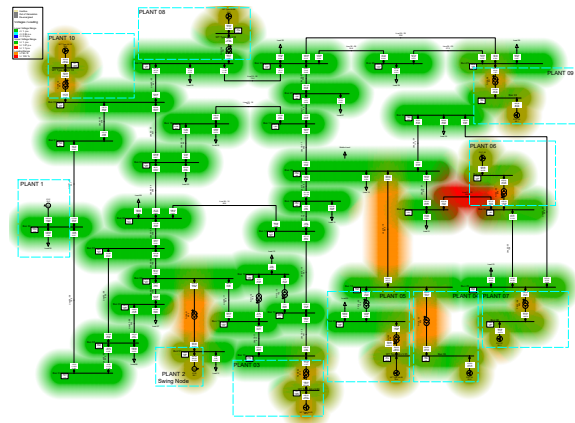
Figure 7.8: Load flow of a test system with 2 SGs, 4 wind turbines with DVC and 4 wind turbines with current control.

A heatmap with presence of grid-forming and grid-following control is shown in figure 7.8 and due to an implementation of type 4 WTs and associated transformers there is an occurrence of a congestion in Line 21-22. Transformers associated with type 4 WTs are modelled differently compared to transformers associated with synchronous generators and WTs with grid-forming controllers. The congestion does not have a massive effect on the performance of the system, since the load flow of the system converges successfully. Such heatmap can indicate a future bottleneck with increased penetration of sources of renewable energy. Such observation might be a good indicator for any future grid expansions. To mitigate potential loses there must be either some new hardware installed or any other sources of distributed energy generation or storage solutions with intent of reducing congestion in the line.

7.1.5. 2 Synchronous Generators, 3 Direct Voltage Controllers, 1 Virtual Synchronous Machine and 4 Wind Turbines with Current Control

One of the objectives for this project was to use different type of grid-forming controllers and evaluate their performance and ability to stabilize the system with massive penetration of PE devices. That is the reason why a controller on one WT was changed from DVC to VSM as indicated in figure 7.9. This figure represents one line diagram of the system which has a VSM associated with power plant 09 compared to DVC in the previous case. The system still includes four grid-following controllers and two synchronous machines.

Heatmap shown in figure 7.10 indicates a similar problem with a line congestion as in the previous case. This congestion is a result of an introduction of a type 4 WTs with current control and associated transformer. Transformer associated with a grid-following controller is modelled differently compared to a transformer associated with other generators. The loading of the line exceeds the limit of the line however the load flow is still able to successfully converge.
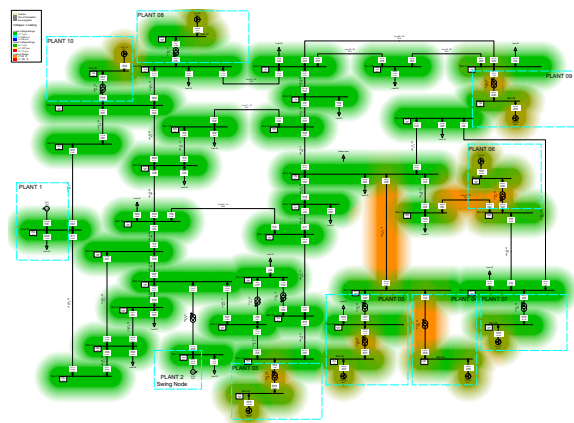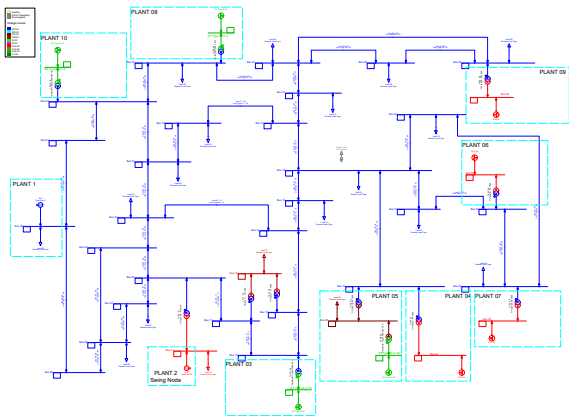
Figure 7.9: One line diagram of a test system with 2 SGs, 3 wind turbines with DVC, 1 wind turbine with VSM and 4 wind turbines with current control.
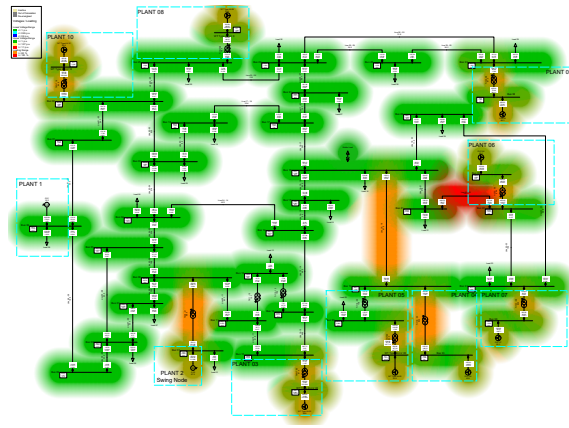
Figure 7.10: Load flow of a test system with 2 synchronous generators, 3 wind turbines with direct voltage control, 1 wind turbine with virtual synchronous machine and 4 wind turbines with current control.

7.2. Case Study 1: Dynamic Behaviour of 10 SG

A dynamic analysis was performed on the standard and unmodified test system to understand the stability and the expected behavior of the current power grid after being subjected to a disturbance. This enables to compare the obtained results of the modified test grids to the base case scenario with 100% penetration of synchronous generation. Final design can be validated by following such an approach, which offers a certain degree of confidence in the proposed approach and obtained results.

7.2.1. Time Domain Simulations

Figure 7.11 indicates a speed of 10 synchronous generators after being subjected to a short circuit event on the Line 16-24 at time = 1 s. A short circuit event is cleared after 0.15 seconds at t = 1.15 s. An event is modelled as a short circuit event with fault impedance characteristics of 1.5 Ohm resistance and 15 Ohm reactance. Such fault impedance characteristics were proposed by DIgSILENT PowerFactory for evaluating the standardized test system. The parameters of the short circuit fault will stay constant for all case scenarios examined in this chapter. A figure 7.11 shows an occurrence of oscillations after an event, where oscillations eventually damp out and speed of all 10 synchronous machines is able to stabilize at the nominal value of 1 p.u.

Figure 7.12 indicates the speed behaviour of 10 synchronous generators after being subjected to a load event at time = 1 second. The active power demand of Load 15 was increased by 15%, which causes the decrease of generator speed of all 10 machines. Similarly to short circuit characteristics, the load event demand will stay constant for the analysis of case scenarios in later section of this chapter. There is a presence of oscillations in case of a load disturbance, however these oscillations are not as significant compared to the short circuit event and they damp out successfully. Due to the increase in demand, all 10 synchronous generators are able to stabilize at the new speed value of around 0.9988 p.u.
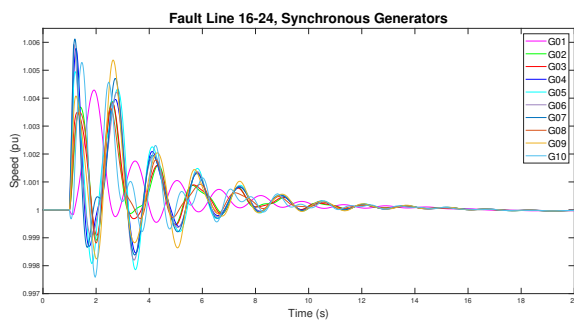
Figure 7.11: A response of 10 synchronous generators to a fault event on Line 16-24.
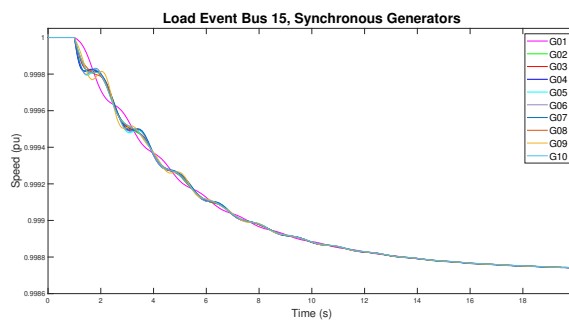
Figure 7.12: A response of 10 synchronous generators to a load event on bus 15.

7.2.2. Eigenvalue Analysis

Eigenvalue analysis has been conducted to study the critical modes of oscillation, to obtain damping ratios and damped frequencies. Such information will help determine and support the time domain observations about the type of present oscillations in the system. Such analysis by examining the real part of the eigenvalues can show whether the system is stable or unstable. In case that one of the modes has a positive real part, this would indicate the unstable system operation.

Modes	Eigenvalues	Damped Frequency	Damping Ratio
Units	[1/s +j rad/s]	[Hz]	[-]
Mode 1	-0.173 ± j 7.053	1.123	0.0246
Mode 2	-0.264 ± j 6.487	1.032	0.0406
Mode 3	-0.324 ± j 4.255	0.677	0.0758
Mode 4	-0.364 ± j 6.734	1.072	0.0539
Mode 5	-0.410 ± j 7.563	1.204	0.0541

Table 7.2: Modal analysis parameters for 10 SGs from PowerFactory analysis.

Critical modes of oscillation have been collected in table 7.2, where 5 modes of oscillation are presented with a corresponding eigenvalue, damped frequency and damping ratio. It has been identified that Mode 3 is a inter-area mode of oscillation according to damped frequency of 0.677 Hz. The damping ratio of the Mode 3 is 0.0758, however Mode 1 has the lowest damping ratio of 0.0246. While Mode 3 is the inter-area mode of oscillation all other modes collected in the table are identified as local modes of oscillation, due to their damped frequency being above 1 Hz and below 3Hz.
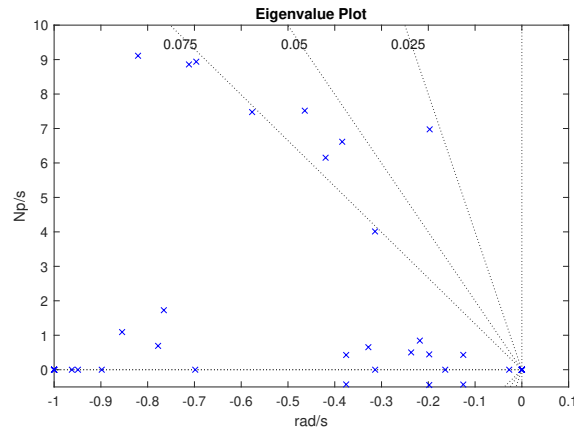
Figure 7.13: Eigenvalue plot indicating critical modes of oscillation for 10 SGs.
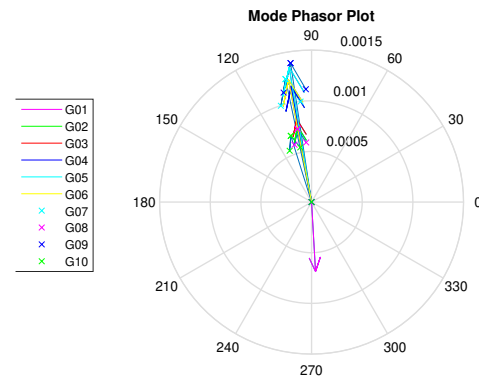
Figure 7.14: Mode phasor plot of the interarea mode of oscillation (mode 3) for 10 SGs.

Eigenvalue plot of oscillations modes is shown in figure 7.13, where the doted lines represent the damping ratios of 0.025, 0.05 and 0.075. This figure supports the previous observations by showing that all modes have a negative real part, which is indicating the stable system operation. In addition to the modes shown in the figure 7.13, there are other modes present in the system. However due to their larger damping ratios they are not included in the eigenvalue plot.

Mode phasor plot has been generated for the inter-area mode of oscillation as shown in figure 7.14, where it is visible that the G01 oscillates against other generators in the system. The presence of inter-area oscillation in the system is supported by the observation that a generator G01 represents a connection to the part of the system that is not modelled in detail. This means that it is not only a generator oscillating against the rest of the system but the whole area oscillating against another.

Overall, standardized test system can be classified as poorly damped system, due to presence of many critical modes of oscillation with low damping ratios. This can be supported by figure 7.13, indicating a high density of modes with damping ratios below or just above 0.075. Damping of the poorly damped system can be improved by tuning the controllers, such as PSS. Interesting to point out is that it has been identified by

DIgSILENT PowerFactory that PSS modelled in the standardized system might not fit well together with the AVR block used [39], which might explain some of the observations.

7.2.3. Prony Analysis

Prony analysis is conducted in order to support results obtained from Modal analysis. Due to presence of many controllers and many controller loops, Modal analysis can produce results which are not aligned with by time-domain simulations. A reason why Prony analysis has been conducted in this project for every scenario is to verify or disproof the obtained results from Modal analysis by analysing the time domain signals. Prony analysis has an ability of identifying the inter-area oscillations and determining the damped frequency and damping ratio.

Parameters	Value	Units
Eigenvalue Traditional Method	-0.239 ± j 4.071	[1/s +j rad/s]
Eigenvalue Modified Method	-0.224 ± j 4.070	[1/s +j rad/s]
Damped Frequency Traditional	0.648	[Hz]
Damped Frequency Modified	0.648	[Hz]
Damping Ratio Traditional	0.0586	[-]

Table 7.3: Parameters observed from Prony analysis for a case with 10 SGs.

There were two different Prony scripts used, labeled as Traditional Prony and Modified Prony. The parameters obtained by both methods are collected in table 7.3. Compering the results from Prony analysis to results collected in table 7.2 from Eigenvalue analysis, it can be seen that values of both analyses match; the biggest mismatch is between real part of the eigenvalue and the damping ratio.
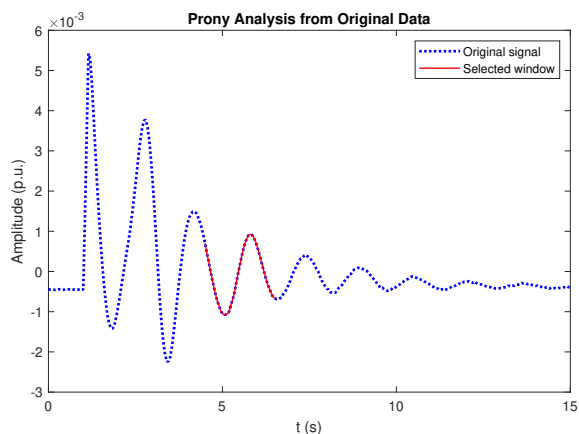
Figure 7.15: Red line identifying the part of the signal selected for the Prony analysis.
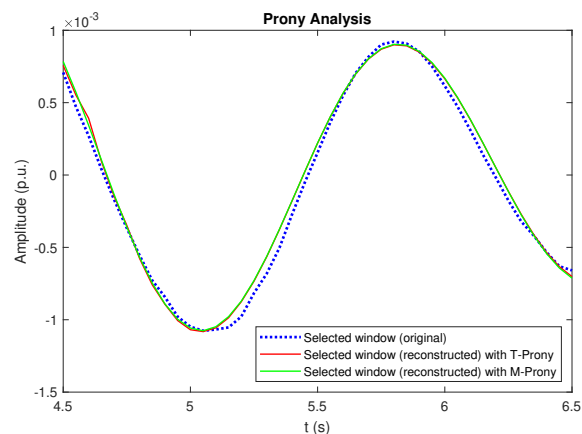
Figure 7.16: The selected window and the reconstructed signal by traditional and modified Prony methods.

Figure 7.16 shows the original time-domain signal and the red part of the signal is the window used for the analysis. The window selected should be in the part of the signal with ring down characteristics, otherwise Prony analysis cannot be applied to the time domain signal. Figure 7.16 shows the original signal as well as the reconstructed signal by traditional and modified Prony analysis. It can be seen that the reconstructed signals match well with the original signal. This indicates the window selected is appropriate for the analysis and that values (eigenvalues, damped frequency and damping ratio) will be correctly generated.

Figure 7.17 shows spectral density of the signal analysed, which identifies the dominant frequencies present in the signal. The observations from the figure support findings from Eigenvalue analysis and indicate that the most dominant frequency value is around 0.670. Results from Prony analysis support observations from Modal analysis, which increases the confidence abut drawing final conclusions. Results produced by only one method can be manipulated to same extent, while two methods giving similar results increase the level of certainty about correctness of the results.
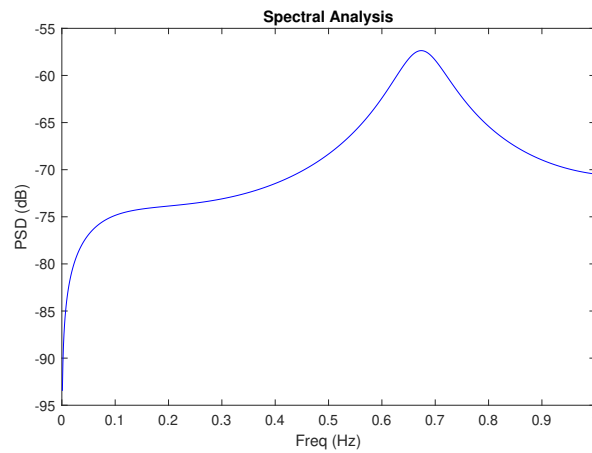
Figure 7.17: Spectral analysis of a generator signal in case of 10 SG.

7.3. Case Study 2: Dynamic Behaviour of 4 SG and 6 WT

This project builds upon results from the findings of the Horizon 2020 MIGRATE Project, which states that grid-following control enables 60% to 70% PE penetration in the grid with correct tuning of the control structures [51]. The intent of this case study is to replicate such observations and following case studies will use grid-forming control to take a step further and increase a total share of PE devices in the system.

7.3.1. Time Domain Simulations

A total share of PE generation was determined by disconnecting synchronous generators step by step until the point when the remainder of the generators lose synchronism. It has been determined that 60% of generation can be obtained from WTs with grid-following control, however such setup cannot withstand any large disturbances such as a short circuit. It can withstand the small disturbance such as the increase in load demand. Such observation can be visible in figure 7.18, where after an initial increase in generator speed, generator signal stabilizes at around 1.01 pu. 7.19 shows a zoomed in version of the same signal response to highlight the oscillations that occur at the beginning of the simulation.
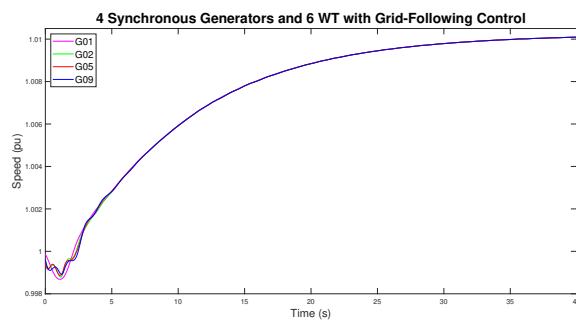
Figure 7.18: Time domain simulations of 4 synchronous generators and 6 WT with grid-following control.
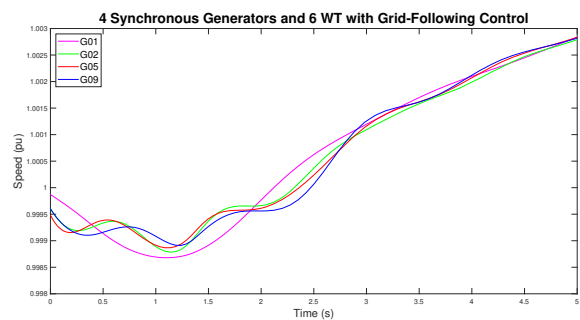
Figure 7.19: Time domain simulations of 4 synchronous generators and 6 WT with grid-following control zoomed in.

7.3.2. Eigenvalue Analysis

Table 7.4 collect five critical modes of oscillation in case only grid-following control is used in addition to synchronous generators. Mode 4 has been identified to be a inter-area mode of oscillation with a damped frequency of 0.667 Hz. Damping ratio of the inter-area mode is 14.5%, while the damping ratio of local modes (Mode 1 and Mode 2) is lower; 6.98% and 6.88% respectively.

Figure 7.20 shows previously mentioned critical modes in a graphical way for easier visualisation. A figure confirms that a Mode 1 and Mode 2 have the lowest damping ratios with a largest imaginary value. This

Modes	Eigenvalues	Damped Frequency	Damping Ratio
Units	[1/s +j rad/s]	[Hz]	[-]
Mode 1	-0.417 ± j 5.954	0.948	0.0698
Mode 2	-0.458 ± j 6.633	1.056	0.0688
Mode 3	-0.512 ± j 1.929	0.307	0.257
Mode 4	-0.615 ± j 4.191	0.667	0.145
Mode 5	-0.780 ± j 1.336	0.213	0.504

Table 7.4: Modal analysis parameters for 4 SGs and 6 WT with grid-following control from PowerFactory analysis.
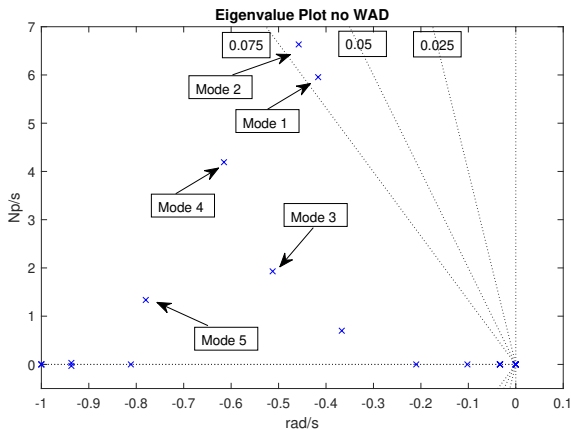
Figure 7.20: Eigenvalue plot indicating critical modes of oscillation for 4 SGs and 6 WT with grid-following control.
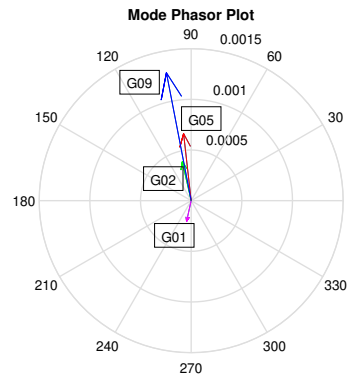
Figure 7.21: Mode phasor plot of the interarea mode of oscillation (mode 4) for 4 SGs and 6 WT with grid-following control.

system is classified as stable due to all modes having a negative real part. Figure 7.21 illustrates the inter-area mode by showing the mode phasor plot of the Mode 4, where generator G01 oscillates against other generators in the system.

7.3.3. Observations, Comparison and Insight

Grid-following control enables integration of PE devices to the power grid with a lower stabilizing effect compared to 100% penetration of synchronous generators. Such behaviour was expected, however grid-following control enables a certain level of RES penetration in the following years during the transition period before higher levels of PE penetrations will be desired. It is also indicated that grid-forming control would be a preferred option due to their stabilizing ability and ability to withstand larger disturbances.

7.4. Case Study 3: Dynamic Behaviour of 2 SG and 8 DVC

It has been proven that grid-forming control is a feasible option for stabilizing the grid following a disturbance even with 80% penetration of RES. Results supporting such statement will be presented in this study case. The remainder of synchronous generation (20%) in the system is supplied either by a generator G01 which represents the connection to the rest of the system and the generator G02 representing the swing node in the grid. There are exactly two synchronous generators present in the modified test system to study the 80% RES penetration in the power grid. This enables a study of the effects of using grid-forming controllers to stabilize the grid following the disturbance.

7.4.1. Time Domain Simulations

Time domain simulations shown in this study case demonstrate that 80% of RES penetration is possible with use of grid forming control. Figure 7.22 shows a speed response of generators G01 and G02 to a short circuit event on the line 16-24. A system is able to withstand a large disturbance, however there is a presence of oscillations in the generator signal. Even though these oscillations are ringing down they cannot completely

damp out and they are present even 20 seconds after introduction of an event. Figure 7.23 shows a response of the generators to a load event, where oscillations are also visible after an introduction of an event. However, these oscillations are able to damp out once the generator speed stabilizes at a new value of around 0.996 pu. An intent of such simulation is to show the ability of the grid-forming control to stabilize the system flowing a large and small disturbance by enhancing rotor angle stability.
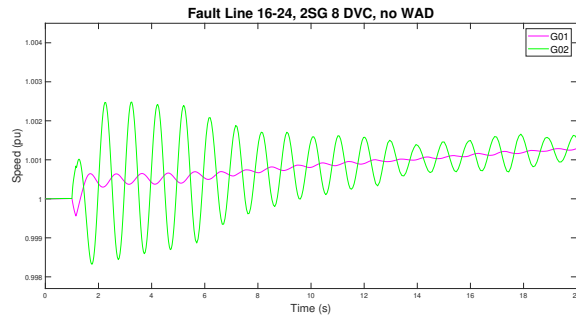
Figure 7.22: A response of 2 SGs to a fault event on Line 16-24 with presence of 8 DVC and without WADC.
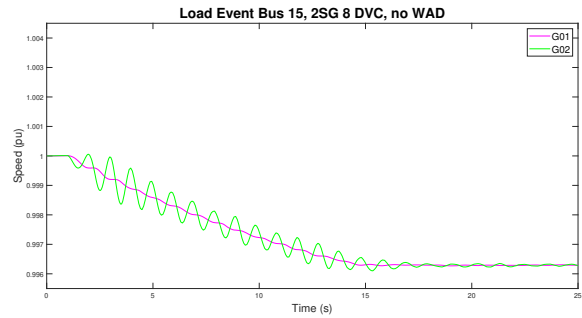
Figure 7.23: A response of 2 SGs to a load event on bus 15 with presence of 8 DVC and without WADC.

7.4.2. Eigenvalue Analysis

Eigenvalue analysis was carried out to evaluate the system stability independent of different disturbances. Such analysis can indicate critical modes of oscillation and can demonstrate the overall system damping and how prone is a system to different types of oscillations. Table 7.5 shows a collection of critical modes of oscillation with corresponding eigenvalues, frequencies and damping ratios. It is identified that there are no interarea modes of oscillation in the system, however the modes listed in the table all fall into local oscillation range. Besides the Mode 1, which has a damping ratio of 8.4%, all other modes are well damped with damping ratios above 28.0%.

Modes	Eigenvalues	Damped Frequency	Damping Ratio
Units	[1/s +j rad/s]	[Hz]	[-]
Mode 1	-0.509 ± j 6.021	0.958	0.084
Mode 2	-2.491 ± j 8.488	1.351	0.282
Mode 3	-9.292 ± j 12.299	1.958	0.603
Mode 4	-15.962 ± j 12.375	1.970	0.790

Table 7.5: Modal analysis parameters for 2 SGs and 8 DVC from PowerFactory analysis.

Figure 7.24: Eigenvalue plot indicating critical modes of oscillation for 2 SGs and 8 DVC.
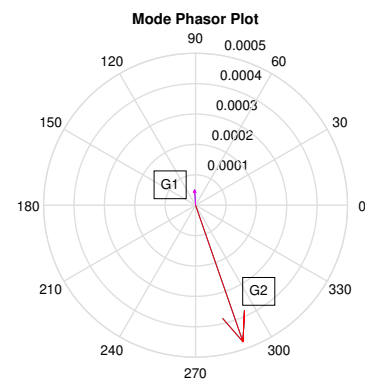
Figure 7.25: Mode phasor plot of the interarea mode of oscillation (Mode 1) for 2 SGs and 8 DVC.

Figure 7.24 illustrates the behaviour explained above, where Mode 1, Mode 2 and Mode 3 are placed in

a figure based on their real and imaginary part. It is shown that Mode 1 has the lowest damping ratio below 10.0% and that Mode 2 has a damping ratio of almost 30.0%. Figure 7.25 shows the mode phasor plot of Mode 1, which illustrates the oscillation of the generator G01 against the generator G02. This is shown by the two arrows pointing in the other direction with almost 180% degrees. These two arrows should point in the same direction, which would indicate that the generators are not oscillating against each other.

7.5. Case Study 4: Dynamic Behaviour of 2 SG and 8 VSM

VSM is another grid-forming control which will be studied in this project and results will be compared to results achieved by using DVC. DVC has been a grid-forming control explored in MIGRATE Project, however analysing additional methods such as VSM will open additional opportunities for research and implementation later on. VSM is not modelled to receive the remote/ stabilising signal, hence it will have a supporting role in this project and will demonstrate its stabilizing ability. VSM grid-forming control will be used in combination with DVC and grid-following control in section 7.9, to demonstrate its ability to damp critical oscillations and further enhance the stability of the grid.

7.5.1. Time Domain Simulations

Time domain simulation shows a response of the generators to a short circuit event and the behaviour of the generators looks very similar to the case with only SGs in the system. Figure 7.26 shows the occurrence of oscillations shortly after an event, which eventually damp out and the generator speed stabilizes around the nominal value of 1 pu. It was expected to observe such behaviour due to a control strategy of VSM, since it simulates the behavior of synchronous machines.
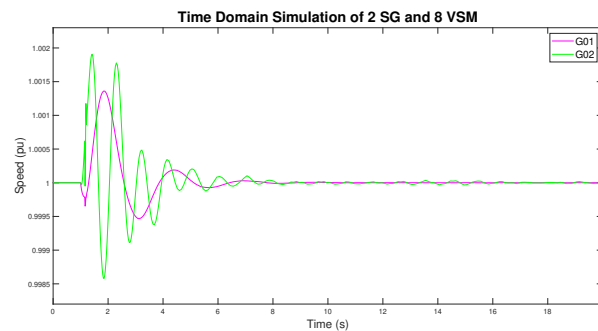
Figure 7.26: Time domain simulations of 2 synchronous generators and 8 VSM - Fault Event.

7.5.2. Eigenvalue Analysis

Eigenvalue analysis shows critical OMs in the system, which are collected in the table 7.6 with corresponding eigenvalues, frequencies and damping ratios. It is shown from the table that there are no inter area modes of oscillations present - even though that both modes listed fall very close to the inter area oscillations range. Mode 1 is identified as a local mode of oscillations and Mode 2 falls into very low frequency osculation range. Mode 2 was selected for further analysis and used to demonstrate that frequency very close to inter area range does not necessary indicate presence of such oscillation in the system.

Modes	Eigenvalues	Damped Frequency	Damping Ratio
Units	[1/s +j rad/s]	[Hz]	[-]
Mode 1	-0.534 ± j 6.900	1.098	0.0772
Mode 2	-0.733 ± j 2.492	0.397	0.282

Table 7.6: Modal analysis parameters for 2 SGs and 8 VSM from PowerFactory analysis.

Figure 7.27 graphically represent the previously mentioned modes of oscillation, where it is visible that Mode 1 has poor damping ratio with less than 10.0% while Mode 2 has a damping ratio of almost 30.0%. Phasor plot is shown in figure 7.28 for Mode 2, where is visible that this mode does not represent the inter-area

oscillations in the system. This is visible by fairly low angle between the two arrows representing different generators. Modal analysis supports observations made by time domain simulations, where it has been determined that VSM is able to enhance stability of the system as well as fairly sufficiently damp oscillations.
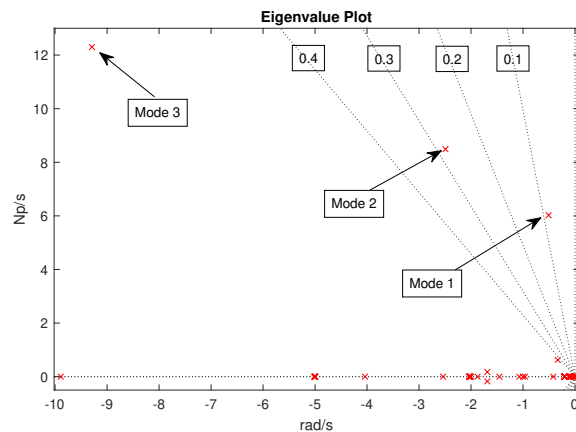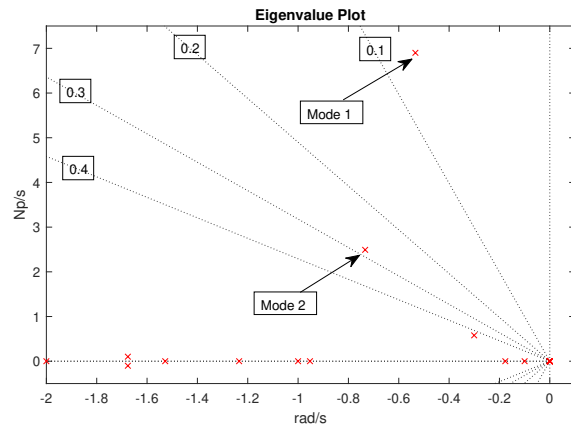

Figure 7.27: Eigenvalue plot indicating critical modes of oscillation for 2 SGs and 8 VSM.
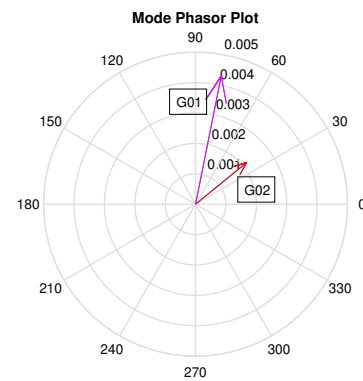
Figure 7.28: Mode phasor plot of the interarea mode of oscillation (mode 2) for 2 SGs and 8 VSM.

7.5.3. Prony Analysis

Prony analysis was carried out to verify the eigenvalue results obtained by Modal analysis as well as to demonstrate the dominant frequencies in the system by generating the spectral analysis figure. Eigenvalues, damped frequencies and damping ratios estimated by traditional and modified Prony is collected in the table 7.7. It is visible that Prony analysis has identified Mode 1 from Modal analysis to be the dominant mode in the signal with its damped frequency of around 1.0 pu. Eigenvalues estimated by both methods overestimate the real part, however imaginary part matches with the imaginary part from Modal analysis.

Parameters	Value	Units
Eigenvalue Traditional Method	$-0.918 \pm j\,6.599$	[1/s +j rad/s]
Eigenvalue Modified Method	$-0.884 \pm j\,6.700$	[1/s +j rad/s]
Damped Frequency Traditional	1.050	[Hz]
Damped Frequency Modified	1.066	[Hz]
Damping Ratio Traditional	0.109	[-]

Table 7.7: Parameters observed from Prony analysis for a case with 2 SGs and 8 VSM.
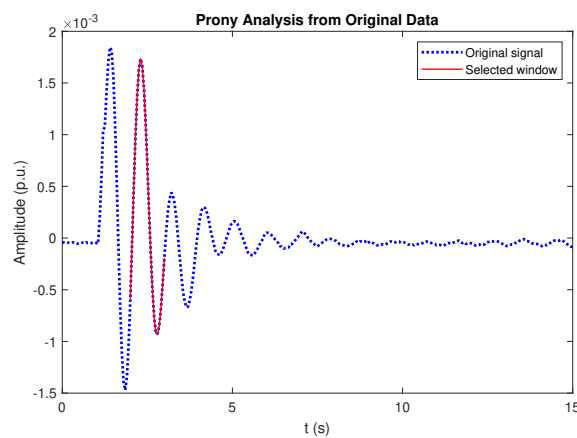
Figure 7.29: Red line identifying the part of the signal selected for the Prony analysis.
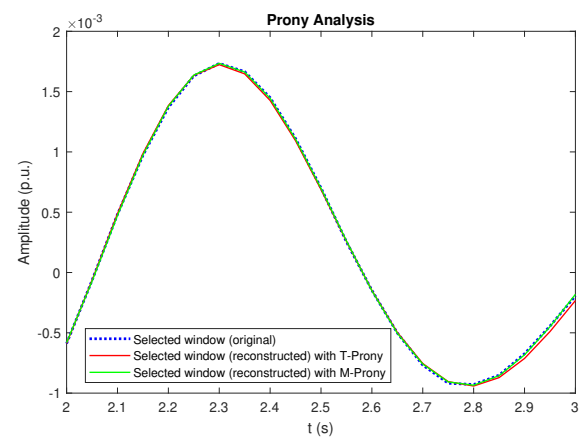
Figure 7.30: The selected window and the reconstructed signal by traditional and modified Prony methods.

Figure 7.29 indicates the part of the signal which has been identified for Prony analysis and which part of the signal has been chosen for estimating the previously mentioned parameters. Figure 7.30 on the other hand shows the part of the signal which has been selected for Prony analysis and also how well traditional and modified Prony is able to match the original signal. If reconstructed signals overlap with the original signal, then the previously presented values match with the input signal from the analysis.
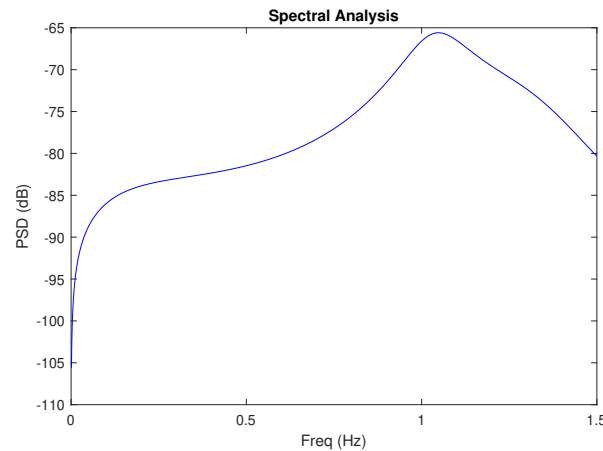
Figure 7.31: Spectral analysis of a generator signal in case of 2 SGs and 8 VSM.

Prony analysis generates the spectral analysis plot, which demonstrates what are the dominant frequencies present in the time domain signal. Figure 7.31 shows the dominant frequencies in the signal when there is 80% of VSM grid-forming controller penetration. It confirms that the most dominant frequency is around 1.0 Hz, which is linked with the Mode 1 from Modal analysis.

7.6. Case Study 5: WAMS with 2 SG and 8 DVC with 8 WADC

Case study 5 is the first case which will be enhanced with WAMS functionality. So far the results presented were either a base case scenario or they were done with intent to replicate the observations from Horizon 2020 MIGRATE Project. So far it has been confirmed that grid-following control allows around 60% of RES penetration in the system and that grid-forming control extends RES penetration to around 80%. Dynamic behaviour of the system with DVC has been shown as well as with VSM and was demonstrated that both methods have sufficient stabilizing and damping ability. It has been pointed out that DVC is a preferred option in this project with the ability to receive the remote/ stabilizing signal which will be used once WADCs are included in the control scheme. Time domain simulations have shown that VSM is a strong candidate for future applications with its stabilizing and damping ability.

7.6.1. Input Signal Selection

Generator	Bus	OI
Power Plant 5	Bus 34	1
Power Plant 7	Bus 36	0.98838
Power Plant 4	Bus 33	0.98246
Power Plant 6	Bus 35	0.981661
Power Plant 3	Bus 32	0.936441
Power Plant 9	Bus 38	0.885768
Power Plant 8	Bus 37	0.716245
Power Plant 10	Bus 30	0.659175

Table 7.8: Observability indices for a case with 2 SGs and 8 DVC with 8 WADCs.

Table 7.8 shows Observability Indexs (OIs) and it is visible that generator buses with highest values of OIs are Bus 34, Bus 36 and Bus 33. It is determined that signals from those buses are able to represent and estimate

the state of the system, which is why it is most appropriate to have PMUs installed on those buses. Deploying only three PMUs will decrease the initial investment as well as the maintenance cost by not compromising the ability to correctly observe the system. A number of PMUs deployed in the system is lower as expected, however such WAMS structure is satisfactory for this project. This is because the main objective of the project is WAMS effect on the controllability of the system.

7.6.2. Time Domain Simulations

Time domain simulations were carried out in order to visualize the oscillations that occur in the system after introduction of an event. There were two different events introduced to the system, a short circuit event on the Line 16-24 and a load event on Load 15 with an increase in active power demand. For the future references, the speed scale is set to be the same between a simulation without a presence of WADC and with a presence of a damping controller. This was done for easier observation of the oscillations, the amplitude of oscillations and the behaviour of the time-domain signal.

Figure 7.32 show the response of the system to a short circuit event when there were zero WADCs linked to WT (green line). Furthermore, the response of the system with correctly tuned WADCs associated to WTs are shown in the same figure (blue line). It is visible that the oscillations generated at the occurrence of an event are able to damp out when the system stabilizes at the new generator speed of around 0.996 pu. Besides, figure 7.33 shows the response of the system as a response to a load event on the Bus 15. Green line shows the original case without WADCs, while a blue line shows a system with eight WADCs connected to the corresponding WT. The generator speed decreases further in case when WADCs are connected to the system, however WADCs increase damping in the system. The signal is able to stabilize at a new value of around 0.995 (at around t = 5 s); sooner compared to the original case without WADCs.
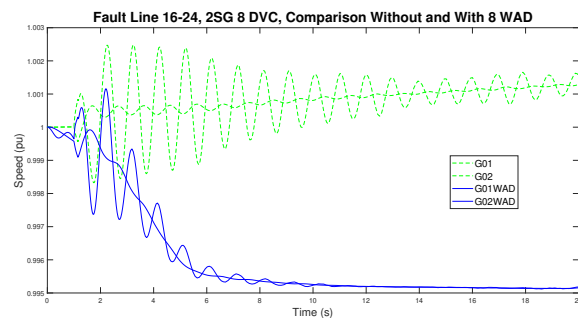
Figure 7.32: A response of 2 SGs to a fault event on Line 16-24 with presence of 8 DVC with and without 8 WADCs.
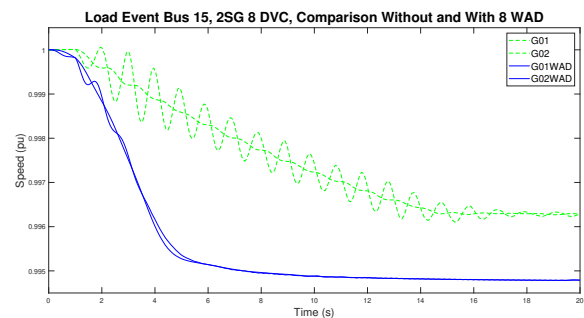
Figure 7.33: A response of 2 SGs to a load event on bus 15 with presence of 8 DVC with and without 8 WADCs.

It was mentioned that WADCs used in this project were subjected to the optimization problem, which means that parameters are tuned to have the highest effect in the system; minimize the difference among the two generator signals. The parameters of all eight different WADCs for a short circuit event are collected in the table 7.14, while a description of each parameter and the units are given below.

Symbol parameter explanation:
- Kpss1 - Controller gain [pu]
- Kpss2 - Controller gain [pu]
- Kpss3 - Controller gain [pu]
- Tw - Integrate time constant [s]
- T1 - Derivative time constant [s]
- T2 - Delay time constant [s]
- T3 - Derivative time constant [s]
- T4 - Delay time constant [s]

Similarly, parameters of all eight WADCs have been tuned for the case when the system has been subjected to the load event on bus 15. By studying and comparing both tables it is visible that the majority of the values are similar among the two tables for the same parameter. Nevertheless, parameters have been tuned individually for both events to observe the desired response in the time domain simulation.

Symbol	Initial	WAD03	WAD04	WAD05	WAD06	WAD07	WAD08	WAD09	WAD10
Kpss1 [pu]	1	0.98930	1.01368	1.00309	1.00512	0.99234	1.01161	0.99537	0.99812
Kpss2 [pu]	1	0.97731	1.03297	0.99821	0.98528	1.00022	0.99323	0.98611	1.17644
Kpss3 [pu]	1	1.01249	0.98581	1.00074	1.00717	0.99385	1.09023	1.00609	0.99626
Tw [s]	10	9.99192	9.98571	9.99965	10.0099	9.99042	9.99024	10.0406	10.0006
T1 [s]	5	4.99151	4.88400	5.00913	5.00256	4.99632	4.99507	5.00145	5.00968
T2 [s]	0.4	0.39153	0.01262	0.40340	0.37498	0.48771	0.43492	0.38458	0.27514
T3 [s]	1	1.00757	0.98059	1.00305	0.99795	1.00271	1.00058	1.04094	0.95476
T4 [s]	0.1	0.0998	0.09967	0.10032	0.10167	0.09919	0.10014	0.10054	0.09981

Table 7.9: Initial and tuned WAD parameters for a case with 2 SGs and 8 DVC.

Symbol	Initial	WAD03	WAD04	WAD05	WAD06	WAD07	WAD08	WAD09	WAD10
Kpss1 [pu]	1	1.12469	0.64617	0.77532	1.05158	1.05525	1.08648	0.85050	1.38765
Kpss2 [pu]	1	0.88593	1.24842	1.08216	0.93197	1.00233	4.99899	0.77123	1.12845
Kpss3 [pu]	1	1.00733	0.89139	0.90298	1.10361	1.01737	1.04791	1.19110	0.93751
Tw [s]	10	10.1343	9.95879	7.03304	9.89302	10.1176	9.87877	10.1164	9.88508
T1 [s]	5	5.08789	5.20659	5.14449	5.04762	4.85885	4.82331	5.10636	4.66281
T2 [s]	0.4	0.22280	0.21745	0.57384	0.27609	0.49139	0.25136	0.34329	0.41406
T3 [s]	1	1.21874	1.36236	1.05036	0.98663	0.95180	1.13708	0.99734	0.79031
T4 [s]	0.1	0.11369	0.08533	0.10881	0.09264	0.11638	0.0951	0.11148	0.05707

Table 7.10: Initial and tuned WAD parameters for a case with 2 SGs and 8 DVC.

7.6.3. Eigenvalue Analysis

Modal analysis was done for the case with eight WADCs connected to DVCs to compare the results to the original case and to support the observations made in the time domain simulations. Table 7.11 collects results for case with eight WADCs as well as for the case without WADCs for easier comparison. Firstly, by comparing the damping ratios it can be noticed that the values actually decreased. Such behaviour is undesired and unexpected, however the explanation can be found in a large number of additional controllers in the system which have a negative impact on damping of individual OMs. Additional work will have to be spent towards optimizing and tuning the whole controls scheme of the system to observe results from Modal analysis which would support results seen in time domain simulations.

Modes	Without Damping Controller			With Damping Controller		
	Eigenvalues	Damped Frequency	Damping Ratio	Eigenvalues	Damped Frequency	Damping Ratio
Units	[1/s +j rad/s]	[Hz]	[-]	[1/s +j rad/s]	[Hz]	[-]
Mode 1	-0.509 ± j 6.021	0.958	0.084	-0.391 ± j 6.110	0.972	0.064
Mode 2	-2.491 ± j 8.488	1.351	0.282	-2.418 ± j 9.246	1.472	0.253
Mode 3	-9.292 ± j 12.299	1.958	0.603	-9.280 ± j 12.278	1.954	0.603

Table 7.11: Modal analysis parameters for 2 SGs and 8 DVCs with 8 WADC from PowerFactory analysis.

Figure 7.34 illustrates the above explained observations, where damping ratios of critical modes decreased with introduction of WADCs. Furthermore, figure 7.35 shows that the angle between the two generators present in the system actually gets closer to 180 °. This means that they are oscillating against each other with a larger angle as they are in the original case. As explained above, such behaviour might be explained by the interaction among newly introduced controllers. They might cause additional oscillations in the system and decrease damping of already present modes of oscillation.

7.6.4. Prony Analysis

Prony analysis was conducted to verify the results from Modal analysis and to verify whether WADCs really have such a negative impact on the system. Table 7.12 collect results from the original case which does not include the WADC signal and from the case when eight WADCs are connected to the system. Results obtained
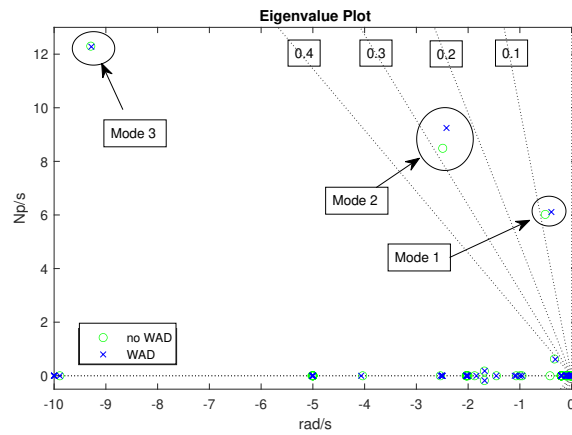
Figure 7.34: Eigenvalue plot indicating critical modes of oscillation without WAD and with 8 WAD.
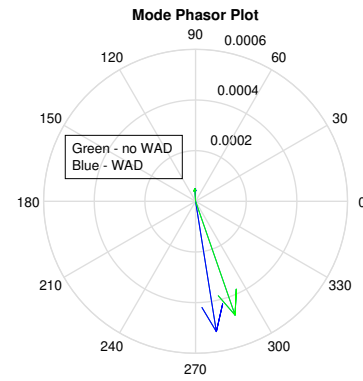
Figure 7.35: Mode phasor plot of the critical mode 1 without WAD and with 8 WAD.

by traditional and modified Prony methods match with results obtained by Modal analysis. By comparing the two cases, it can be noticed that Prony analysis actually estimated a higher damping ratio of the dominant mode compared to the base case. Such observation will be later supported by spectral analysis.

Parameters	Without Damping Controller		With Damping Controller	
	Value	Units	Value	Units
Eigenvalue Traditional Method	-0.395 ± j 6.370	[1/s +j rad/s]	-0.968 ± j 6.253	[1/s +j rad/s]
Eigenvalue Modified Method	-0.458 ± j 6.4305	[1/s +j rad/s]	-0.600 ± j 6.030	[1/s +j rad/s]
Damped Frequency Traditional	1.014	[Hz]	0.995	[Hz]
Damped Frequency Modified	1.019	[Hz]	0.960	[Hz]
Damping Ratio Traditional	0.0619	[-]	0.0965	[-]

Table 7.12: Parameters observed from Prony analysis.
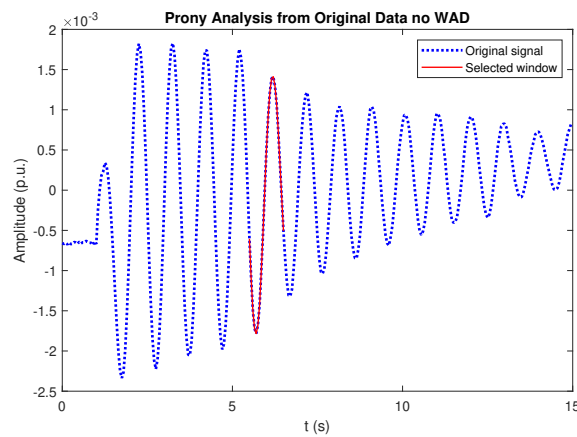
Figure 7.36: Red line is identifying the part of the signal selected for the Prony analysis.
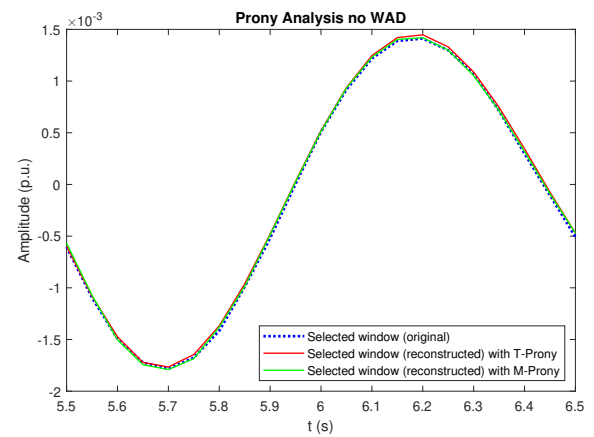
Figure 7.37: The selected window and the reconstructed signal by traditional and modified Prony function.

Figure 7.36 shows a time window selected for the analysis in case without WAMS architecture and figure 7.37 shows an original signal as well as signals reconstructed by traditional and modified Prony analysis. The reconstructed signals match well with the original data, which means that the eigenvalue, damped frequency and damping ratios determined by Prony analysis were correctly interpreted from the signal provided. Figure 7.38 shows a selected window of the time domain signal of the case with WAMS which was determined for the Prony analysis. Furthermore, 7.39 shows the original signal selected for the analysis and the reconstructed signals by modified and traditional Prony analysis. It can be concluded that parameters estimated by Prony analysis represent the time domain signal based on the observation that the reconstructed signals match with

the original signal.
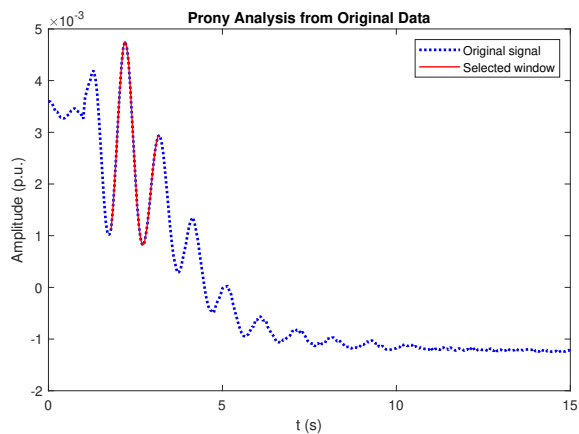
Figure 7.38: Red line is identifying the part of the signal selected for the Prony analysis.
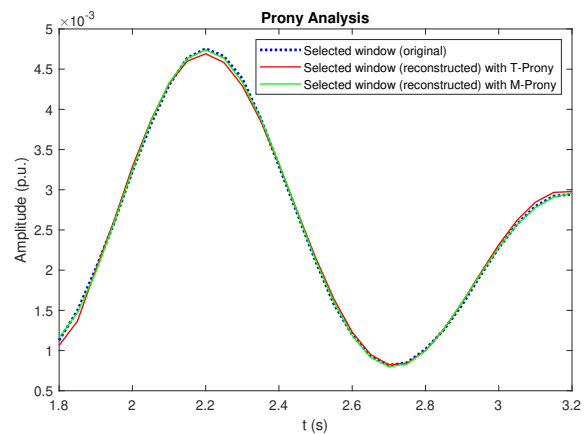
Figure 7.39: The selected window and the reconstructed signal by traditional and modified Prony function.

Figure 7.40 show the spectral density of the original case without using WADCs. High peak around frequency 1.0 Hz can be noticed, which indicates a dominant frequency in the system. It can also be concluded that this frequency is poorly damped if the results are compared to figure 7.41, which shows spectral density of the signal with presence of eight WADCs in the system. Even though that damping of frequency around 1.0 Hz is enhanced, the occurrence of ultra low frequency oscillations is caused in the system due to introduction of new controllers.
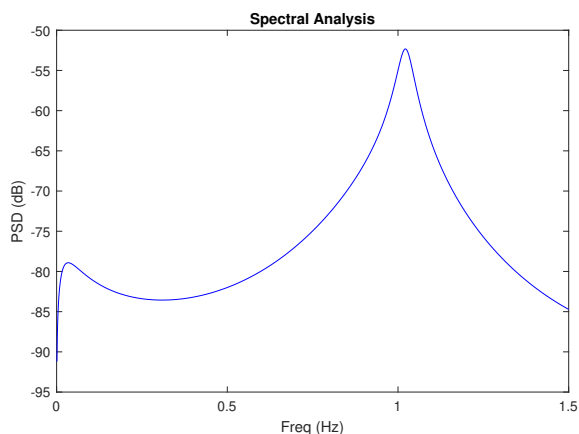
Figure 7.40: Spectral analysis of a generator signal without the use of WAD.
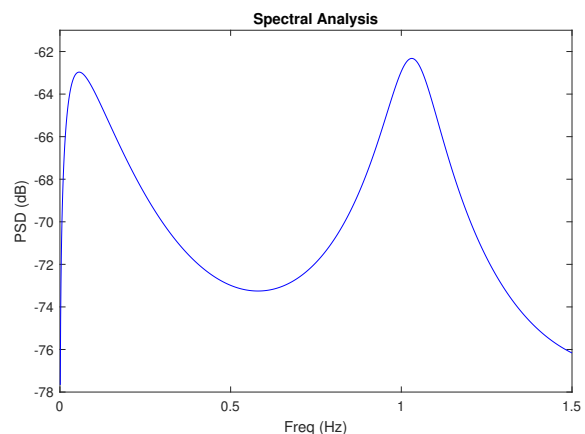
Figure 7.41: Spectral analysis of a generator signal with the use of WAD.

7.6.5. Observations, Comparison and Insight

This case has demonstrated that deploying WADC on every grid-forming controller present in the system might not bring the intended improvements to the system. The explanation might be found in a large number of additional controllers in the system and interactions among them. Another case study with three WADCs is conducted to verify whether less additional controllers in the system will have the intended effect. This might be a better option before an analysis is done for understanding the effects of controller interaction.

7.7. Case Study 6: WAMS with 2 SG and 8 DVC with 3 WADC

This case study examines an effect of WAMS on system stability and system damping while deploying three WADCs in the system. Output signal selection methodology is deployed in this case study to determine the location of WADCs to extract the highest effect out of these controllers.

The methodology used for implementation and analysis of this Case Study is as following:

1. Replace generators G03 to G10 with WTs with DVC grid-forming control. There are two synchronous generators kept in the system, since G01 represents the connection to the non modelled part of the original grid and generator G02, which is modelled as a swing generator; hence why it is required to keep it in the grid. The second reason why there are exactly two synchronous generators present in the modified test system is to study the 80% PE penetration to the power grid. This would give the ability to study the effects of using grid-forming controllers to stabilize the grid following the disturbance and the use of WAMS to damp oscillations.

2. The input and output signal selection method is executed for the grid with DVC grid-forming controllers without the presence of PMUs and without damping controllers, which enables identification of buses in the grid with the highest observability and controllability indices. Buses with highest observability indices will be candidates for PMU deployment and generators connected to buses with highest controllability indices will be candidates for WADC deployment.

3. The WADC will be connected to three WTs with associated buses that have the highest controllability indices in the system. Only power plants with DVC are considered to receive the stabilizing signal from WAMS, because this kind of control strategy enables the use of a remote signal. In other words, the synchronous generators G01 and G02 are not candidates to receive the PMU signal in this design.

4. The WADC implemented in the previous step will receive a PMU signal from the buses identified to have the highest observability indices. There will be a total of three PMUs in the system and WADC is designed to receive total of three voltage measurements from PMUs. The signal from the WADC will then be combined with the local control to enhance damping of oscillations and overall stability of the system.

7.7.1. Input and Output Signal Selection

Table 7.13 shows collected information about OI and Controllability Index (CI) for generator buses. OIs and CIs are listed in the table with associated power plants and corresponding generator buses. Power plants are listed in order from highest OIs and CIs towards the lowest index. OIs are the same as listed in the previous case study, however CIs have to be calculated to determine the candidates to have WADCs associated.

Generator	Bus	OI	Generator	Bus	CI
Power Plant 5	Bus 34	1	Power Plant 2	Bus 31	1
Power Plant 7	Bus 36	0.98838	Power Plant 7	Bus 36	0.861558
Power Plant 4	Bus 33	0.98246	Power Plant 6	Bus 35	0.818519
Power Plant 6	Bus 35	0.981661	Power Plant 4	Bus 33	0.780735
Power Plant 3	Bus 32	0.936441	Power Plant 5	Bus 34	0.77897
Power Plant 9	Bus 38	0.885768	Power Plant 9	Bus 38	0.755563
Power Plant 8	Bus 37	0.716245	Power Plant 3	Bus 32	0.738151
Power Plant 10	Bus 30	0.659175	Power Plant 8	Bus 37	0.576952
-	-	-	Power Plant 10	Bus 30	0.48112
-	-	-	Power Plant 1	Bus 39	0.056414

Table 7.13: Observability and Controllability indices for a case with 2 SGs and 8 DVC.

CIs collected in the right part of the table indicate generator buses where the injection of active power have the highest stabilizing effect on the system. As described in chapter 5: Wide Area Monitoring for Improved Controllability, this was determined based on introducing a mobile load to every generator bus and observing where does the active power injection have the highest effect on the system. Highest CIs is associated with a Power Plant 2, however this power plant is not a candidate to receive the stabilizing signal; hence the next three highest values of CIs were selected to be candidates for deployment of WADCs. Power plants that are receiving the stabilizing signal and have a presence of a wide area damping controller associated to their control structure are Power Plant 7, Power Plant 6 and Power Plant 4.

7.7.2. Time Domain Simulations

Short circuit event in the system with eight WTs with grid-forming control has been studied without and with the presence of WAMS structure. Activation of a WAMS structure means presence of PMUs and WADCs in the

system. Figure 7.42 shows the time domain response of generators G01 and G02 after being subjected to the short-circuit event. Figure shows generator response in case when there was no WAMS in the system and in case when WAMS was deployed. Both curves are shown in the same figure for easier visualization and evaluation of the effect of WAMS on the controllability.

The oscillations visible in the figure occur with the introduction of an event and they start to damp out, however generator speed is not able to stabilize around the nominal value in case without WAMS (green line). Figure also shows a response of the generators G01 and G02 after being subjected to the event however due to the presence of WAMS oscillations are able to damp out shortly after the event (blue line). Speed of generators stabilizes after around 14 seconds at the new value of around 1.004 pu. Figure confirms that correctly tuned parameters of WADCs as part of WAMS structure has a positive effect on damping oscillations in the system in case of a short circuit disturbance.
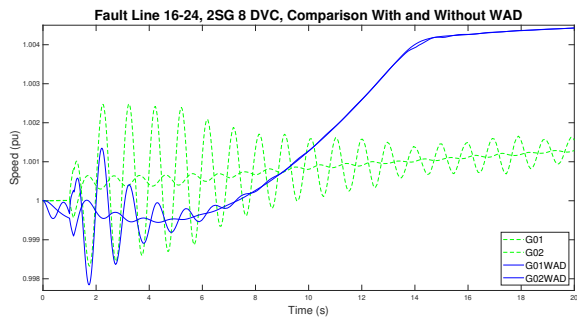
Figure 7.42: A response of 2 SGs to a fault event on Line 16-24 with presence of 8 DVC with and without WADCs.
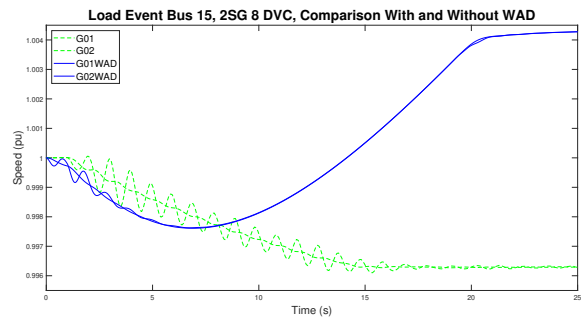
Figure 7.43: A response of 2 SGs to a load event on bus 15 with presence of 8 DVC with and without WADCs.

Response of the system to a load event for Bus 15 has been studied without and with the presence of WAMS. Figure 7.43 shows the time-domain response of the system to the increase in active power demand on Load 15 at time = 1 second. The generator speed of G01 and G02 decreases after an introduction of an event in case when there is no WADC in the system (green line). At time around t = 15 second generator speed stabilizes at the new value of around 0.9963. On the other hand, figure 7.43 shows the response of the system with present of WADC in the control structure of DVC (blue line). There are still some oscillations present after an event, which damp out shortly after. There are no oscillations visible anymore at time = 20 seconds, where generators stabilize at value around 1.004 p.u.

WADCs selected for enhancing the damping in the system were WADC 04, WADC 06 and WADC 07. An initial values of the parameters of all three damping controllers were the same, as listed in the table 7.14. The selected WADCs were subjected to the optimization process, where the set objective was to minimize the difference between the time-domain signal response of both generators present in the system after being subjected to a short circuit event.

Symbol	Initial Values	WAD 04	WAD 06	WAD 07
Kpss1 [pu]	1	0.475188	4.233772	2.25934
Kpss2 [pu]	1	0.837866	0.096978	0.980238
Kpss3 [pu]	1	3.789916	3.599287	1.548673
Tw [s]	10	8.002287	11.94835	7.059065
T1 [s]	5	9.793561	5.074099	3.200958
T2 [s]	0.4	0.039881	0.040087	0.769054
T3 [s]	1	1.901543	0.552523	1.293007
T4 [s]	0.1	0.116355	0.009934	0.30812

Table 7.14: Initial and tuned WAD parameters for a case with 2 SGs and 8 DVC.

Selected WADCs for enhancing the damping in the system were subjected to the optimization process, however in this case with intent of minimizing the oscillations of the generator G01 against generator G02 after a load event. Tuned parameters of all three WADCs in case of a load event are collected in the table 7.15.

Symbol	Initial Values	WAD 04	WAD 06	WAD 07
Kpss1 [pu]	1	0.449323	4.282183	2.253745
Kpss2 [pu]	1	3.860345	0.096418	0.957666
Kpss3 [pu]	1	3.713403	3.544565	1.542007
Tw [s]	10	7.960741	11.87091	7.040721
T1 [s]	5	9.767166	5.071509	3.189806
T2 [s]	0.4	0.030778	0.002078	0.793144
T3 [s]	1	1.848232	0.554959	1.211252
T4 [s]	0.1	0.113791	0.007897	0.314317

Table 7.15: Initial and tuned WAD parameters for 2SG 8DVC.

7.7.3. Eigenvalue Analysis

Eigenvalue analysis has been executed for both cases; without and with the presence of WAMS system, similarly to time-domain simulation analysis. Four critical modes of oscillation were identified and are collected in table 7.16 with its corresponding eigenvalue, damped frequency and damping ratio. Left part of the table summarizes the values observed without including WAMS and values listed on the right part of the table were observed with presence of WAMS. None of the modes fall in range between 0.3 Hz and 0.7 Hz, which means that there are no inter-area oscillations in the system. Other listed modes fall in range of local modes of oscillation with damped frequency just below 1.0 Hz or above 1.0 Hz. Such scenario can be seen for both cases analysed, without and with the presence of WAMS.

Modes	Without Damping Controller			With Damping Controller		
	Eigenvalues	Damped Frequency	Damping Ratio	Eigenvalues	Damped Frequency	Damping Ratio
Units	[1/s +j rad/s]	[Hz]	[-]	[1/s +j rad/s]	[Hz]	[-]
Mode 1	-0.509 ± j 6.021	0.958	0.084	-0.481 ± j 6.107	0.972	0.079
Mode 2	-2.491 ± j 8.488	1.351	0.282	-3.428 ± j 9.006	1.433	0.356
Mode 3	-9.292 ± j 12.299	1.958	0.603	-9.372 ± j 12.222	1.945	0.609
Mode 4	-15.962 ± j 12.375	1.970	0.790	-16.022 ± j 12.295	1.957	0.793

Table 7.16: Modal analysis parameters for 2 SGs and 8 DVCs from PowerFactory analysis.

Eigenvalue analysis is used to analyse the effect of WAMS on improvement in damping ratios of every critical mode. It can be seen that for the Mode 1, damping ratio actually decreases with presence of WAMS, however Mode 2, Mode 3 and Mode 4 experience an improvement in their damping ratios. Damping ratios of these critical modes are actually very large, which might lead towards concluding that oscillation modes are well damped in this system.
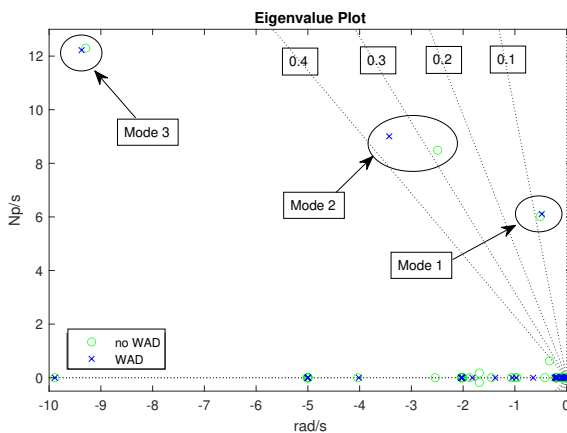

Figure 7.44: Eigenvalue plot indicating critical modes of oscillation without WAD and with WAD.
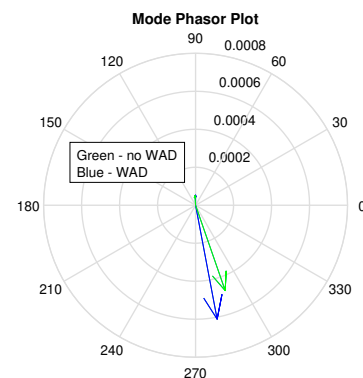

Figure 7.45: Mode phasor plot of the critical mode 1 without WAD and with WAD.

Similar observations can be drawn from the visual representation of critical modes of oscillation as shown in figure 7.44. Purple crosses denote modes of oscillation in case without WAMS and WADCs present in the system, while green circles denote critical modes in case when WAMS is present. From figure it can be seen a slight decrease in damping ratio for Mode 1 and an improvement in damping ratios for Mode 2 and Mode 3. Mode phasor plot has also been constructed for Mode 1, since Mode 1 is the closest to the inter-area oscillation range. It can be seen that mode phasor plot confirms that damping ratio for this specific mode does not increase with use of WAMS, because the angle between each generator increases. This can be explained as a consequence of adding new control loops and tuning would be required.

7.7.4. Prony Analysis

Prony analysis was conducted on the time domain signal output of the synchronous machines present in the modified system for cases without and with WAMS system with corresponding PMUs and WADCs. The values of eigenvalue, damped frequency and damping ratio obtained by Prony analysis for two different cases are shown in figure 7.17. There were two different Prony analyses used: traditional and modified Prony analysis, hence two values are listed in the table for each parameter. By comparing the results from Prony analysis to results in table 7.16, it can be observed that similar mode has been observed as an inter-area mode with similar characteristics. Eigenvalues obtained by both methods can compare to Mode 1 from table 7.16, as well as the damped frequency. Damping ratio for the analysis done by Prony analysis in case there is no WAMS in the system is lower and it has a value of 0.0619 compared to 0.084 from eigenvalue analysis with presence of WAMS. Prony analysis gives a value of 0.0965 compared to 0.079 from eigenvalue analysis with the presence of WADCs.

Parameters	Without Damping Controller		With Damping Controller	
	Value	Units	Value	Units
Eigenvalue Traditional Method	-0.395 ± j 6.370	[1/s +j rad/s]	-0.968 ± j 6.253	[1/s +j rad/s]
Eigenvalue Modified Method	-0.458 ± j 6.4305	[1/s +j rad/s]	-0.600 ± j 6.030	[1/s +j rad/s]
Damped Frequency Traditional	1.014	[Hz]	0.995	[Hz]
Damped Frequency Modified	1.019	[Hz]	0.960	[Hz]
Damping Ratio Traditional	0.0619	[-]	0.0965	[-]

Table 7.17: Parameters observed from Prony analysis.

Figure 7.46 shows a time window selected for the analysis with presence of WAMS functionalities and figure 7.47 shows an original signal as well as signals reconstructed by traditional and modified Prony analysis. Reconstructed signals match the original time-domain signal, however the traditional Prony analysis does not reconstruct the signal as well as the modified analysis does. Values provided by Prony analysis should not have significant deviations among the two techniques used and values are summarized in the table 7.17.
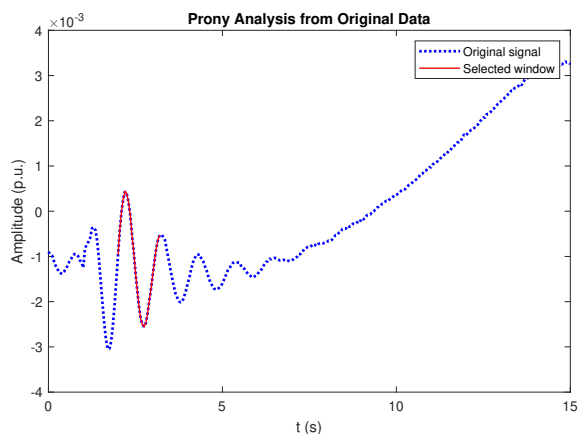

Figure 7.46: Red line is identifying the part of the signal selected for the Prony analysis.
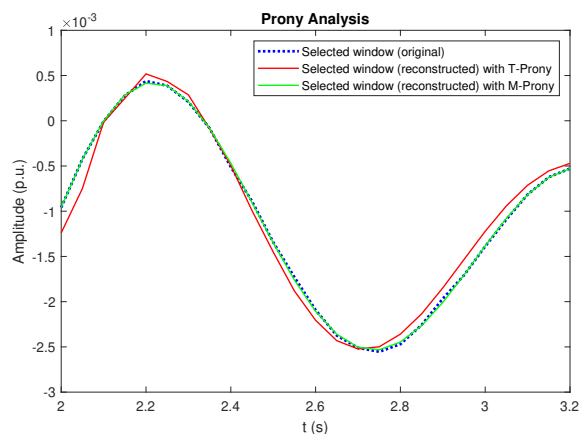
Figure 7.47: The selected window and the reconstructed signal by traditional and modified Prony function.

Figure 7.40 and figure 7.48 show spectral density of the frequencies present in the time signal for cases

without and with WAMS implemented, respectively. These figures confirm previous observations from eigen-value analysis, by showing that dominant frequencies do not fall into range between 0.3 Hz and 0.7 Hz, which does in fact indicate that there are no inter-area oscillations in the system and that frequencies above 1.0 Hz are dominant.
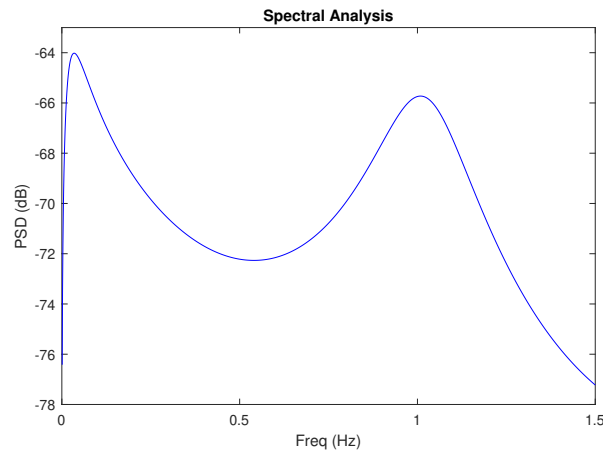

Figure 7.48: Spectral analysis of a generator signal with the use of WAD.

7.7.5. Observations and Comparison to the Base Case

Comparing results of a time domain simulations of the system with presence of eight DVCs to the base case of having ten synchronous generators indicates and confirms an occurrence of new oscillations and highly dynamic behaviour of the system. Oscillations in the base case were able to damp out shortly after an event and in case of 80% RES penetration oscillations are present, however the WADCs increase damping in the system. When three WADCs are present in the system some oscillations are visible shortly after an event, however these oscillations start to ring-down. Eventually lines of both generators start overlapping, which means that they do not swing against each other. This was achieved with correctly tuning damping controller parameters with the objective of minimizing the oscillations of the generators.

Results of the eigenvalue analysis show that the system with RES penetration have well damped modes of oscillation compared to the base case. Such behaviour was not expected and might be indicating some flaws in the control structure of the base case system with ten synchronous generators. Furthermore, a system in this case does not have any inter area modes of oscillation, only local modes of oscillation compared to the base case. This could be due to the ability of grid-forming controllers to receive a signal from a remote location compared to synchronous generators that do not have such an ability in this project. Prony analysis is done to verify and confirm the results of the eigenvalue analysis and to indicate critical modes of oscillation. Even though there is no inter area mode of oscillation in this case, Prony analysis identified a mode of oscillation which was very similar to Mode 1 from eigenvalue analysis with the damped frequency around 1.0 Hz.

7.8. Case Study 7: WAMS with 2 SG, 4 DVC and 4 WT

In this section, the analysis of how many DVC grid-forming controllers can be replaced with grid-following current control will be conducted as well as an effect of such modifications on system stability will be studied. The methodology for the case study 3 is as following:

1. Keep the existing DVC grid-forming control which are part of WAMS structure in the system and replace other with grid-following control. Determine whether the system is able to stabilize following an disturbance.
2. In case that the system does not stabilize, add one additional DVC grid-forming controllers. Which power plants to include grid forming control is determined by the analysis summarized in table 7.13, where the order of power plants with decreasing observability indices is located. The fourth grid-forming controller added to the system would then be the power plant with the fourth largest observ-

ability index.

3. Due to the layout of the test system and since the power plant with the fourth largest observability index is located in the same part of the system as already activated grid-forming controllers, a power plant with the fifth largest observability index was selected to include grid-forming controller strategy.

4. The results observed with implementation of one additional grid-forming controller (with previous three implemented) were satisfactory based on criteria that the system is able to stabilize after an event.

Such a methodology is considered to mimic the realistic implementation of control strategies in the future power grids, where the existing current control on WTs will not be replaced with grid-forming control and the extend of using WAMS technology to enhance selective damping is studied in this section.

7.8.1. Input and Output Signal Selection

Table 7.18 shows the OIs for all power plants in the system, however in this case there are two different state variables considered. This is because there are two different controllers (DVC and grid-following controller) associated with WTs in the system.

Generator	Bus	OI
Power Plant 7	Bus 36	1
Power Plant 6	Bus 35	0.98824
Power Plant 4	Bus 33	0.95325
Power Plant 9	Bus 38	0.87992
Power Plant 10	Bus 30	0.17752
Power Plant 3	Bus 32	0.14144
Power Plant 8	Bus 37	0.09451
Power Plant 2	Bus 31	0.07624
Power Plant 5	Bus 34	0.07062
Power Plant 1	Bus 39	0.00691

Table 7.18: Observability and controllability indices for 2 SGs, 4 DVCs and 4 WTs with current control.

In this case PMUs are installed on Bus 36, Bus 35 and Bus 33, as suggested in the table 7.18. Three out of four power plants with DVC present in this study case have been identified to have the highest OIs and such phenomenon was explained in the previous paragraph. Comparing the values of OIs to the previous case study it is visible that Bus 36, Bus 35 and Bus 33 were preferred candidates in the previous case study just behind a value of Bus 34. These three buses being an option for deployment of PMUs might not be such a bad option after all and the results of the analysis will support the observation.

7.8.2. Time Domain Simulations

Figure 7.49 shows a time response of the generators to a short circuit event, with four DVCs and four WTs with current control connected to the system. There are oscillations visible following the disturbance before the generators stabilize around a new value of 1.004 p.u. Figure 7.50 shows a response of the system with a presence of WAMS structure, where a system is able to damp the oscillations shortly after an event. The system in both cases stabilizes at value around 1.004 p.u., however the amplitude of the oscillations is lower than in case without WAMS. It is also important to point out from the figure that at time around t = 1 second the generator G02 gets out of step before the oscillations become periodical, which is seen as sudden changes in speed signal. For this project is important that the system is able to stabilize and the generators do not lose synchronism, even though such behaviour is not ideal and can cause serious damage on generator windings.

Damping controller parameters have been tuned by PSO algorithm to achieve the highest effect of WAMS implementation. Properly tuned parameters of the damping controller have the desired effect on the speed signal of the generators. Parameters taken into consideration for tuning and values achieved by PSO algorithm when a system is subjected to a short circuit event are collected in table 7.19. DVCs associated with Power Plant 4, Power Plant 6 and Power Plant 7 are chosen to receive the stabilizing signal, hence the parameters of associated WADCs have to be tuned to obtain the desired result. The parameters' symbols are the same as explained in the previous study case, hence Study Case 2 can be referred to for the names of the parameters.
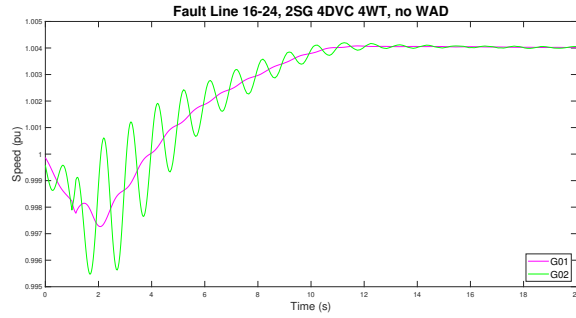
Figure 7.49: A response of 2 SGs to a fault event on Line 16-24 with presence of 4 DVCs, 4 WTs and without WADC.
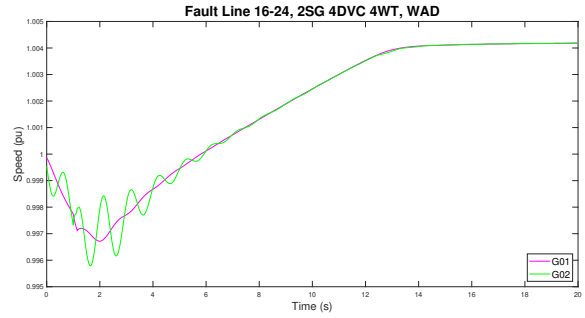

Figure 7.50: A response of 2 SGs to a fault event on Line 16-24 with presence of 4 DVCs, 4 WTs and with WADC on G07, G06, G04.

Symbol	Initial Values	WAD 04	WAD 06	WAD 07
Kpss1 [pu]	1	0.687975	0.030464	4.202095
Kpss2 [pu]	1	0.662225	0.660137	0.687463
Kpss3 [pu]	1	0.737080	0.511362	0.422322
Tw [s]	10	9.938308	10.28073	10.08579
T1 [s]	5	9.881687	4.996715	4.922270
T2 [s]	0.4	0.017139	0.250242	0.059595
T3 [s]	1	1.002742	0.588831	1.014443
T4 [s]	0.1	0.115245	0.096275	0.098532

Table 7.19: Initial and tuned WAD parameters for 2SG 4DVC 4WT.

A time domain response of a system with four grid-following controllers to a load event at time = 1 second is shown in figure 7.51. After an initial drop in generator speed, the system is able to stabilize and the generator speed increases to the value just below 1.002 p.u. Figure illustrates the presence of oscillations over the entire period shown, even more than 10 seconds after a load event. On the other hand, WAMS is able to damp these oscillations in the system shortly after an event as shown in figure 7.52. Similar behaviour is shown since speed initially drops to a lower value and recovers shortly after. The value of generator speed is able to stabilize at the later value and it is not visible in this figure since the main intent is to show the presence of oscillations and the ability of WAMS to damp those oscillations. The figure which indicates the value of when generators are able to stabilize is shown later.

Figure 7.51: A response of 2 SGs to a load event on bus 15 with presence of 4 DVC, 4 WTs and without WADC.
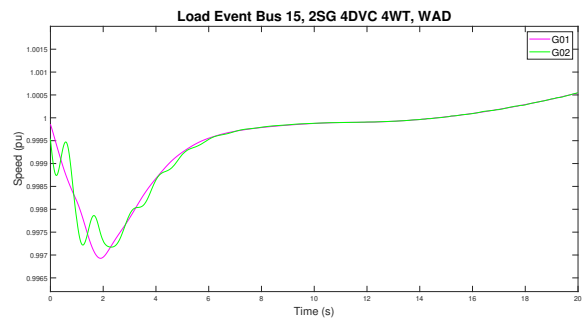
Figure 7.52: A response of 2 SGs to a load event on bus 15 with presence of 4 DVC, 4 WTs and with WADC on G07, G06, G04.

Table 7.20 collects initial and tuned parameters of wide area damping controllers in case the system is subjected to a load event. The generator signal following the disturbance with presence of WAMS is not as effectively damped as the ones shown in the figure in case that parameters are not tuned specifically to the disturbance. Even though the effect of wide area damping controllers is slightly less effective in those instances, the overall improvement over the standard case without damping controllers is visible. In reality, parameters of damping controllers cannot be tuned for every disturbance, however parameter values of WADC usually follow a similar trend. There might be one parameter value per controller that has a different magnitude, however this might be due to the nature of the tuning algorithm and its methodology of determining the best

solution.

Symbol	Initial Values	WAD 04	WAD 06	WAD 07
Kpss1 [pu]	1	0.677308	0.598364	3.574130
Kpss2 [pu]	1	4.811894	0.691442	0.682926
Kpss3 [pu]	1	0.683829	0.439301	0.420463
Tw [s]	10	9.851473	10.01094	10.08554
T1 [s]	5	9.891694	4.972223	4.925936
T2 [s]	0.4	0.061935	0.280791	0.547317
T3 [s]	1	1.012137	0.649938	1.015117
T4 [s]	0.1	0.112296	0.100110	0.104813

Table 7.20: Initial and tuned WAD parameters for 2SG 4DVC 4WT for Load event.

Figure 7.53 shows the generator signals of G01 and G02 as a response to the short circuit disturbance in case without and with WAMS functionalities. The difference in oscillation amplitude, system's ability to damp oscillations and the behaviour of the signal can be compared and studied side by side. Similarly, figure 7.54 shows the signals of the generators, however in this case following the load event. Important to note for this figure is that the time period shown is t = 70 seconds, with an intent of showing the whole period before the signal stops ramping up and stabilizes at around 1.004 p.u. There are still oscillations visible in the figure for a signal without presence of WAMS, however the main intention of showing this figure is to see how in case with WAMS signal is able to stabilize sooner at around time t = 35 seconds.
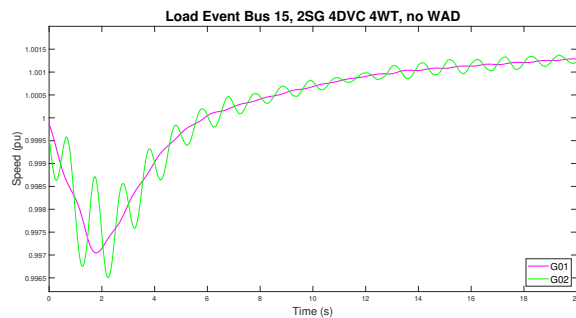

Figure 7.53: A response of 2 SGs to a fault event on Line 16-24 with presence of 4 DVC, 4 WTs with and without WADCs.

Figure 7.54: A response of 2 SGs to a load event on bus 15 with presence of 4 DVC, 4 WTs with and without WADCs.

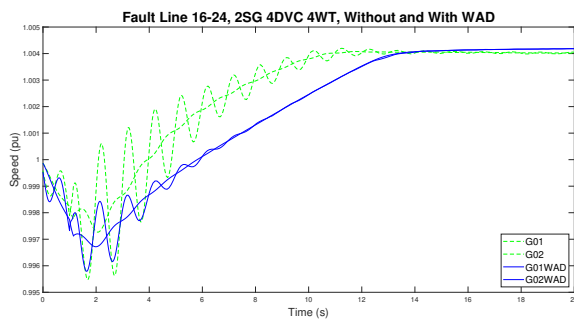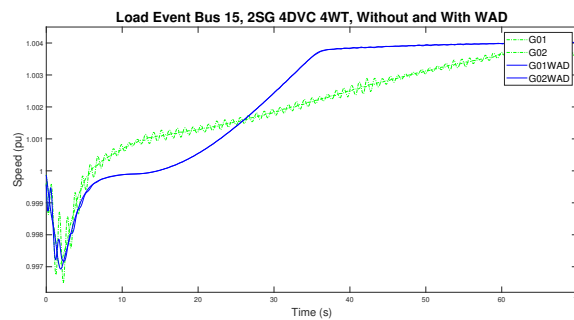It is interesting to point out that in both cases and for both disturbances the signals follow a similar trend. Initially, following the disturbance the signal decreases with a high rate of change, however at some point all generators start to speed up until they reach a new value where they stabilize. This behaviour is different from the base case as well as from the case when only grid-forming control with synchronous machines are present in the system. This means that such behaviour occurs due to grid-following control or less grid-forming ability in the system.

7.8.3. Eigenvalue Analysis

Eigenvalue analysis was performed to study damping of the system with four grid-forming controllers associated with WTs, four grid-following controllers and two synchronous machines. Three critical modes of oscillation are collected in figure 7.21, where Mode 1, Mode 2 and Mode 3 are all identified as local modes of oscillation. Modified system does not have a presence of inter area mode of oscillation, which might be due to lack of rotating masses in the system and the system oscillates locally. System is well damped with only Mode 2 having a damping ratio below 10%. All other critical modes have a damping ratio of more than 35%, with WAMS as well as without the presence of WAMS. It must be pointed out that damping ratios of all three critical modes decrease with presence of WAMS, which is not an ideal outcome. A possible explanation for such behaviour might be a presence of additional control loops and interaction of current control with WADCs.

Previously observed behaviour of the system and relatively high damping ratios can be confirmed by ex-

Modes	Without Damping Controller			With Damping Controller		
	Eigenvalues	Damped Frequency	Damping Ratio	Eigenvalues	Damped Frequency	Damping Ratio
Units	[1/s +j rad/s]	[Hz]	[-]	[1/s +j rad/s]	[Hz]	[-]
Mode 1	-0.441 ± j 6.094	0.970	0.0721	-0.361 ± j 6.141	0.977	0.0587
Mode 2	-3.656 ± j 8.746	1.392	0.3857	-3.738 ± j 9.597	1.527	0.3621
Mode 3	-9.599 ± j 11.982	1.907	0.6252	-9.587 ± j 12.222	1.945	0.6172

Table 7.21: Modal analysis parameters for 2 SGs, 4 DVCs and 4 WTs from PowerFactory analysis.

amining figure 7.55, where three modes for both cases are highlighted in the figure. The doted lines indicated the damping ratios of 0.1, 0.2, 0.3 and 0.4. From the figure is visible that critical modes of oscillation for a case without presence of WADC (green circles) have higher damping ratios than blue crosses which represent the case with presence of WAMS. Such behaviour was explained by analyzing table 7.21 and is visually represented in this figure.
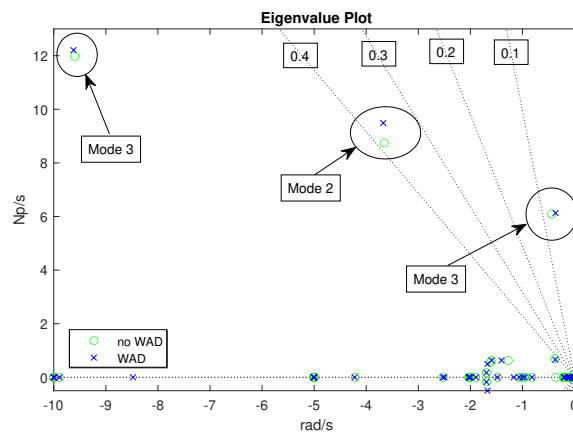

Figure 7.55: Eigenvalue plot indicating critical modes of oscillation without WAD and with WAD.

7.8.4. Prony Analysis

Prony analysis was conducted to verify whether the behaviour from eigenvalue analysis will be visible in the time domain response. Prony analysis will verify whether system's ability to damp oscillations with a presence of WADC is in fact lower than without the presence of such a controller. Information collected in table 7.22 show that there is actually higher damping of the dominant mode in a system without the presence of WAMS, which is definitely surprising after observing the time domain response of the system. This observation presents an opportunity for future research and improvements of control structure of heavily penetrated system with RES. The existing model could serve as a base case to study an effect of other advanced solutions for solving these issues.

Parameters	Without Damping Controller		With Damping Controller	
	Value	Units	Value	Units
Eigenvalue Traditional Method	-0.435 ± j 6.174	[1/s +j rad/s]	-0.374 ± j 6.498	[1/s +j rad/s]
Eigenvalue Modified Method	-0.225 ± j 6.469	[1/s +j rad/s]	-0.336 ± j 6.253	[1/s +j rad/s]
Damped Frequency Traditional	0.9826	[Hz]	1.0342	[Hz]
Damped Frequency Modified	1.0296	[Hz]	0.9952	[Hz]
Damping Ratio Traditional	0.0703	[-]	0.0575	[-]

Table 7.22: Parameters observed from Prony analysis 2SG 4DVC 4WT.

Prony analysis supports the observed damping ratio and a collection of information present in table 7.22 show that other parameters (eigenvalues and damped frequencies) are successfully estimated from the time domain signal. Figure 7.56 shows the selected window of the time domain signal for Prony analysis. Figure

7.57 shows that Prony analysis is able to reconstruct the signal and estimate eigenvalues, damped frequency and damping ratios in line with Modal analysis.
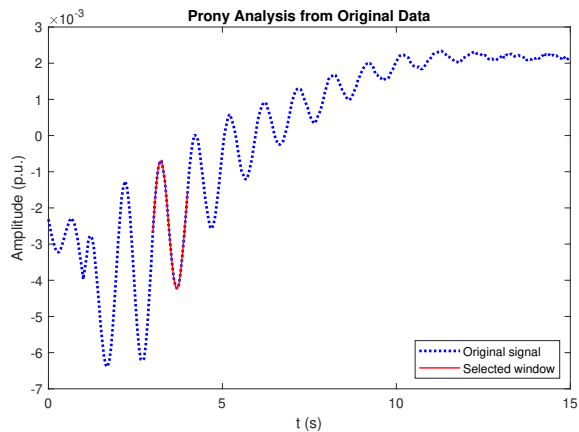

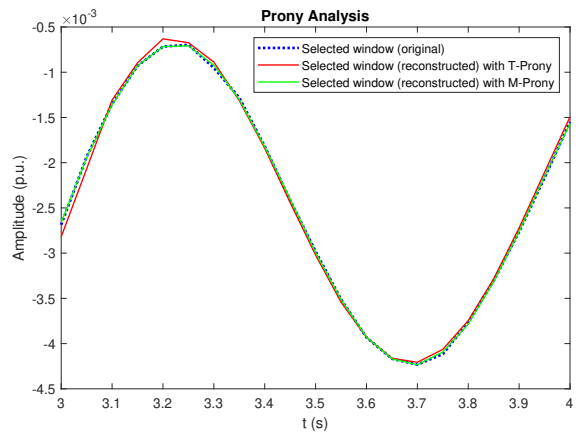Figure 7.56: Red line is identifying the part of the signal selected for the Prony analysis.

Figure 7.57: The selected window and the reconstructed signal by traditional and modified Prony function.

Presence of WAMS makes a selection of the appropriate time window for Prony analysis challenging and figure 7.58 shows the selected window which was considered for the analysis. The reconstructed signals by Prony analysis are shown in 7.59, where a traditional Prony method produced a signal which does not completely overlap with the original data. Table 7.22 has shown that there are no significant differences between values estimated with the two methods used.
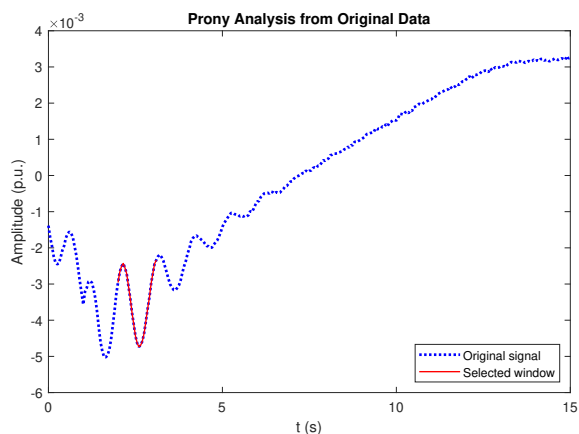

Figure 7.58: Red line is identifying the part of the signal selected for the Prony analysis.
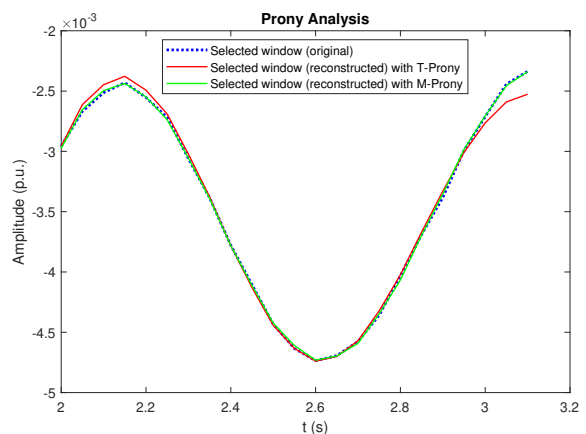

Figure 7.59: The selected window and the reconstructed signal by traditional and modified Prony function.

The presence of dominant frequencies in the time domain signal is shown by spectral analysis in range between 0 Hz and 1.5 Hz. Figure 7.60 shows the spectral density of the signal when WAMS was not activated in the system and it highlights that the dominant mode of oscillations is around or just above 1.0 Hz as summarized in the table 7.22. Similarly, figure 7.61 follows the same results as indicated in the figure, however it shows a high density of very-low frequency oscillations. Such behaviour might lead towards the conclusion that controllers present in the system (grid-following, grid-forming and control associated with synchronous machines) will have to be tuned to improve the behaviour of the system.

7.8.5. Observations and Comparison to to Previous Study Cases

Obtained time domain simulation results follow a similar trend as time domain simulation results of the Study Case 6 when the WAMS is activated in the system. The response of the generators after being subjected to the disturbance is similar in both cases (with and without WAMS) and for both disturbances. A difference of having WAMS in the system is visible by reduced amount of oscillations present in the time domain signal and
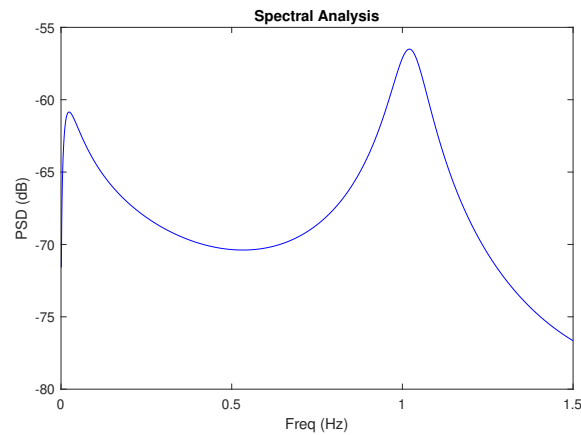
Figure 7.60: Spectral analysis of a generator signal without the use of WAD.
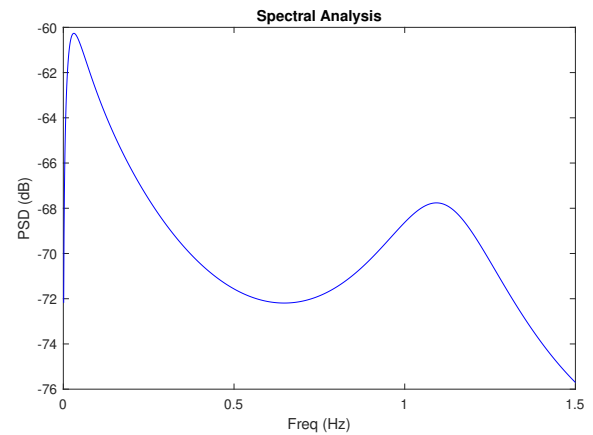

Figure 7.61: Spectral analysis of a generator signal with the use of WAD.

the time that it takes for the signal to stabilize at new value. The major difference between study cases 5 and 7 is that in case of a short circuit event, a system for the base case stabilizes at the nominal values shortly after an event. Another difference between different study cases is seen in case of a load event, where a decrease in generator speed is visible when synchronous generators are present in the system. In case of a presence of grid-forming and grid-following control there is actually an increase in generator speed.

Eigenvalue and Prony analysis do not support the observations of increased damping in the system from the time domain simulations, where the damping of critical modes of oscillations actually deceases with presence of WAMS. Such behaviour is not desired and WAMS was actually designed to enhance damping in the system. It was also observed that the overall damping of the system with grid-following control has been improved similarly to the Study Case 6. This study case can be concluded by saying that a system is able to withstand significant disturbances even if there is a presence of grid-following control on some of the WTs. It is important to point out that 40% of all generation is generated by WTs with grid-following control, which is significant for designing future power grids. This study should be taken into consideration when planning future modification and introducing RES penetration to the grid.

7.9. Case Study 8: WAMS with 2 SG, 3 DVC, 1VSM and 4 WT

For a purpose of analysing an effect of having different types of grid-forming controllers connected in the grid at the same time, the DVC grid-forming controller has been combined with VSM. A study of a complete replacement of DVC controller strategy with VSM is not possible in this project, because VSM is not modeled to receive the voltage signal from the remote location; hence the VSM grid-forming control does not have an ability to receive the signal from WAMS. An attempt was made to modify such SVM controller to be able to receive the remote signal, however more effort and more understanding of the particular control structure is required for successful implementation. Furthermore, it was stated in the scope of this thesis project that this project will focus on application of already existing controllers to design a system where WAMS will improve the overall damping and stability of the system. Results would be explained by performing eigenvalue analysis as well as by studying the time-domain results.

It has been described in the section 7.8 that the presence of four grid-forming controllers in the grid is required in order for the test system to stabilize after an introduction of a short-circuit fault. The WAMS signal will be as described in the previous section fed to DVC grid forming controllers, since this type of a controller has an ability to receive a signal from the remote location. The purpose of adding the VSM to the grid is to study an impact of additional grid-forming controllers and its interaction with already present controllers. This analysis will be a great indication whether such a controller has a potential to be successful at stabilizing the system following the disturbance and whether such controller could be used for WAMS applications to receiving the stabilizing signal.

The methodology of implementation additional grid-forming controllers to the system is as following:
   1. The system will consists of two synchronous generators (G01 and G02), three DVC grid forming con-

trollers, one VSM grid forming controller and four grid-following current controllers.

2. VSM will replace DVC controller on a Power Plant 09, which does not receive the remote WAMS signal. Grid-following control is associated with power plants determined by signal selection analysis done in section 7.7.

3. The effect of having another controller with stabilizing ability in the system with a different structure will be studied and an effect will be determined by time-signal analysis and with eigenvalue analysis.

4. PMUs are installed on Bus 36, Bus 35 and Bus 33, which has been determined in section 7.8 and is summarized in a table 7.18. Power plants with WADCs are Power Plant 7, Power Plant 6 and Power Plant 4 as determined in section 7.7.

7.9.1. Time Domain Simulations

The effect of adding VSM and replacing an existing DVC has a positive effect on the stabilization of a time domain signal as seen in figure 7.62. The speed of the generators is able to stabilize at a much lower value of around 1.0005 p.u. and despite the presence of oscillations such result is very promising. Furthermore, figure 7.63 shows even more promising results since the speed of the generators is able to stabilize almost at the nominal value of 1.0 p.u. Addition of VSM has a positive effect on the system damping, where oscillations are successfully damped shortly after the disturbance despite the fact that there are four grid-following controllers present.
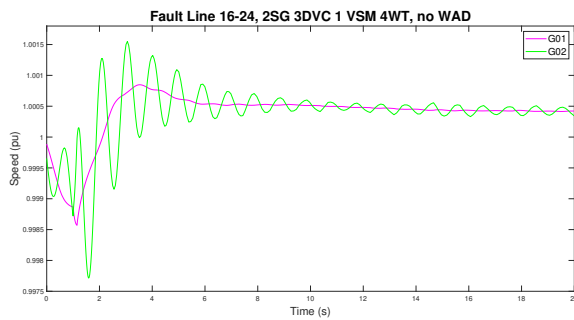

Figure 7.62: A response of 2 SGs to a fault event on Line 16-24 with presence of 3 DVCs, 1 VSM, 4 WTs and without WADC.
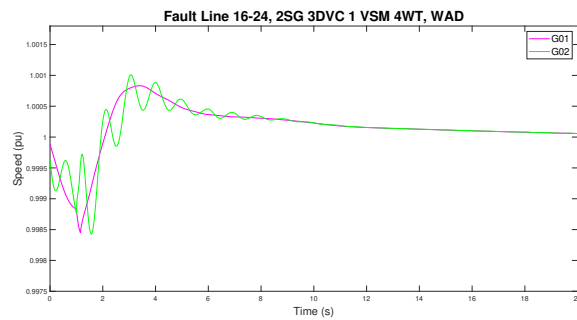
Figure 7.63: A response of 2 SGs to a fault event on Line 16-24 with presence of 3 DVCs, 1 VSM, 4 WTs and with WADC on G07, G06, G04.

Symbol	Initial Values	WAD 04	WAD 06	WAD 07
Kpss1 [pu]	1	0.494324	0.501072	0.502572
Kpss2 [pu]	1	0.499986	0.499931	0.508624
Kpss3 [pu]	1	0.502228	1.269081	0.495787
Tw [s]	10	10.0053	9.992328	10.00533
T1 [s]	5	4.999588	5.00366	5.000902
T2 [s]	0.4	0.404339	0.01394	0.395943
T3 [s]	1	1.004071	0.996125	1.000827
T4 [s]	0.1	0.099637	0.099564	0.061862

Table 7.23: Initial and tuned WAD parameters for 2SG 3DVC 1VSM 4WT.

Initial and tuned parameters of individual WADCs present in the structure are summarized in table 7.23. These parameters are tuned with an intent to minimize the oscillations among the generators G01 and G02. The symbols shown in the figure are the same as in the previous sections so please refer to those for a description and units.

The response of both synchronous generators to a load event is shown in figure 7.64 in case when WAMS is not present in the system and figure 7.65 shows the response of the generators when WAMS is activated. Enhanced damping is visible when WAMS is present during the simulation. Table 7.24 collects the initial and tuned parameters of the three WADCs present in the system, WADC 04, WADC 06 and WADC 07. A description of the symbols can be found in the previous section, since the same parameters are used for the optimization problem.
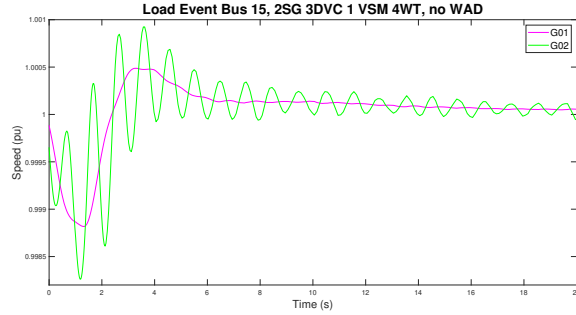
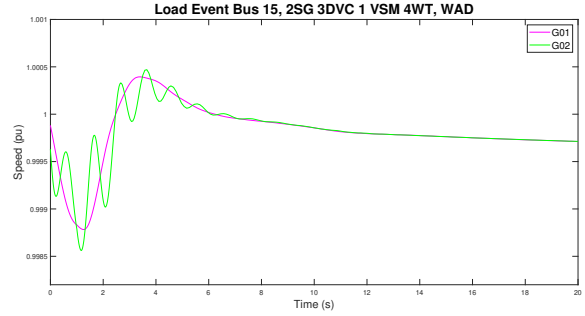Figure 7.64: A response of 2 SGs to a load event on bus 15 with presence of 3 DVCs, 1 VSM, 4 WTs and without WADC.

Figure 7.65: A response of 2 SGs to a load event on bus 15 with presence of 3 DVCs, 1 VSM, 4 WTs and with WADC on G07, G06, G04.

Symbol	Initial Values	WAD 04	WAD 06	WAD 07
Kpss1 [pu]	1	0.504771	0.590096	0.215352
Kpss2 [pu]	1	3.856223	0.097397	0.635215
Kpss3 [pu]	1	4.747128	1.020172	0.169688
Tw [s]	10	10.03691	10.04491	9.841836
T1 [s]	5	4.668739	4.931563	5.076405
T2 [s]	0.4	0.081284	0.480715	0.484011
T3 [s]	1	1.031895	1.090087	1.053072
T4 [s]	0.1	0.030948	0.197457	0.099871

Table 7.24: Initial and tuned WAD parameters for 2SG 3DVC 1VSM 4WT.

Figure 7.66 shows the response of the system with and without WAMS activated in the system in case of a fault event. The response of the signal is very similar independent of WAMS, however there is substantially less oscillations with presence of WAMS. Figure 7.67 shows the generator speed of G01 and G02 when subjected to a load event and the response of an individual generator is very similar independent on presence of WAMS. In is interesting to note that the system has almost the same response when subjected to short-circuit event as well as when subject to a load disturbance. There is a significant contribution of just a single VSM grid-forming controller and the biggest benefit is to enable a system to stabilize shortly after an event an for generator speed to return to its nominal value independent on the disturbance.
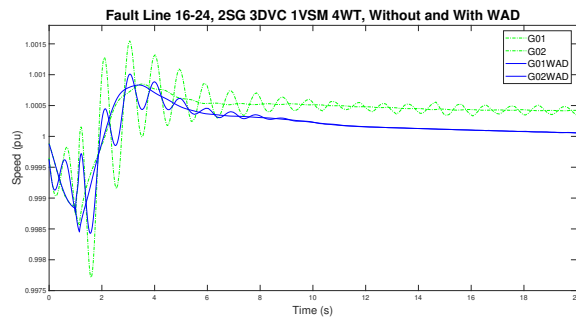
Figure 7.66: A response of 2 SGs to a fault event on Line 16-24 with presence of 3 DVCs, 1 VSM, 4 WTs with and without WADC.
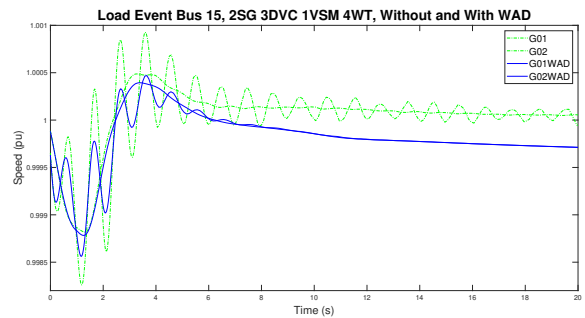
Figure 7.67: A response of 2 SGs to a load event on bus 15 with presence of 3 DVCs, 1 VSM, 4 WTs with and without WAMS.

7.9.2. Eigenvalue Analysis

Eigenvalue, damped frequency and damping ratio of critical modes of oscillation are collected in table 7.25, for cases with and without WAMS activated during the analysis of the system. Table shows that damping of the modes of oscillation decreases with the introduction of WAMS, which was also seen in the Study Case 7. Furthermore, modes of oscillation listed in the table are all local modes without any critical OMs falling into a range of inter area modes of oscillation.

Modes	Without Damping Controller			With Damping Controller		
	Eigenvalues	Damped Frequency	Damping Ratio	Eigenvalues	Damped Frequency	Damping Ratio
Units	[1/s +j rad/s]	[Hz]	[-]	[1/s +j rad/s]	[Hz]	[-]
Mode 1	-0.460 ± j 6.386	1.016	0.0718	-0.427 ± j 6.390	1.017	0.0667
Mode 2	-6.121 ± j 9.910	1.577	0.526	-6.008 ± j 10.910	1.737	0.482
Mode 3	-17.969 ± j 11.673	1.858	0.839	-18.031 ± j 11.583	1.844	0.841

Table 7.25: Modal analysis parameters for 2SG 3DVC 1VSM 4WT PowerFactory analysis.

Figure 7.68 highlights two critical modes of oscillation collected in the table, since Mode 3 has a relatively large positive value and high damping ratio. Mode 1 was considered for the mode phasor plot representation as shown in figure 7.69 since it is the closest to the inter-area oscillation range. Figure supports previous observation about damping ratio decreasing with introduction of WAMS, where blue lines, which represents the generators with the presence of WADC, oscillate against each other with an angle close to 180 degrees. On the other hand, green lines, which represent generators when WAMS was not included to the system during the simulation oscillate against each other with a smaller angle compared to the blue lines, which indicates a better damped mode.
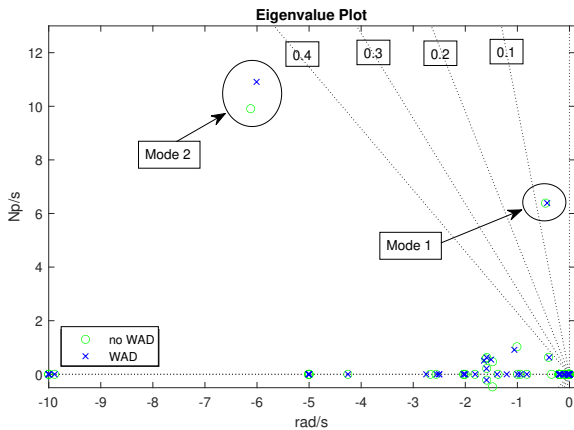

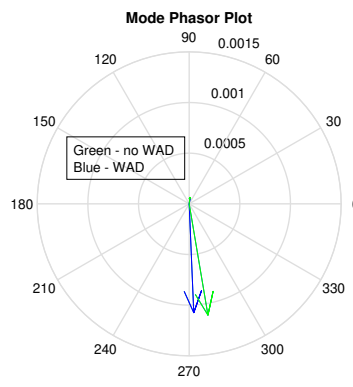Figure 7.68: Eigenvalue plot indicating critical modes of oscillation without WAD and with WAD.

Figure 7.69: Mode phasor plot of the critical mode 1 without WAD and with WAD.

7.9.3. Prony Analysis

Table 7.26 shows the parameters estimated by traditional and modified Prony analysis and the identified mode of oscillation can be compared to Mode 1 from Eigenvalue analysis shown in table 7.25. The real part of the eigenvalue determined by both methods does not match with the real part from the eigenvalue analysis, where the traditional Prony estimated a higher value and a traditional method estimated a lower value. Prony estimates a similar imaginary part well as well as the damped frequency and damping ratio. Table also shows that the damping ratio estimated from the test system with WAMS improved over the test system with WAMS disconnected. Prony analysis results in that aspect do not match with eigenvalue analysis results and such observation indicates that increased damping is visible from the time domain signal. Similar predictions about the cause of such behaviour can be made as in Study Case 7, where any additional controller loops might be a root of the problem observed.

A window selected for the Prony analysis when WAMS is deactivated can be seen in figure 7.70 and the reconstructed signal of both Prony methods can be visible in 7.71. The appropriate time window for Prony analysis to give correct results due to the behaviour of the signal is easily determined in this study case. Values previously seen in the table can accurately represent the time domain signal based on the observation that reconstructed signals match with the original signal.

Time window selected for the Prony analysis in case when WAMS is connected to the system is shown in figure 7.72. Such setup can be observed from the figure based on less visible oscillations in the signal, which

Parameters	Without Damping Controller		With Damping Controller	
	Value	Units	Value	Units
Eigenvalue Traditional Method	-0.521 ± j 6.474	[1/s +j rad/s]	-0.675 ± j 6.865	[1/s +j rad/s]
Eigenvalue Modified Method	-0.262 ± j 6.463	[1/s +j rad/s]	-0.260 ± j 6.440	[1/s +j rad/s]
Damped Frequency Traditional	1.0304	[Hz]	1.0927	[Hz]
Damped Frequency Modified	1.0286	[Hz]	1.0249	[Hz]
Damping Ratio Traditional	0.0803	[-]	0.0979	[-]

Table 7.26: Parameters observed from Prony analysis 2SG 3DVC 1VSM 4WT.

Figure 7.70: Red line is identifying the part of the signal selected for the Prony analysis.

Figure 7.71: The selected window and the reconstructed signal by traditional and modified Prony function.

also means that finding the right window might turn out slightly more difficult that in case without WAMS. A proof of the correctly selected window is figure 7.73, where reconstructed signals of both methods match with the original signal. A red line, which shows the reconstructed signal with traditional Prony method, slightly deviates from the original signal towards the end of the selected time window, while blue line tracks the original signal throughout the whole window. Nevertheless, the table shown before indicates that both methods were able to match the original line and correctly estimate the parameters.
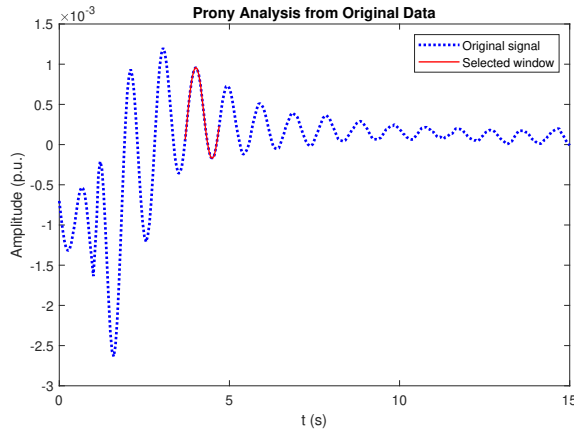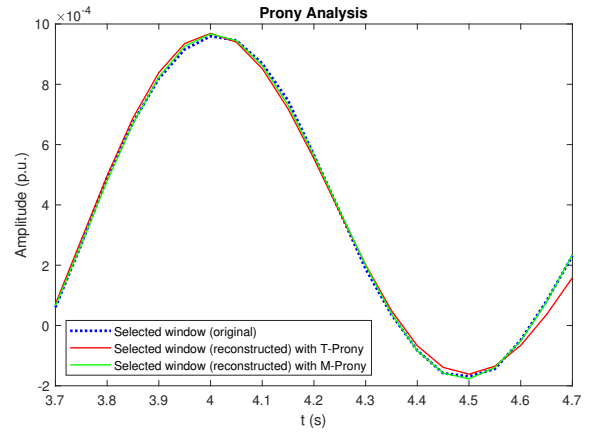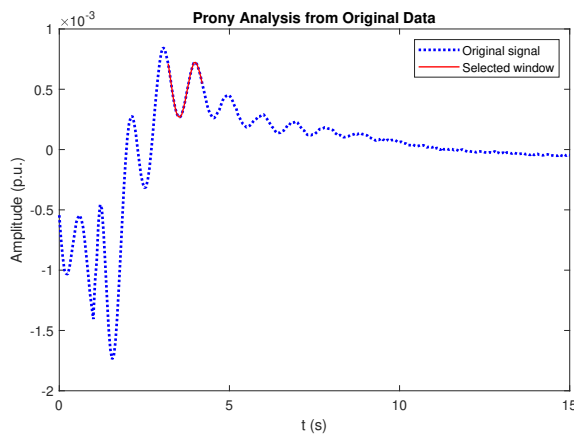

Figure 7.72: Red line is identifying the part of the signal selected for the Prony analysis.
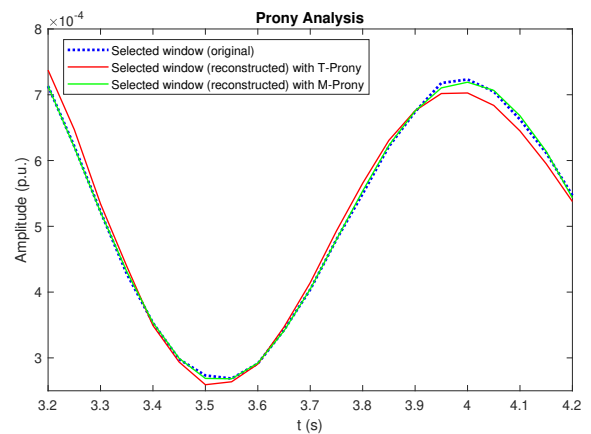
Figure 7.73: The selected window and the reconstructed signal by traditional and modified Prony function.

Figure 7.74 and figure 7.75 show spectral densities of the frequencies present in the time signal in case when system did not include WAMS and when WAMS was activated. Both figures indicate that there no inter area oscillations in the system because frequencies in range between 0.3 Hz ans 0.7 Hz are not dominant in the signal. However, furthermore 7.75 indicates that presence WADC significantly decreased frequencies around 1.0 Hz, which highlights the damping ability of WAMS.

Figure 7.74: Spectral analysis of a generator signal without the use of WAD.
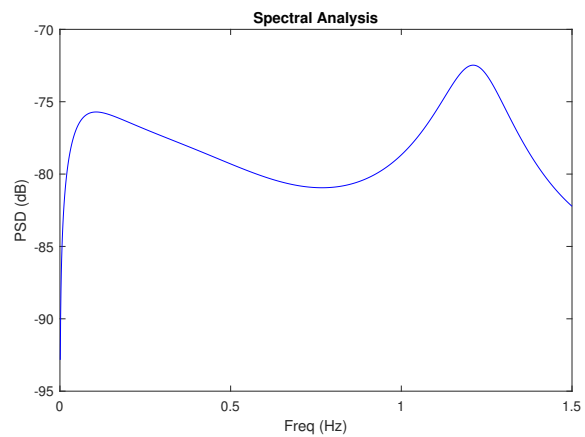
Figure 7.75: Spectral analysis of a generator signal with the use of WAD.

7.9.4. Observations and Comparison to Previous Study Cases

The biggest outcome of this study case is a positive effect of introducing VSM grid-forming controller to the system on the overall stability and it would be very interesting to see an effect when VSM would be able to receive a stabilizing signal from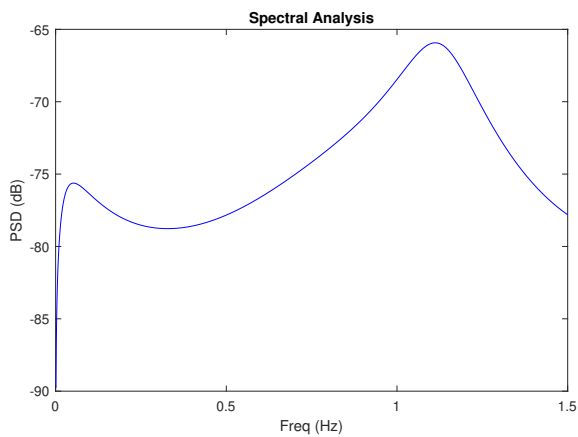 WAMS. From time domain simulations is visible that following the initial dip system responds in a very similar way as a base case, where generator speed is able to stabilize very close to its nominal value of 1.0 p.u. Study Case 8 shows a potential of VSM in further enhancing the system stability and motivates for conducting future research in area of enhancing controllability of grid-forming controllers by introducing WAMS functionalities.

Another observation made in this study case is increase in damping ratios of critical modes of oscillation compared to results in Study Case 7. Mode 1 can be compared to previous study case and a slight improvement in damping ratio can be observed, however the significant improvement in time domain simulations can conclude that VSM enhanced stability limits of the system as seen in figures 7.66 and 7.67.

8

Conclusion and Future Work

The objective of this Master's Thesis project was twofold: to study an effect of massive penetration of PE devices to the power grid and to propose means and technologies for utilizing gained knowledge by developing DNV's NextGen GridOps Knowledge Framework. Applying gained knowledge to real-world situations means that the proposed solution needs to be as realistic as possible to be feasible for clients to decide to optimize for such procedures. A work carried in this this project build upon findings developed during Horizon 2020 MIGRATE project, where it has been identified that grid-following control enables 60% penetration of RES to the power grid. It has been also stated that grid-forming control enables higher penetration of RES and at some point it would even allow 100% penetration. In this thesis work results of MIGRATE were reconstructed, where grid-following control enables 60% penetration of RES. Furthermore, two different methods were used to prove that grid-forming control enables higher levels of penetration, to go with findings from MIGRATE project. The two methods used were a DVC and a VSM method. Unfortunately, only DVC method is able to receive the remote stabilizing signal; hence DVC grid-forming control has been the used for studying the impacts of WAMS mitigation solutions on the system.

Different case studies with implemented WAMS were performed to determine:
- how significant is the effect of WAMS functionality and what are the observed benefits,
- does a higher number of WADCs cause higher stabilizing and damping effect,
- what is the percentage of grid-forming control required in the system and what percentage can be grid-following control, and
- what is the effect of adding VSM control to the system and whether two different control strategies can be implemented to the system at the same time.

The latest two case studied were done with intent of mimicking realistic implementations, where a certain percentage of RES will have grid-following control. Furthermore, different kinds of grid-forming control will be deployed in the future grid with different stabilizing characteristics and it is important to realize possible benefits of such behaviour.

A final design proposed, which takes explained motivation into consideration is as following: massively penetrated system with RES consists of 2 synchronous generators and eight wind power plants, which are able to match previous power output achieved by synchronous generators. About forty percent of all power generation comes from wind power plants with grid-forming ability and about forty percent of total power output comes from wind power parks with grid-following ability. There are a total of three PMUs installed in the system as well as three WADCs despite the fact there are a total of ten power plants in the system. This was done to preserve an initial investment and operational costs in the future grids. Results obtained from time-domain simulations and from eigenvalue analysis confirms that application of WAMS enhances controllability and consequently enhances system stability and increases damping in heavily RES penetrated systems. It has been determined that further knowledge is required to understand controllers and interactions among them, since the occurrence of very low frequency oscillations can be assigned to their existence. Tuning of controllers and system control schemes might solve these issues without installing any new hardware.

8.1. Answers on Research Questions

Following research questions will be answered to highlight important points, methods and findings achieved in this project and to emphasize the value of the research conducted.

1. What modifications are required with respect to a standardized test system to enable a study of different case studies with 80% penetration of RES? How will control models (grid forming and grid following), phasor measurement units and wide area monitoring system (WAMS) be modelled in DigSILENT PowerFactory?

The standardized IEEE 39 Bus New England system has been considered for the Master's Thesis project, which consists of ten synchronous generators equipped for steady-state and for dynamic analysis. Eight WTs have been added to the system to replace eight synchronous generator to study massive penetration of PE devices to the power grid and to study effects of those devices on transient and small signal stability. These eight WTs have been modelled to either have a grid-forming or grid-following control associated. WTs have been added to the system as static generators, which were defined to act as WTs in the system by introducing various control structures: DVC, VSM or current control.

The objective of the project is to study the impacts of massive penetration of RES and observe the mitigating effect of WAMS structure on occurring oscillations in the system. PMU devices as well as WADC have to be introduced to the system for a proper design and introduction of WAMS functionalities. It has been decided that three PMUs and three WADCs will be introduced to the system to study an effect of WAMS on enhancing overall stability and damping of the system. PMUs were modelled in the system as voltage measurement, which provide a measurement from the analytically determined buses, while WADC have been modelled as a composite model in PowerFactory and applied to a modified structure of DVCs.

2. How should a phasor measurement unit be deployed to provide measurements for a wide area damping controller to have the highest observability of the system state?

The effect of damping controller is not only dependent on the location of such a controller but also based on the signal such controller is receiving. A control input signal is provided by a total of three PMUs distributed around the system and located on the generator buses. Voltage measurement from the determined buses will act as inputs to the WADC and generated signal will be in the DVC structure subtracted from the reference voltage. Magnitude of the selected voltage has been selected for the controller input due to the structure of the WADC, even though that the voltage angle would give better observability and would be more appropriate; it could be considered for future research. A location of each individual PMU is determined based on the observability indices which are determined by constructing a state-space matrix C and combining this information with the right eigenvector of the modal analysis to identify which buses in the system have the highest observability in the system. Such approach enables to preserve some of the initial and operational costs by not installing PMUs on every generators bus, however the reduced number of PMUs in the system should not jeopardize the effectiveness of WAMS structure.

The approach considered might not be ideal, because voltage magnitude has been identified for the stabilizing signal. Much more appropriate would be the voltage angle, because it carries more information about the state of the system. However, the design considered should provide the satisfying outputs because the main focus of this project was to study the effect of WAMS on controllability of the system. Voltage magnitude has been used for the stabilizing signal because DVC has been previously designed to accept such measurements. This analysis lacks insight about a number of required PMUs in the system and it should be considered while evaluating observability capabilities of the design.

3. Where should a wide area damping controller be deployed to have the highest impact on controllability of the system? Does deploying wide area damping controller on every power plant bring significant improvements over a case when only a handful of WADC are deployed on analytically determined bases?

Determining the location of supplementary damping controllers is based on the ability to have the highest possible effect on the stability of the system without over designing the number of forming controllers in the system. Similar behaviour as explained with PMUs is deployed to avoid any unnecessary investment and operational costs, however at the same time still having the intended effect of such controllers. Controllability indexes are determined for system generators based on a combination of information from state-space matrix B and left eigenvectors. Matrix B is not available as an export option in PowerFactory since it depends on the user definition and is in this project constructed by introducing a mobile load to every generator bus.

This is done by running a script, where mobile load introduces an active power injection of 100 MW to the system. Addition of stabilizing control to highly impactful points in the system means that there are less devices needed in the system for a similar effect.

This Master's Thesis did not focus on developing a method which would identify the number of WADCs which are required to achieve the desired level of controllability in the system. Two scenarios were considered, with eight and with three WADCs and the results show that larger number does not necessary mean better results. Determining what specific PE interfaced devices at specific locations should be the best candidate for WADC is also not studied in this project, because DVC was the only technology able to receive the remote signal.

4. What control approach (Direct Voltage Control, Virtual Synchronous Machine or grid following control) or combination of controllers show the highest effectiveness against different disturbances? What control approach or combination of controllers prove to be the most effective as well as realistic for future implementation?

A combination of control approaches which has been determined to be the most successful at enhancing the system stability as well as mimicking the real world implementation consists of two synchronous generators and eight acpwt. Four of those eight WTs have grid-forming control associated with them and four WTs have grid-following control associated. Three WTs have DVC grid-forming control associated due it their ability to receive the stabilizing signal from WAMS and one WT has a SVM grid-forming control associated which has proven to bring significant enhancements to system stability in heavily RES penetrated power grids. Four WTs have grid-following control associated to represent a real world implementation of RES, where not every control on existing WTs will get replaced in the future. This project has made a step towards understanding and designing future grid as well as proposing initial steps that will enhance future energy consultancy and future grid operations. Nevertheless, there is room for improvements in many areas and specific topics will be summarized in the section "Future Work."

5. What results should be implemented into NextGen GridOps Framework and how should they be modelled to support future system operations?

Results and information implemented into NextGen GridOps Knowledge Framework do not include technical details, but rather a collection of implementation strategies, maturity levels and roadmaps as well as procedures for real world deployment of a specific solution. Such information will be used by DNV in the future to enhance their consultancy and advising their clients on future grid operations. Information implemented in the framework will serve as project acceleration, since information needed during the execution of new project will be stored in one place and associated with relevant information, reference and internal experts in the field. Framework will be used as a knowledge sharing tool among experts at DNV and it will be used for creating a large picture about applications and processes that will happen in the future grid operations. Information collected in one place gives the ability for an easy identification of areas needing an improvement and later also allows to check whether such approach or solution might clash with some already existing methods or regulations. Most importantly, NextGen GridOps Framework will be DNV's internal tool which will strengthen the confidence of grid operators through better better being able to manage the ever-increasing complexity of the power grids.

8.2. Future Work

Many interesting topics and topic which were out of the scope of the project were identified throughout the execution of the project and it might be beneficial to study those topics in the future to further explore the impact of RES penetration to the power grid. Topics identified are:

1. Effect of having other renewable source of energy or storage present in the grid.

Other sources of energy have a different kind of controllers associated, which would have a different effect on the overall stability of the system. It would be very interesting to observe the processes in the system once storage or electrical vehicles are introduced to the system and what effect do those have on the transmission system and its stability. It would be interesting to observe the effect on the congestion management and the overall power transfer through the network. The standardized system considered for the analysis consists of loads, which are modelled as consumers of power with the constant demand. Introduction of loads, which are not only consumers but can also produce electricity, would have an interesting effect on the system due to bidirectional flow of energy.

2. Stochastic availability of natural resources such as wind and solar.

WTs modelled in this project have a constant power output, however in real world power output of RES depends on the availability of natural sources of energy; availability of wind in case of WTs and availability of sun in case of solar panels. Addition of wind power curves to influence the output power of the WTs would enable to study an effect of stochastic behaviour on introduction of new oscillations in the system and how can WAMS contribute towards damping of occurred oscillations. While power curves provide information about the power output depending on the speed of wind, it would also be beneficial to implement information about availability of sun and wind throughout a whole year. It is obvious that solar panels are not able to produce any power during the night, with a bulk of power generated during the day when a system typically experiences lower demand as in the morning and in the evening. Introduction of storage solutions might also become very important and control associated with them might be another source of oscillations in the future.

3. Modifying other grid-forming controllers to gain the ability to receive a remote wide area monitoring system signal.

This Master's Thesis project has demonstrated the effect of adding a stabilizing signal and combining it with a local signal to damp oscillations visible in the time domain signal. A grid-forming control able to receive a remote signal was DVC, however VSM and current control associated with WTs do not have an ability to receive a stabilizing system. These control structures would require modifications to be able to receive a remote signal and consequently receive a signal from WAMS. It has been demonstrated that VSM has a great ability to further stabilize heavily RES penetrated power systems, which suggests that system stability might benefit from their ability to receive a stabilizing signal from WAMS.

4. Tuning of controller parameters and adjusting the whole system control configuration to enhance results from eigenvalue analysis.

Eigenvalue analysis results in this project do not always match with results observed from the time domain simulations while performing different case studies and for different scenarios. While significant damping was seen in time domain simulation, damping ratios of critical modes of oscillation observed during eigenvalue analysis did not always improve when WAMS was activated. This is a reason why existing control structures should be adjusted and further refined to increase damping of critical modes as well as not cause new oscillations in the system. Spectral analysis has shown a high density of very low frequency oscillations where controllers and interaction among them might be the main cause for such oscillations.

5. Occurrence of very low frequency oscillations in the system with addition of new controllers.

Future power grid might be prone to very low frequency oscillation and it would be beneficial to study the effect of such frequencies. Development of methods for detection of such frequencies and indication of sources of oscillations should be considered in the future. It would be interesting to study what mitigations would be required to damp such oscillation, with either implementation of new hardware to the system or with focusing more on tuning controllers in the system. Tuning controllers and understanding interaction among them might be an answer to solve future issues in power grids, which is a reason why more effort should be dedicated to understanding and mitigating those issues.

A

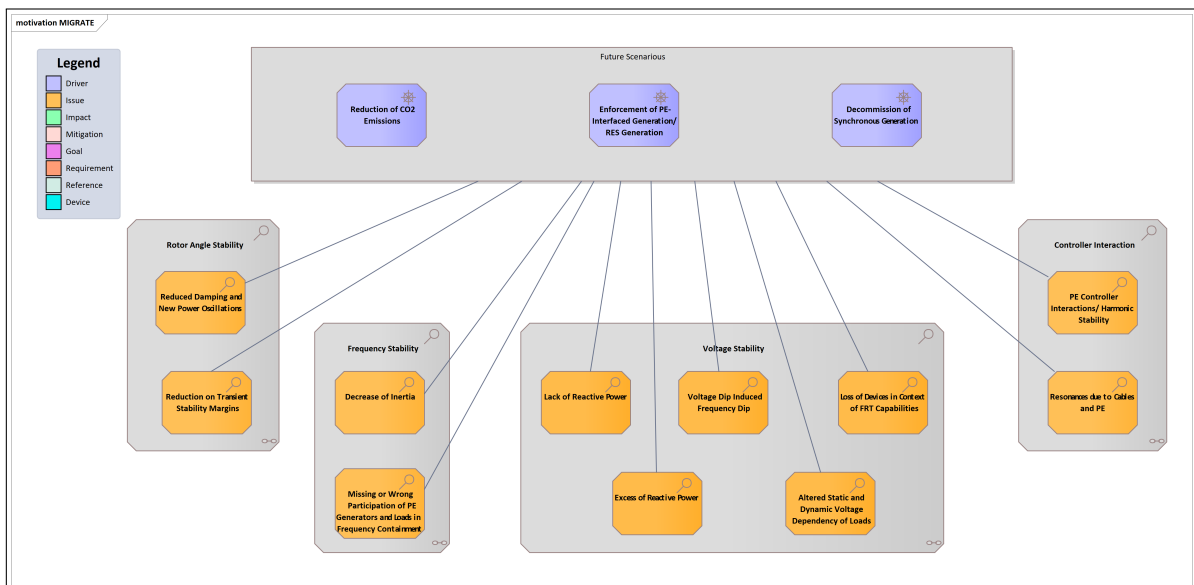# NextGen GridOps Knowledge Framework - Enterprise Architecture Implementation

Figure A.1: Implementation of MIGRATE project findings regarding identified issues into NextGen GridOps Framework built in Enterprise Architect.
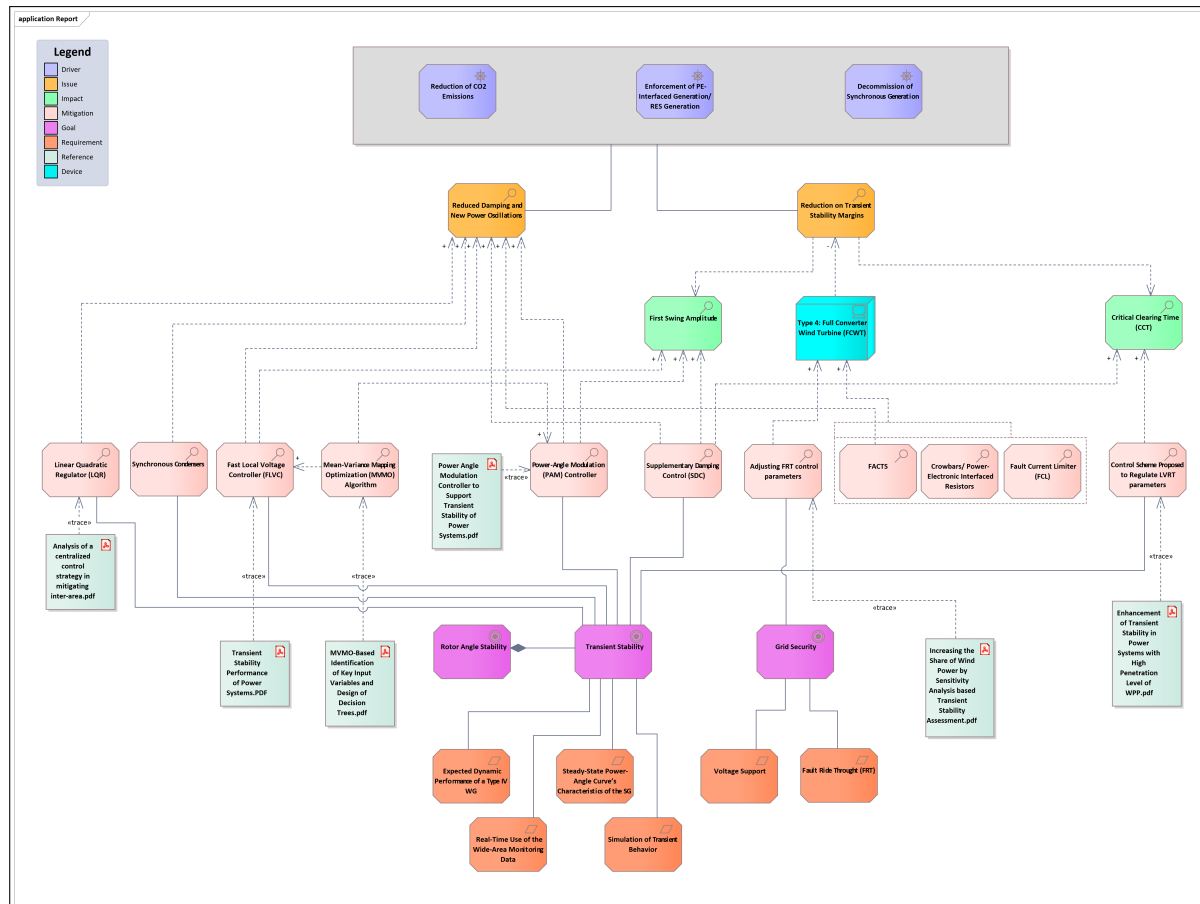
Figure A.2: Issues related to rotor angle stability with corresponding mitigations, goals and requirements.
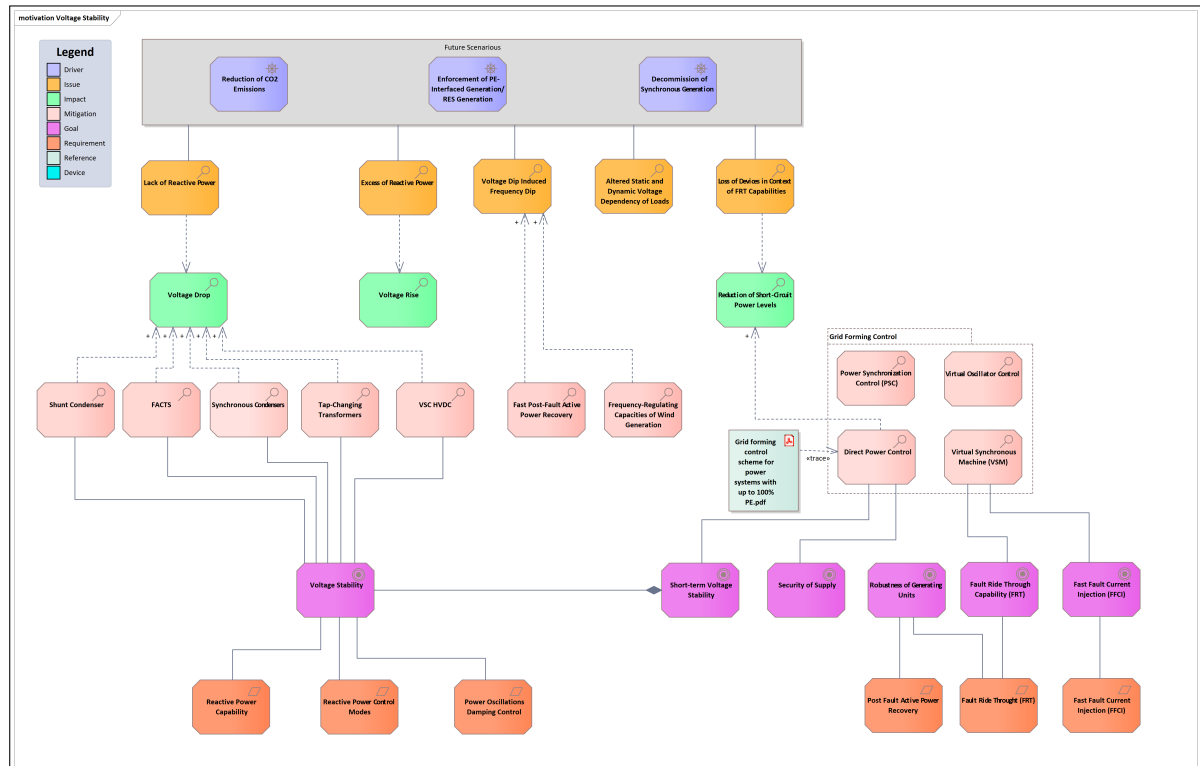

Figure A.3: Issues related to voltage stability with corresponding mitigations, goals and requirements.
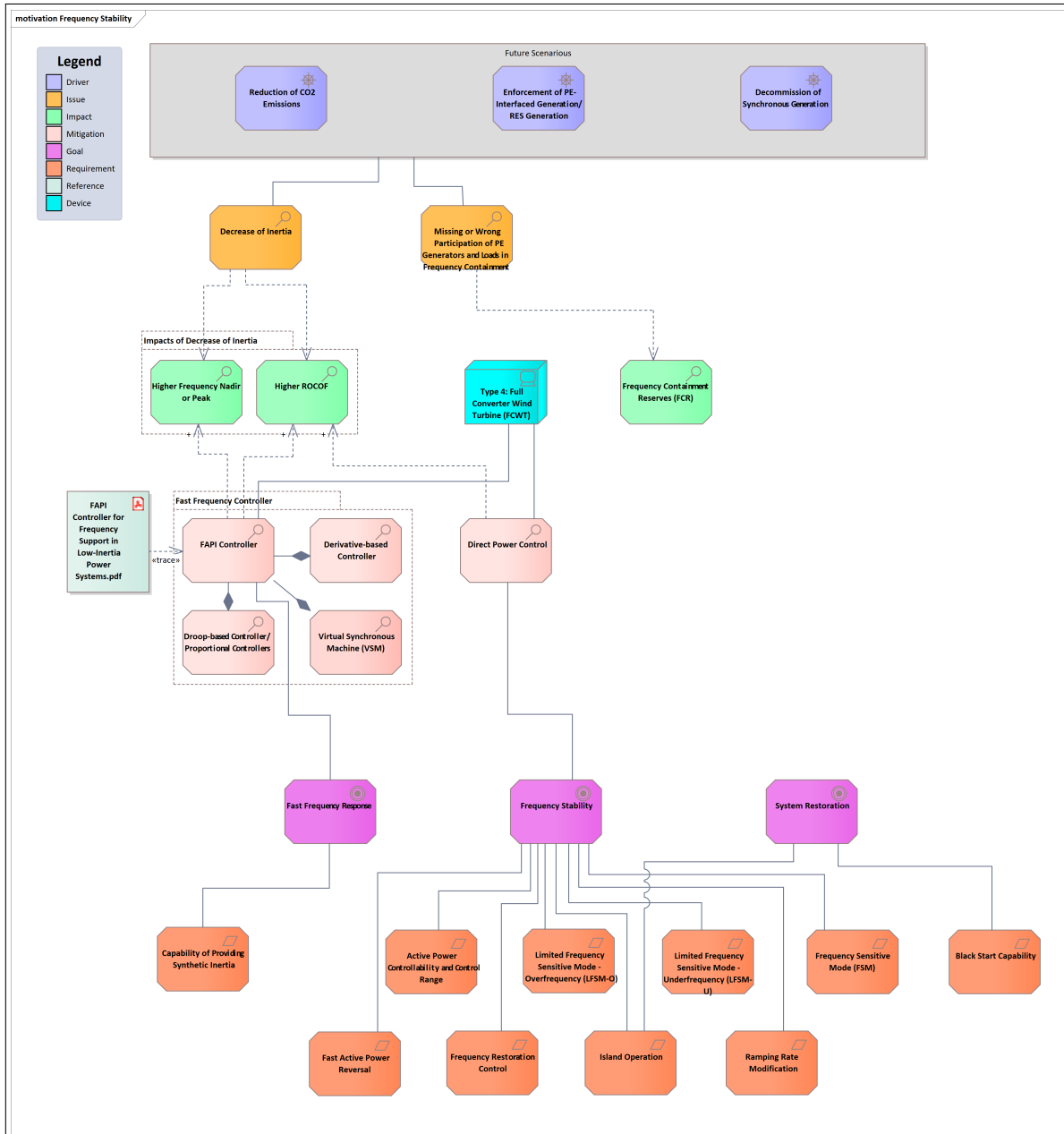
Figure A.4: Issues related to frequency stability with corresponding mitigations, goals and requirements.
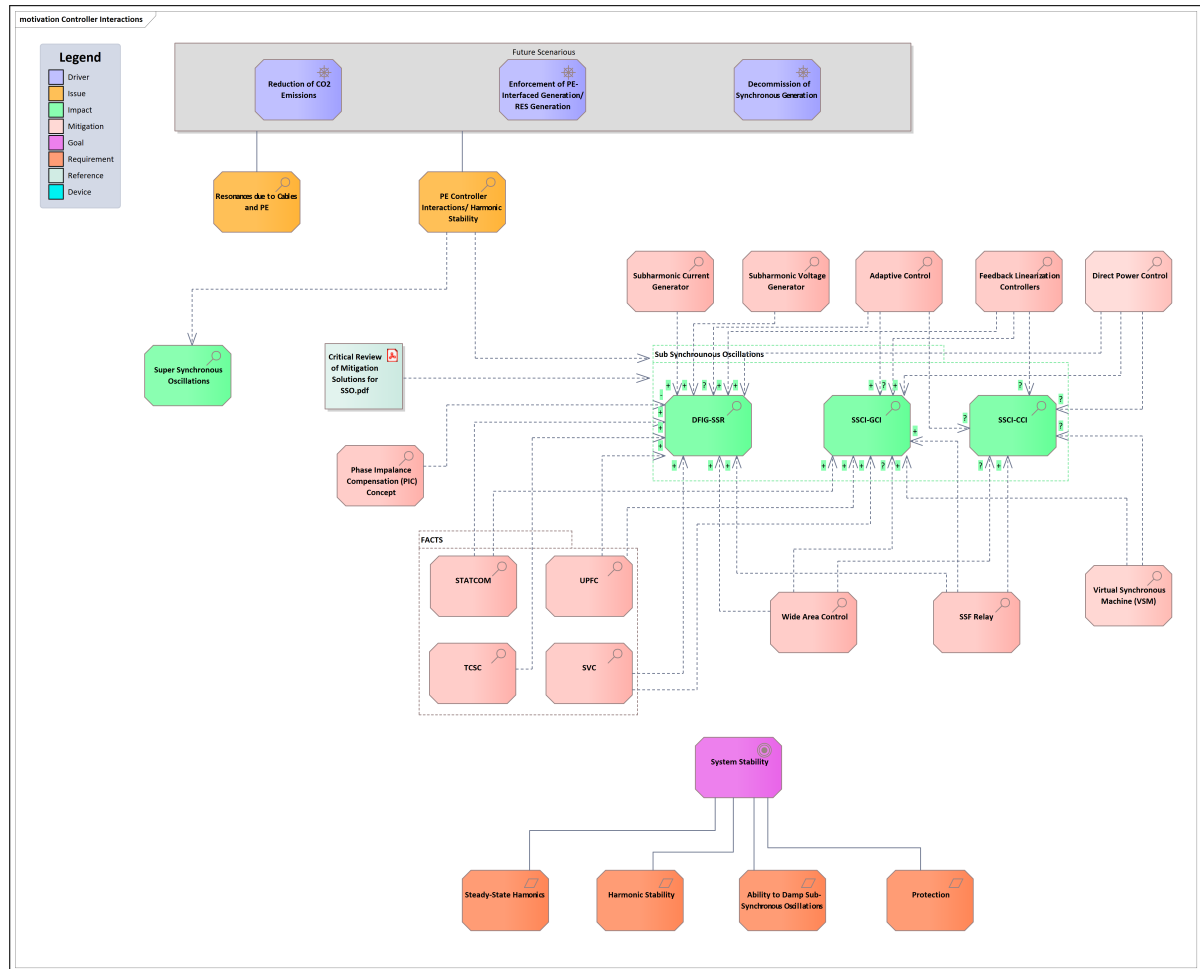
Figure A.5: Issues related to controller interactions with corresponding mitigations, goals and requirements.

B

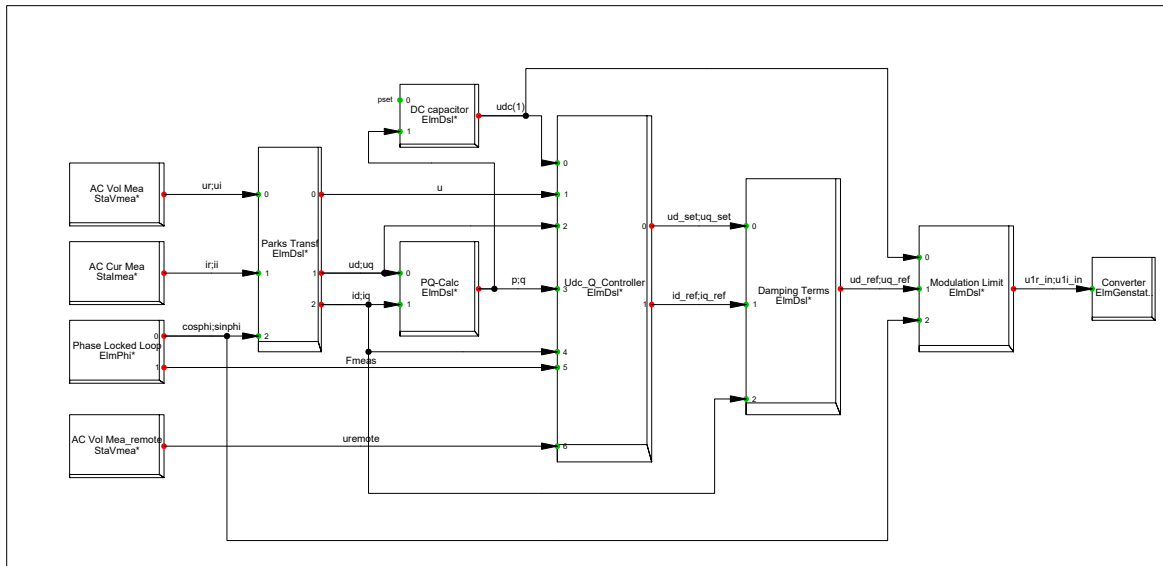## Direct Voltage Control - DIgSILENT PowerFactory Implementation

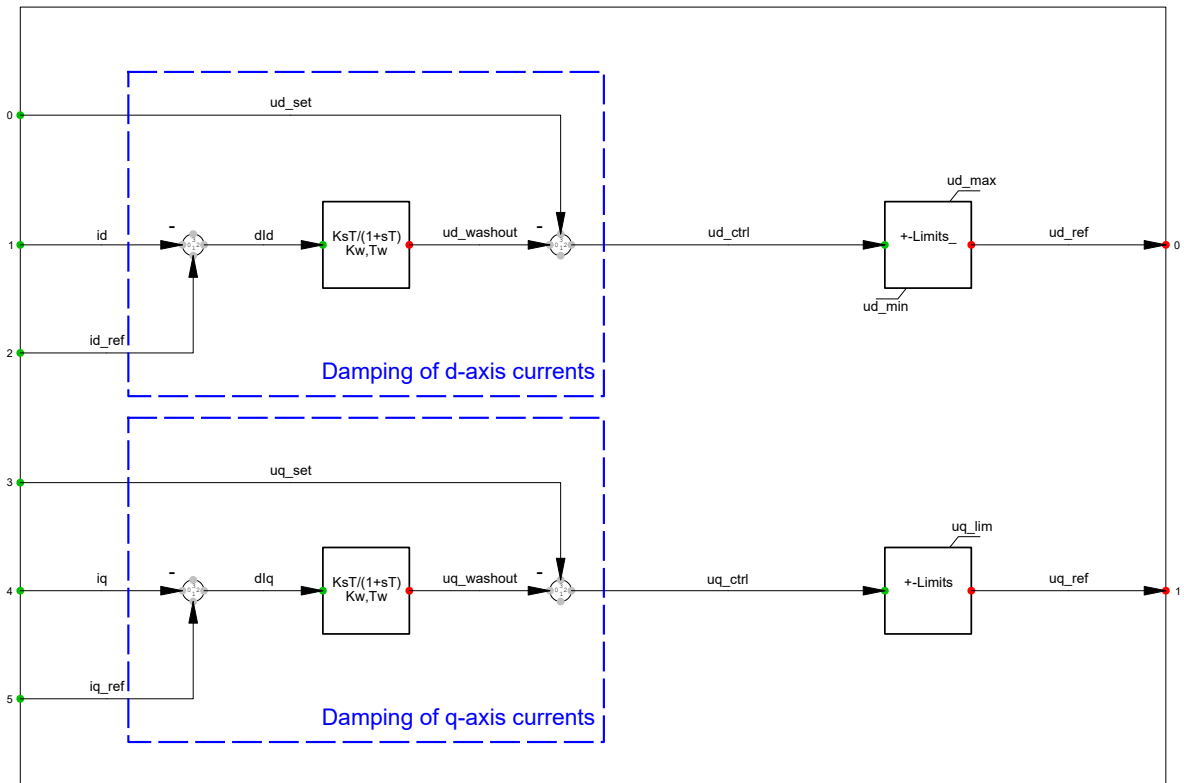Figure B.1: Direct Voltage Control composite frame.

Damping Terms:

Figure B.2: Direct Voltage Control Damping Terms.
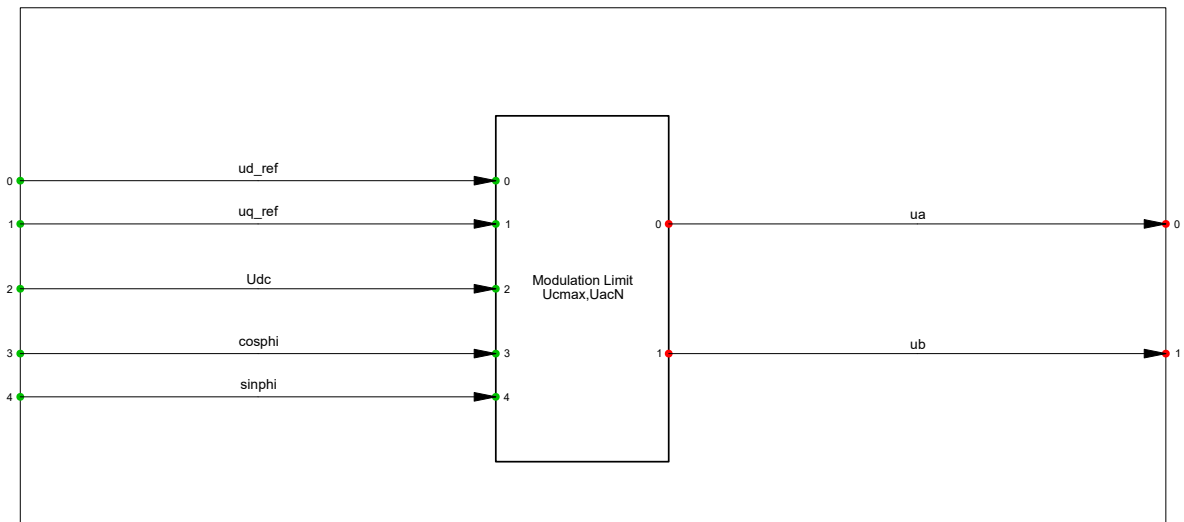
Modulation Limitation:

Figure B.3: Direct Voltage Control Modulation Limitation.

DC Bushbar and Capacitor:

Figure B.4: Direct Voltage Control DC Bushbar and Capacitor.
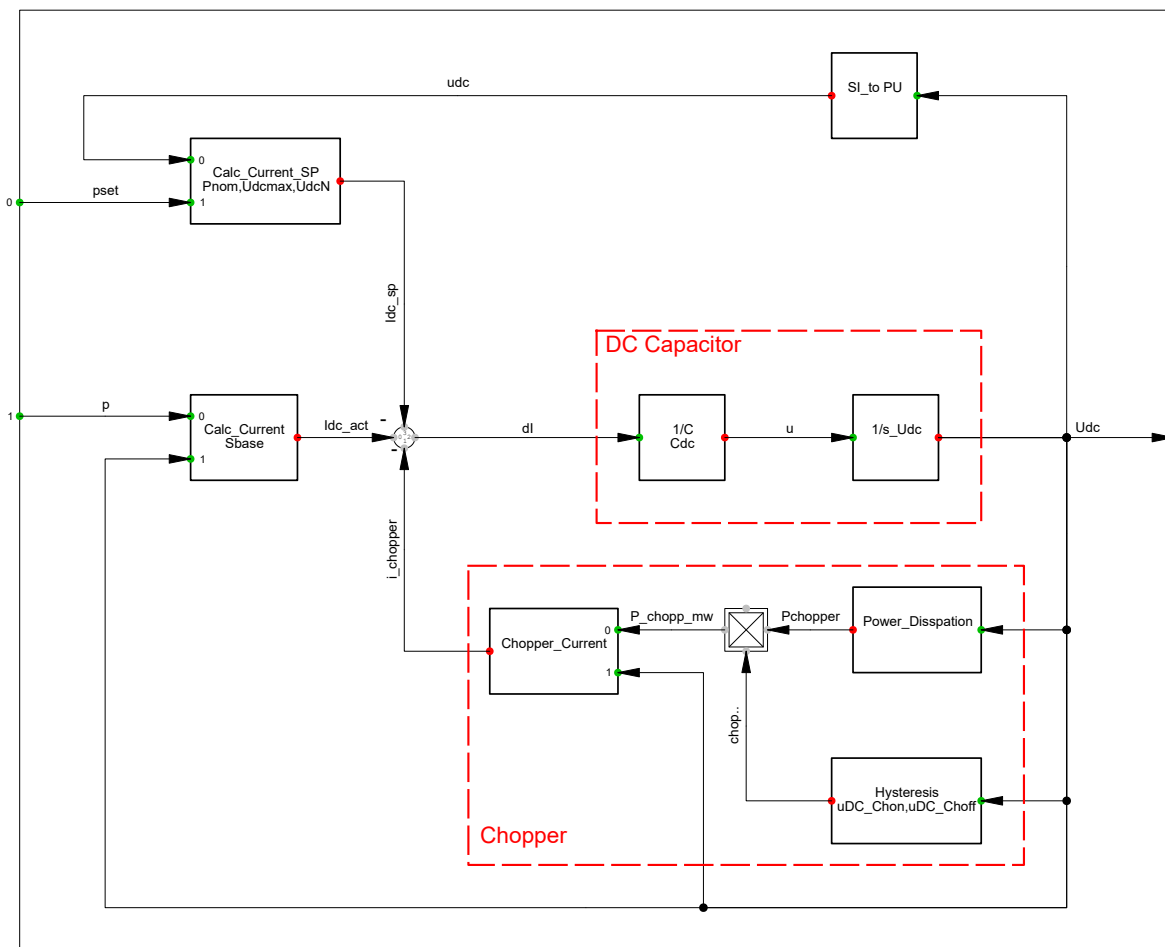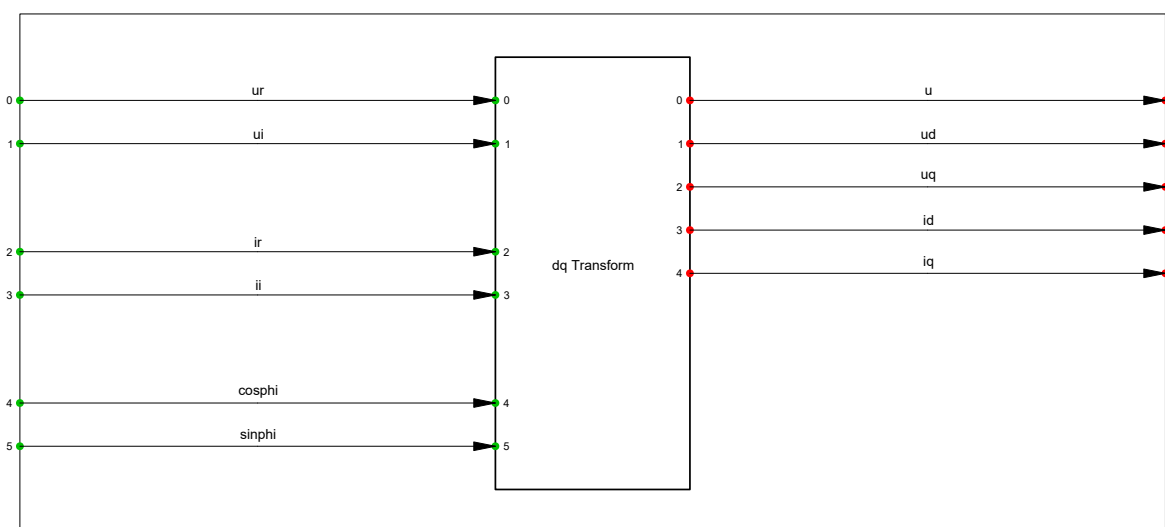
Park Transformation:

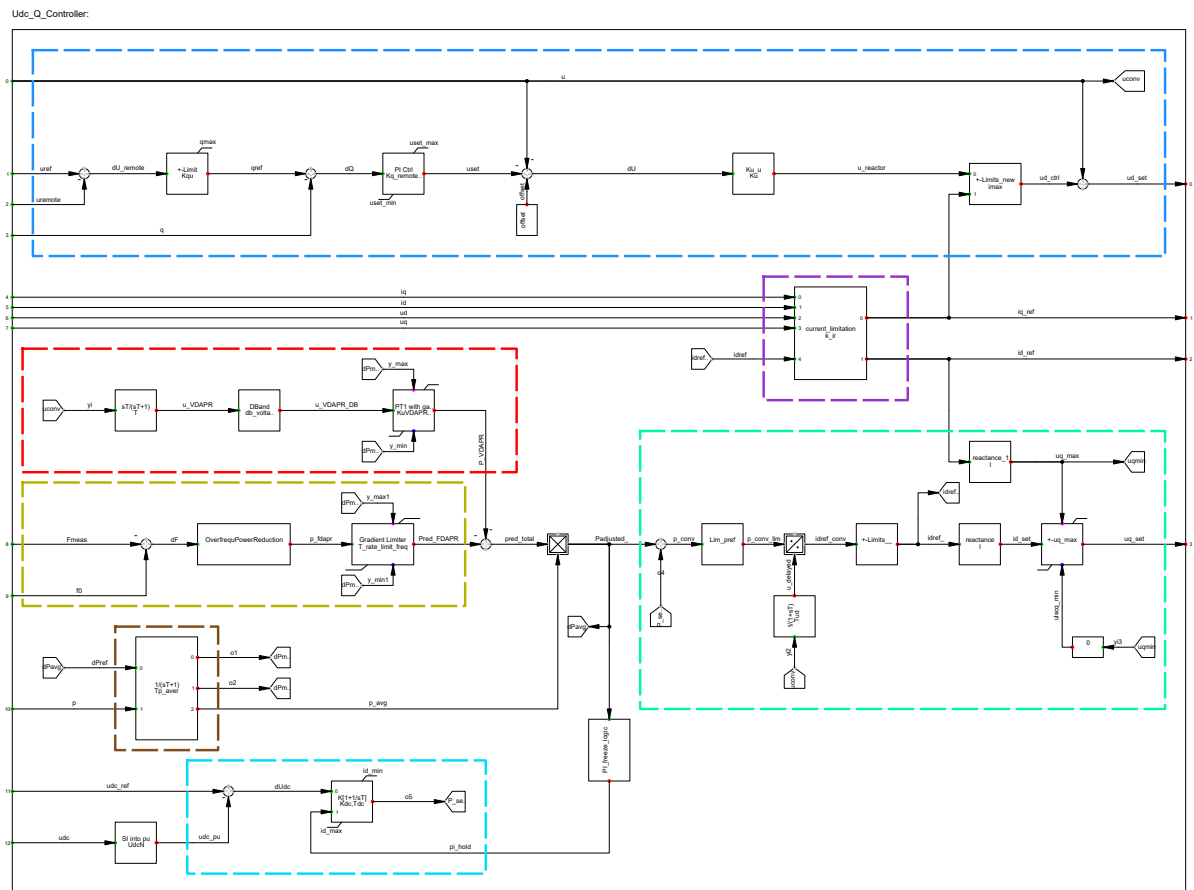Figure B.5: Direct Voltage Control Park Transformation.

Figure B.6: Direct Voltage Control Udc Q Control.

C

Wide Area Damping Control - DIgSILENT PowerFactory Implementation
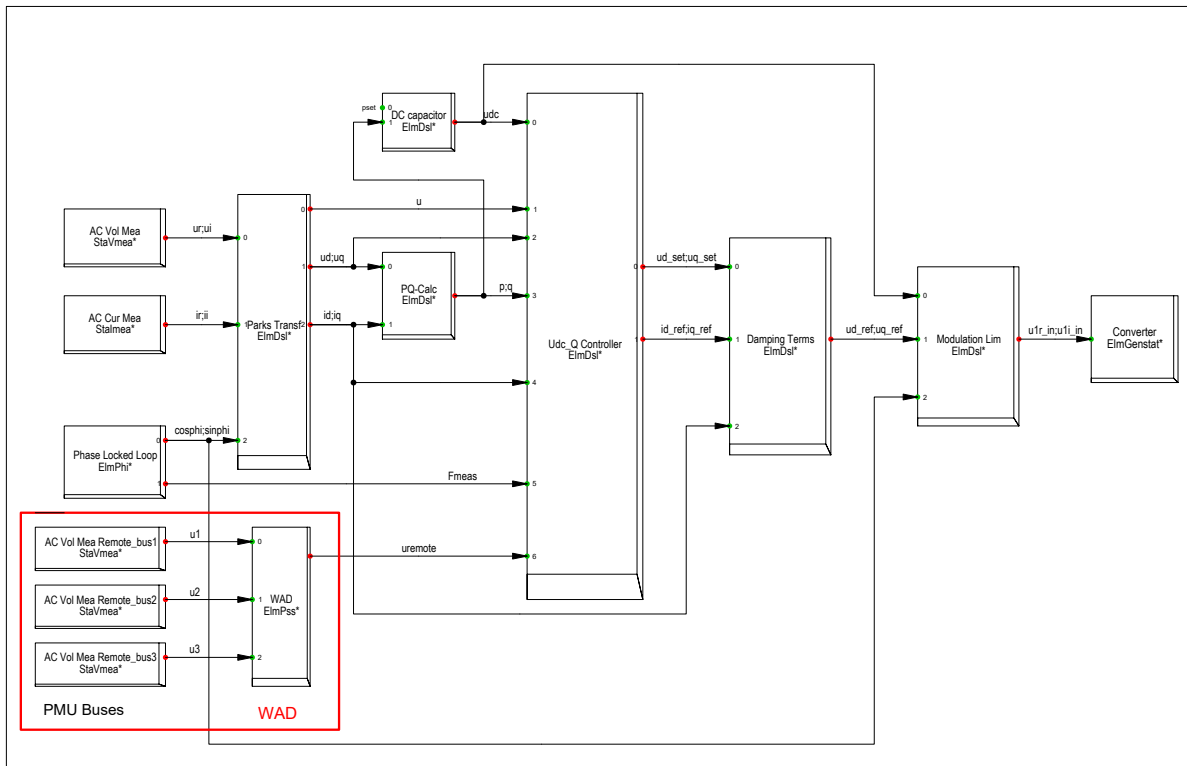
Converter Frame WAD:

Figure C.1: Application of WADC block to the existing control structure
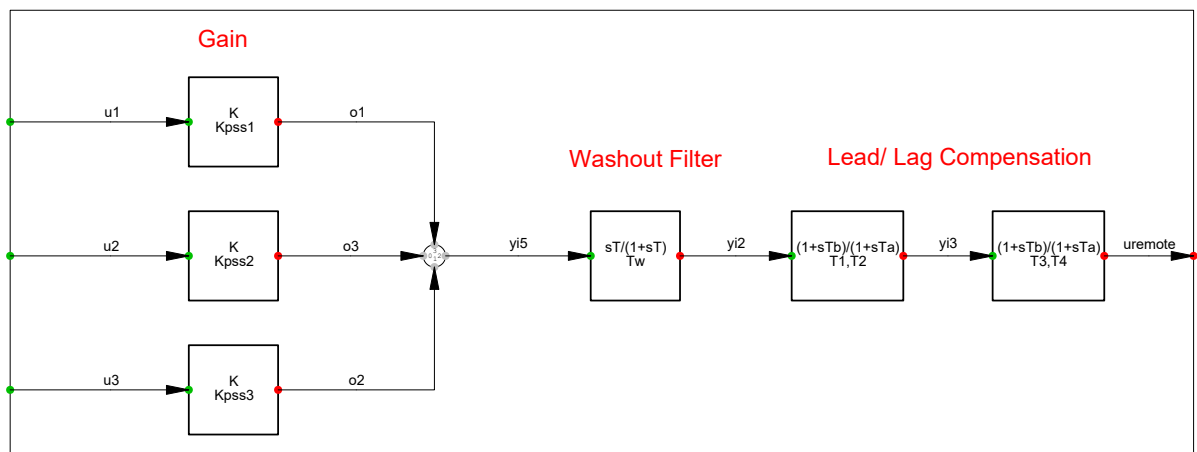
Figure C.2: Structure of WADC block modelled in PowerFactory

Bibliography

[1] MIGRATE. Clean energy - the european green deal. Available at `https://ec.europa.eu/commission/presscorner/detail/en/fs_19_6723`, 2019.

[2] DNV GL. Energy transition outlook, 2020.

[3] MIGRATE. Massive integration of power electronic devices. Available at `www.h2020-migrate.eu`, 2016.

[4] MIGRATE Work Package. (Responsible partner: TenneT GmbH). Migrate deliverable 1.1: Report on systemic issues, 2016.

[5] M. Ndreko, S. Rüberg, and W. Winter. Grid forming control scheme for power systems with up to 100% power electronic interfaced generation: a case study on great britain test system. *IET Renewable Power Generation*, 14(8):1268–1281, 2020. doi: 10.1049/iet-rpg.2019.0700.

[6] S. V. Dhople, B. B. Johnson, and A. O. Hamadeh. Virtual oscillator control for voltage source inverters. In *2013 51st Annual Allerton Conference on Communication, Control, and Computing (Allerton)*, pages 1359–1363, 2013. doi: 10.1109/Allerton.2013.6736685.

[7] A. Korai, J. Denecke, J. L. Rueda Torres, and E. Rakhshani. New control approach for blackstart capability of full converter wind turbines with direct voltage control. In *2019 IEEE Milan PowerTech*, pages 1–6, 2019. doi: 10.1109/PTC.2019.8810684.

[8] M. R. Younis and R. Iravani. Wide-area damping control for inter-area oscillations: A comprehensive review. In *2013 IEEE Electrical Power Energy Conference*, pages 1–6, 2013. doi: 10.1109/EPEC.2013.6802938.

[9] F. M. Gonzalez-Longatt and J. L. Rueda Torres. *Advanced Smart Grid Functionalities Based on PowerFactory*, pages 1–371. Springer International Publishing, 2018. ISBN 978-3-319-50532-9. doi: "10.1007/978-3-319-50532-9_1.

[10] N. Hatziargyriou, J. V. Milanovic, C. Rahmann, V. Ajjarapu, C. Canizares, I. Erlich, D. Hill, I. Hiskens, I. Kamwa, B. Pal, P. Pourbeik, J. J. Sanchez-Gasca, A. M. Stankovic, T. Van Cutsem, V. Vittal, and C. Vournas. Definition and classification of power system stability revisited extended. *IEEE Transactions on Power Systems*, pages 1–1, 2020. doi: 10.1109/TPWRS.2020.3041774.

[11] P. Kundur. *Power System Stability and Control.* McGraw-Hill, 1994.

[12] F. M. Gonzalez-Longatt and J. L. Rueda Torres. *Modelling and Simulation of Power Electronic Converter Dominated Power Systems in PowerFactory*, pages 1–377. Springer International Publishing, 2021. ISBN 978-3-030-54124-8. doi: 10.1007/978-3-030-54124-8.

[13] G. Denis, T. Prevost, M. Debry, F. Xavier, X. Guillaud, and A. Menze. The migrate project: the challenges of operating a transmission grid with only inverter-based generation. a grid-forming control improvement with transient current-limiting control. *IET Renewable Power Generation*, 12(5):523–529, 2018. doi: 10.1049/iet-rpg.2017.0369.

[14] V. N. Sewdien, M. van der Meijden, T. Breithaupt, L. Hofmann, D. Herwig, A. Mertens, B. W. Tuinema, and J. L. Rueda Torres. Effects of increasing power electronics on system stability: Results from migrate questionnaire. In *2018 International Conference and Utility Exhibition on Green Energy for Sustainable Development (ICUE)*, pages 1–9, 2018. doi: 10.23919/ICUE-GESD.2018.8635602.

[15] M. G. Molina and P. E. Mercado. Modelling and control design of pitch-controlled variable speed wind turbines. In Ibrahim Al-Bahadly, editor, *Wind Turbines*, chapter 16. IntechOpen, Rijeka, 2011. doi: 10.5772/15880.

[16] V. Yaramasu, B. Wu, P. C. Sen, S. Kouro, and M. Narimani. High-power wind energy conversion systems: State-of-the-art and emerging technologies. *Proceedings of the IEEE*, 103(5):740–788, 2015. doi: 10.1109/ JPROC.2014.2378692.

[17] M. Ndreko. *Electrical Power Systems of the Future*, chapter Dynamic Stability at High Variable Renewable Energy Source Penetration, pages 1–14. Delft University of Technology, 2020.

[18] Y. Solbakken. Vector control for dummies. Available at `https://www.switchcraft.org/learning/ 2016/12/16/vector-control-for-dummies`, 2017.

[19] P. Unruh, M Nuschke, P. Strauß, and F. Welck. Overview on grid-forming inverter control methods. *Energies*, 13(10):2589, 2020. doi: 10.3390/en13102589.

[20] L. Ramirez Elizondo and P. Bauer. *DC and AC Microgrids*. Delft University of Technology, 2018.

[21] Jiabing Hu and Bin Hu. Direct active and reactive power regulation of grid connected voltage source converters using sliding mode control approach. In *2010 IEEE International Symposium on Industrial Electronics*, pages 3877–3882, 2010. doi: 10.1109/ISIE.2010.5637630.

[22] H. Nian, P. Cheng, and Z. Q. Zhu. Coordinated direct power control of dfig system without phase-locked loop under unbalanced grid voltage conditions. *IEEE Transactions on Power Electronics*, 31(4):2905–2918, 2016. doi: 10.1109/TPEL.2015.2453127.

[23] T. Neumann, I. Erlich, B. Paz, A. Korai, M. K. Zadeh, S. Vogt, C. Buchhagen, C. Rauscher, A. Menze, and J. Jung. Novel direct voltage control by wind turbines. In *2016 IEEE Power and Energy Society General Meeting (PESGM)*, pages 1–5, 2016. doi: 10.1109/PESGM.2016.7741744.

[24] S. Zhu, Y. Zhang, D. Le, and A. A. Chowdhury. Understanding stability problems in actual system — case studies. In *IEEE PES General Meeting*, pages 1–6, 2010. doi: 10.1109/PES.2010.5590041.

[25] A. M. Almutairi and J. V. Milanovic. Comparison of different methods for input/output signal selection for wide area power system control. In *2009 IEEE Power Energy Society General Meeting*, pages 1–8, 2009. doi: 10.1109/PES.2009.5275576.

[26] M. Beiraghi and A. M. Ranjbar. Additive model decision tree-based adaptive wide-area damping controller design. *IEEE Systems Journal*, 12(1):328–339, 2018. doi: 10.1109/JSYST.2016.2524518.

[27] D. Dotta, A. S. e Silva, and I. C. Decker. Wide-area measurements-based two-level control design considering signal transmission delay. *IEEE Transactions on Power Systems*, 24(1):208–216, 2009. doi: 10.1109/TPWRS.2008.2004733.

[28] A. Heniche and I. Kamwa. Assessment of two methods to select wide-area signals for power system damping control. *IEEE Transactions on Power Systems*, 23(2):572–581, 2008. doi: 10.1109/TPWRS.2008. 919240.

[29] J. C.-H. Peng and N.-K. C. Nair. Comparative assessment of kalman filter and prony methods for power system oscillation monitoring. In *2009 IEEE Power Energy Society General Meeting*, pages 1–8, 2009. doi: 10.1109/PES.2009.5275656.

[30] J. L. Rueda and I. Erlich. Input/ouput signal selection for wide-area supplementary damping controllers based on probabilistic eigenanalysis. *IFAC Proceedings Volumes*, 46(6):42–47, 2013. ISSN 1474-6670. doi: 10.3182/20130522-3-RO-4035.00007.

[31] N. Modi, M. Lloyd, and T. K. Saha. Wide-area signal selection for power system damping controller. In *AUPEC 2011*, pages 1–6, 2011.

[32] H. Nguyen-Duc, L. Dessaint, A. F. Okou, and I. Kamwa. Selection of input/output signals for wide area control loops. In *IEEE PES General Meeting*, pages 1–7, 2010. doi: 10.1109/PES.2010.5589788.

[33] O. Mäki, J. Seppänen, L. Haarla, K. Zenger, J. Turunen, and A. Nikkilä. Analysis of a centralized control strategy in mitigating inter-area power oscillations. In *IEEE PES Innovative Smart Grid Technologies, Europe*, pages 1–6, 2014. doi: 10.1109/ISGTEurope.2014.7028960.

[34] C. A. Juárez, J. L. Rueda, I. Erlich, and D. G. Colomé. Probabilistic approach-based wide-area damping controller for small-signal stability enhancement of wind-thermal power systems. In *2011 IEEE Power and Energy Society General Meeting*, pages 1–4, 2011. doi: 10.1109/PES.2011.6039650.

[35] H. M. Ayres, I. Kopcak, M.S. Castro, F. Milano, and V. F. da Costa. A didactic procedure for designing power oscillation dampers of facts devices. *Simulation Modelling Practice and Theory*, 18(6):896 – 909, 2010. ISSN 1569-190X. doi: https://doi.org/10.1016/j.simpat.2010.02.007.

[36] F. M. Gonzalez-Longatt and J. L. Rueda Torres. *PowerFactory Applications for Power System Analysis*, pages 391–420. Springer International Publishing, 2014. ISBN 978-3-319-12958-7. doi: 10.1007/978-3-319-12958-7.

[37] O. AL-Masari and M. AL-Masari. Enhancement of small signal stability of wind farms by using statcom and hvdc link. *International Journal of Emerging Science and Engineering (IJESE)*, 3(4):4–10, 2015. ISSN 2319–6378.

[38] S. Peyghami, P. Davari, M. Fotuhi-Firuzabad, and F. Blaabjerg. Standard test systems for modern power system analysis: An overview. *IEEE Industrial Electronics Magazine*, 13(4):86–105, 2019. doi: 10.1109/MIE.2019.2942376.

[39] DIgSILENT GmbH. 39 bus new england system, 2020.

[40] Power System Dynamic Performance Committee. Dynamic models for turbine-governors in power system studies. *IEEE Power & Energy Society*, 2013.

[41] IEEE recommended practice for excitation system models for power system stability studies. *IEEE Std 421.5-2005 (Revision of IEEE Std 421.5-1992)*, pages 1–93, 2006. doi: 10.1109/IEEESTD.2006.99499.

[42] DIgSILENT GmbH. Description, modelling and simulation of a benchmark system for converter dominated grids (part 1), 2018.

[43] IEC 61400-27-1:2020. Wind energy generation system - part 27-1: Electrical simulation models - generic models. 2020.

[44] DIgSILENT GmbH. Description, modelling and simulation of a benchmark system for converter dominated grids (part 2), 2018.

[45] S. D'Arco and J. A. Suul. Equivalence of virtual synchronous machines and frequency-droops for converter-based microgrids. *IEEE Transactions on Smart Grid*, 5(1):394–395, 2014. doi: 10.1109/TSG.2013.2288000.

[46] DIgSILENT GmbH. Digsilent powerfactory 2021: Technical reference, grid-forming converter templates, 2020.

[47] DIgSILENT GmbH. Digsilent powerfactory 2021: User manual, 2020.

[48] A. R. Akkawi, Muhamad Haj Ali, L. A. Lamont, and L. El Chaar. Comparative study between various controllers for power system stabilizer using particle swarm optimization. In *2011 2nd International Conference on Electric Power and Energy Conversion Systems (EPECS)*, pages 1–5, 2011. doi: 10.1109/EPECS.2011.6126806.

[49] IEEE guide for phasor data concentrator requirements for power system protection, control, and monitoring. *IEEE Std C37.244-2013*, pages 1–65, 2013. doi: 10.1109/IEEESTD.2013.6514039.

[50] A. Dubey. Load flow analysis of power systems. *International Journal of Scientific and Engineering Research*, 7:06, 2016. ISSN 2229-5518.

[51] MIGRATE Work Package. (Responsible partner: TenneT GmbH). Migrate deliverable 1.6: Demonstration of mitigation measures and clarification of unclear grid code requirements, 2019.